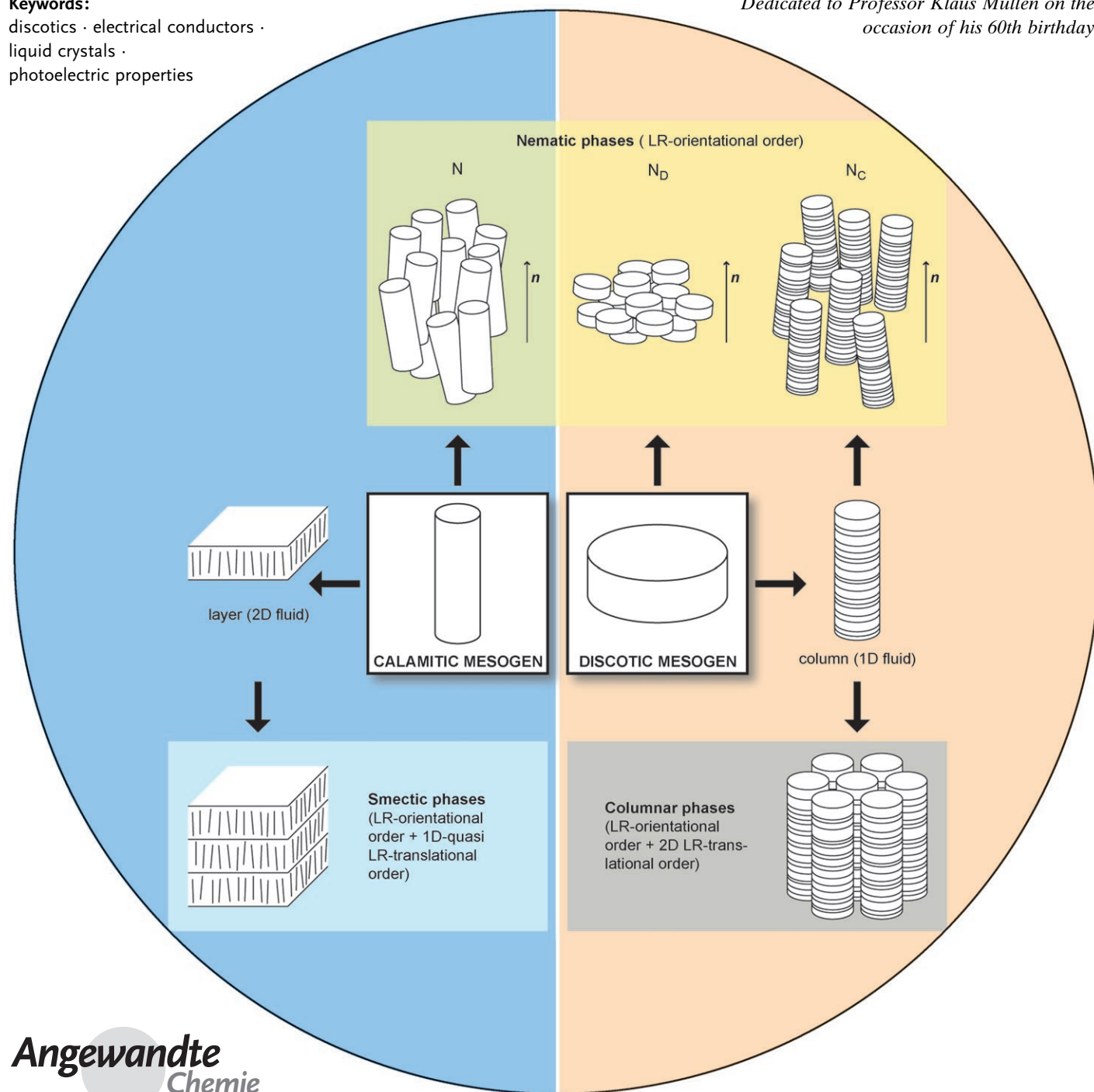# Discotic Liquid Crystals: From Tailor-Made Synthesis to Plastic Electronics

Sabine Laschat,* Angelika Baro, Nelli Steinke, Frank Giesselmann,*
Constanze Hägele, Giusy Scalia, Roxana Judele, Elisabeth Kapatsina, Sven Sauer,
Alina Schreivogel, and Martin Tosoni

Dedicated to Professor Klaus Müllen on the
occasion of his 60th birthday

*M*ost associate liquid crystals with their everyday use in laptop computers, mobile phones, digital cameras, and other electronic devices. However, in contrast to their rodlike (calamitic) counterparts, first described in 1907 by Vorländer, disklike (discotic, columnar) liquid crystals, which were discovered in 1977 by Chandrasekhar et al., offer further applications as a result of their orientation in the columnar mesophase, making them ideal candidates for molecular wires in various optical and electronic devices such as photocopiers, laser printers, photovoltaic cells, light-emitting diodes, field-effect transistors, and holographic data storage. Beginning with an overview of the various mesophases and characterization methods, this Review will focus on the major classes of columnar mesogens rather than presenting a library of columnar liquid crystals. Emphasis will be given to efficient synthetic procedures, and relevant mesomorphic and physical properties. Finally, some applications and perspectives in materials science and molecular electronics will be discussed.

From the Contents

1. Introduction

Since the end of the 19th century when Friedrich Reinitzer, Otto Lehmann, and others introduced the liquid-crystalline state of matter into science, the exact connection between the formation of liquid-crystalline phases and the structure of the constituent molecules became a major topic of debate.[1] In his classic study on the *Influence of molecular configuration on the crystalline-liquid state*,[2] Daniel Vorländer reported in 1907 that *"… the crystalline-liquid state results from a molecular structure which is as linear as possible"*. Over the next seventy years the linear rodlike shape of mesogenic molecules became a generally accepted principle in liquid-crystal research, which then developed into a mature field of science.

In the year 1977, however, when the thermotropic liquid crystals of rodlike molecules started to revolutionize commercial display technologies, Sivaramakrishna Chandrasekhar et al. reported *"… what is probably the first observation of thermotropic mesomorphism in pure, single-component systems of relatively simple plate-like, or more appropriately disc-like, molecules"*.[3] Even though there had been theoretical predictions[4–7] and experimental hints[8] that assemblies of disklike molecules might also form thermotropic mesophases, this study was the first clear-cut evidence for *"Liquid crystals of disc-like molecules"*[3] by Chandrasekhar et al. which then opened a whole new field of fascinating liquid-crystal research. Soon after this study by Chandrasekhar et al., the French research groups of Dubois and Levelut reported further liquid crystals formed by disklike molecules.[9, 10]

Today with the liquid-crystal displays an essential part of our everyday life, it seems quite clear that liquid crystals of disklike molecules ("discotic liquid crystals") cannot compete with their rodlike counterparts ("calamitic liquid crystals") in terms of electrooptic performance. Their unique structural and electronic properties, however, open completely different aspects of possible applications in topical research fields such as molecular electronics and high-efficiency organic photovoltaics.[11, 12] Discotic liquid crystals thus now receive increasing attention. This Review aims to summarize the rapid development of the field in recent years from the chemist's point of view.

A more general survey on the self-organization of discotic mesogens in comparison to their calamitic (rodlike) counterparts will be discussed before a detailed description. The rodlike configuration of a typical calamitic mesogen such as methoxybenzylidene-*p-n*-butylaniline (MBBA, the first room-temperature nematic material for display applications[13]) is usually represented by an elongated uniaxial ellipsoid or cylinder (Figure 1), and the structure of its liquid crystalline phase(s) described as a packing of these cylinders. Even though the representation of the detailed molecular structure by a simple elongated cylinder seems to be a rather

[*] Prof. Dr. S. Laschat, Dr. A. Baro, Dr. N. Steinke, Dr. R. Judele,
Dipl.-Chem. E. Kapatsina, Dipl.-Chem. S. Sauer,
Dipl.-Chem. A. Schreivogel, Dipl.-Chem. M. Tosoni
Institut für Organische Chemie
Universität Stuttgart
Pfaffenwaldring 55, 70569 Stuttgart (Germany)
Fax: (+49) 711-685-64285
E-mail: sabine.laschat@oc.uni-stuttgart.de

Prof. Dr. F. Giesselmann, Dipl.-Chem. C. Hägele
Institut für Physikalische Chemie
Universität Stuttgart
Pfaffenwaldring 55, 70569 Stuttgart (Germany)
Fax: (+49) 711-685-62569
E-mail: f.giesselmann@ipc.uni-stuttgart.de
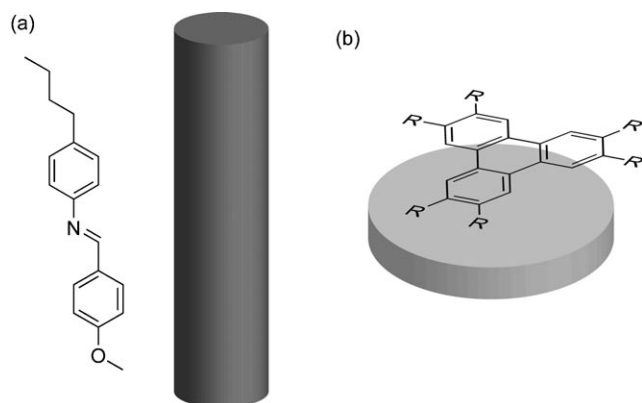
Dr. G. Scalia[+]
Max-Planck-Institut für Festkörperforschung
Heisenbergstrasse 1, 70596 Stuttgart (Germany)

[+] permanent address: ENEA, C.R. Portici
80055 Neapel (Italy)

Supporting information for this article is available on the WWW under http://www.angewandte.org or from the author.

Figure 1. A calamitic (a) and a discotic (b) mesogen, and a representation of their effective molecular shapes as rods and disks, respectively.

crude simplification, this approach turned out to be quite successful since mesogens in fluid phases are basically free to rotate (at different rates) around their molecular axes and the cylinder thus represents the average (or effective) shape of the molecule in the liquid-crystalline packing.

Simple discotic mesogens such as the triphenylenes (Figure 1b) have a more or less rigid planar core with typically six or eight flexible chain substituents laterally attached to the core. Following the same reasoning as in the calamitic case its effective shape is represented by a flat disk. While disks and cylinders both represent rather anisometric molecular shapes, the principal axis of the calamitic mesogen is given by the long axis of the cylinder, whereas the short axis (normal to the plane of the disk) represents the principal axis of a discotic mesogen.

The self-organization of (calamitic as well as discotic) mesogenic molecules into the various liquid-crystalline phases (that is, spontaneously anisotropic ordered fluids) is driven by the anisotropy in the intermolecular interactions (mainly steric and dispersion interactions) between the highly anisometric molecules. In the simplest case the usual nematic phase (N) is formed when calamitic mesogens align their principal axes to a certain degree along a common direction, which defines the so-called director n (see Figure 11). Thus a long-range orientational order with full rotational symmetry around n results, whereas the molecular centers of mass are—as in an ordinary fluid—translationally disordered in all directions. Basically the same nematic structure is obtained

when the short molecular axes of discotic mesogens align along n (N_D phase, Figure 11).[14] In addition to this N_D phase, another option for disklike molecules to form a nematic phase has been observed.[15] The disklike mesogens pile up into extended one-dimensional (1D) columns which tend to align with their column axes parallel to each other to form the so-called columnar nematic phase (N_C). The columns thus act as supramolecular rods which—similar to single rodlike molecules—are the building blocks of a nematic phase. Even though it has become common practice to distinguish between N, N_D, and N_C phases, these three phases all have the same symmetry and thus—in terms of strict crystallographic notation—the distinction seems unnecessary.

The stacking of disklike molecules into 1D columns is a rather characteristic motive in the self-organization of discotic molecules, and inherent to their most typical liquid-crystalline phases: the family of columnar phases. Different types of stacking are observed depending on the details of the intracolumnar interactions: "disordered columns" with an irregular stacking of the disks, "ordered columns" in which the cores are stacked in a regular ordered (equidistant) fashion while the flexible tails are still disordered, and "tilted columns" where the cores of the disks are tilted with respect to the column axis. As none of these types has perfect translational order, these extended supramolecular columns can in general be considered as 1D fluids.[16a] In the columnar phases these columns are arranged in a 2D lattice with the column axes parallel to each other. The variety of columnar phases can thus be thought of as 1D fluid (along the columns) and 2D crystalline (along the 2D lattice vectors) structures; the different types of which are distinguished by their intracolumnar order (disordered, ordered, tilted) and the symmetry of the 2D intercolumnar lattice (hexagonal, rectangular, oblique) (Figure 2 and 3).
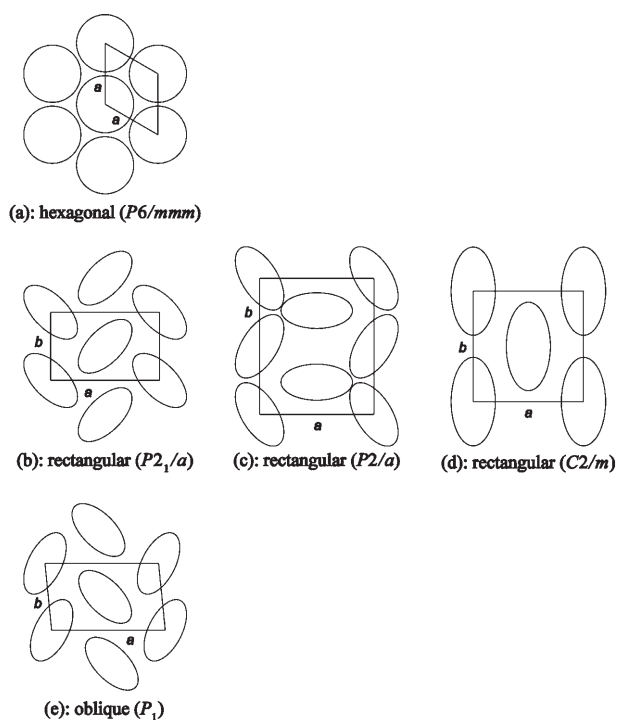
Even though columnar phases are most characteristic for discotic mesogens, they are by no means unique: surfactants which aggregate into columnar micelles to form lyotropic columnar phases ("middle soap")[17] have been known for a long time, and even some calamitic mesogens were found to show thermotropic columnar phases.[18] The general picture is completed by smectic (or lamellar) phases that are all signified by a 1D periodic stack of "smectic layers" formed by orientationally ordered mesogenic molecules. In the typical cases of fluid and hexatic smectic mesophases, each layer can be seen as a 2D liquid. Smectic phases thus have a

Sabine Laschat studied chemistry from 1982 to 1987 at the Universität Würzburg and received her PhD in 1991 from the Universität Mainz under the supervision of Horst Kunz. After a postdoctorate with Larry Overman, she finished her habilitation in 1996 at the Universität Münster (mentor: Gerhard Erker). In 1997 she was appointed Associate Professor of Organic Chemistry at the Technische Universität in Braunschweig. Since 2002 she has held a Chair in Organic Chemistry at the Universität Stuttgart, and is speaker of the collaborative research center SFB 706.

Frank Giesselmann studied chemistry and received his PhD from the Technischen Universität Clausthal-Zellerfeld. During his postdoctoral studies on phase transitions in liquid crystals, he worked with Peter Zugenmaier (Clausthal), W. Kuczynski (Poland), and Sven T. Lagerwall (Sweden). In 1998 he finished his habilitation and received the venia legendi in Physical Chemistry. Since 2002 he has been Professor of Physical Chemistry at the Universität Stuttgart, where he also joined the International Max Planck Research School on Advanced Materials.

(a): hexagonal (*P6/mmm*)

(b): rectangular (*P2₁/a*)　(c): rectangular (*P2/a*)　(d): rectangular (*C2/m*)

(e): oblique (*P₁*)

Figure 2. Plan views of the 2D lattices in hexagonal (a), rectangular (b–d), and oblique (e) columnar mesophases. Point-group symmetries in parentheses are according to the "International System".
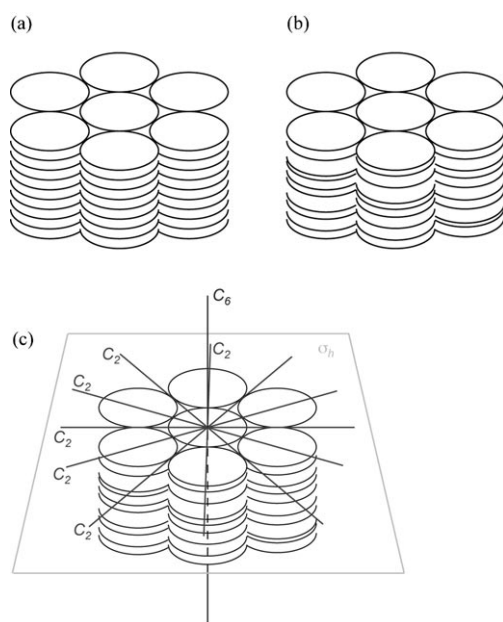
Figure 3. The stacking of the mesogen cores in the columns: a) ordered stacking, b) disordered stacking, and c) symmetry elements of a Col_h mesophase: the point group D_{6h} has one C_6 axis, and perpendicular to this axis, six C_2 and a mirror plane σ_h. For clarity, only the cores of the molecules are shown.

fluid structure in two dimensions combined with a (quasi) long-range translational order in the third dimension, normal to the smectic layers.[16b] In the case of disklike mesogens, smectic phases are quite rare.

In light of these principles, a comment on the current terminology is necessary: soon after the discovery by Chandrasekhar et al. of the columnar liquid-crystalline phases formed by disklike molecules, terms such as "discotic phases" or "discotics" were coined to denote the disklike molecules as well as the (mostly but not exclusively) columnar phases formed by them. As this incorrect synonym for the structure of a (macroscopic) phase and the shape of its constituting molecules created a constant source of ambiguities, in 1998 Chandrasekhar himself pointed out: *"Strictly speaking, it is the molecules that are discotic and not the mesophases, which may be columnar, nematic, or lamellar"*.[19] In this Review we will thus clearly distinguish between "discotic molecules" and "columnar liquid crystals".

2. Structures of liquid crystalline phases

This chapter will be devoted to the detailed structures of the various liquid-crystal phases of discotic molecules,[20] their chiral variants, and their experimental identification and characterization by X-ray diffraction and polarizing optical microscopy.

2.1. The hexagonal columnar mesophase Col_h

The planar space group of a hexagonal columnar mesophase is *P6/mmm*, which is equivalent to *P6/m2/m* in the International System (Figure 2) and belongs to the point group D_{6h} in Schoenflies notation. The symmetry elements are shown in Figure 3c.

The 2D diffraction pattern and the small-angle X-ray scattering (SAXS) profiles of an unorientated (powder) sample of a Col_h mesophase are shown in Figure 4 and Figure 5. In the small-angle regime a few distinct peaks can be observed. The sharpness of these reflections is due to the long-range intercolumnal order. According to Fontes et al., the correlation length of the 2D hexagonal lattice, measured in strands, is at least 4000 Å or approximately 200 columns.[21] This lower limit of the correlation length is set by the instrumental resolution.

Figure 6 shows the 2D lattice planes that correspond to the (10) and (11) reflections, d_{10} and d_{11}, respectively. These two *d* spacings follow the Equation (1).

$$d_{11} = \frac{d_{10}}{2\cos 30°} = \frac{d_{10}}{\sqrt{3}} \tag{1}$$

Thus, the *d* spacings of the (10) and (11) reflections show the ratio $1:1/\sqrt{3}$. More geometric considerations result in the characteristic ratios of $1:1/\sqrt{3}:1/\sqrt{4}:1/\sqrt{7}:1/\sqrt{9}:1/\sqrt{12}:1/\sqrt{13}$ for the *d* spacings of the (10), (11), (20), (21), (30), (22), and (31) reflections of a 2D hexagonal lattice in the small-angle regime.

As can also be seen in Figure 6, the d_{hk} spacings (in which *h* and *k* are the Miller indices of the associated reflection) are related to the lattice constant *a* according to Equation (2).
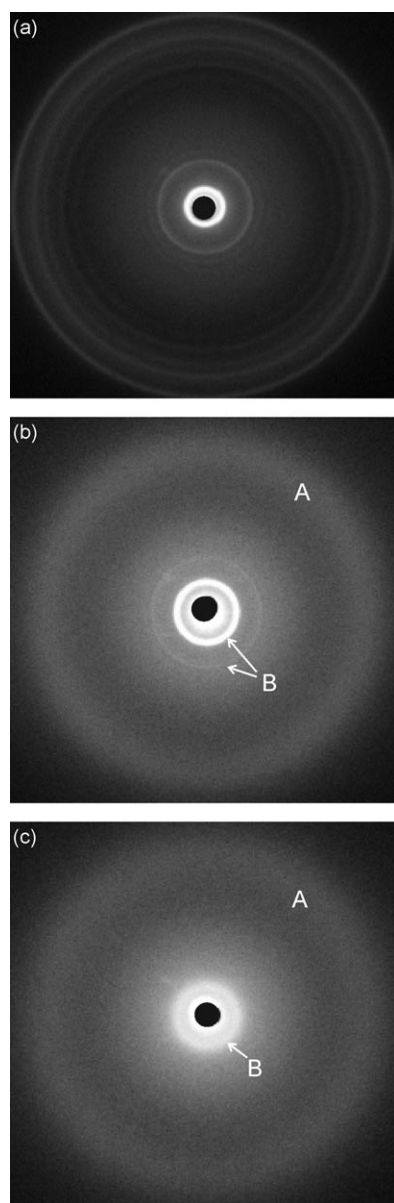
Figure 4. 2D X-ray diffraction patterns of an unorientated sample of tetraphenylene **78e**. a) Crystalline phase and b) liquid-crystalline phase: A) diffuse halo caused by the liquidlike order of the alkyl side chains; B) distinct reflections in the small-angle regime, which result from the long-range intercolumnar ordering. c) A diffuse ring is observed in the isotropic melt in the small-angle regime as a result of the loss of long-range order of the columns.

One example that demonstrates these characteristic ratios is shown in Table 1.

$$\frac{1}{d_{hk}^2} = \frac{4}{3}\frac{h^2 + k^2 + hk}{a^2} \qquad (2)$$

Further evidence of the hexagonal arrangement of the columns is obtained by a 2D diffraction pattern of a monodomain sample. For a powder sample of a columnar hexagonal mesophase, scattering rings are observed. If a monodomain sample is available, six point-shaped reflections
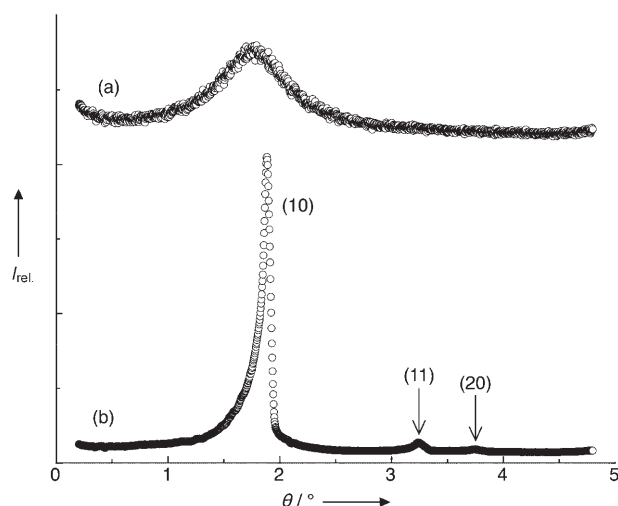
Figure 5. Small-angle X-ray scattering profiles of tetraphenylene **78** (R = COC$_{14}$H$_{29}$). a) Isotropic melt, b) Col$_h$ mesophase: the reflections (10), (11), and (20) are due to the long-range intercolumnar ordering.
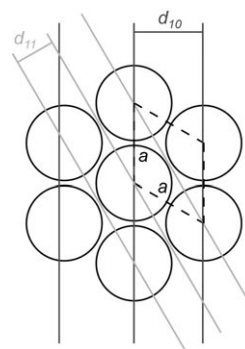
Figure 6. In a hexagonal lattice, the d spacings of the (10) and (11) reflections show the characteristic ratio $1:1/\sqrt{3}$.

Table 1: d Spacings and lattice parameter for a columnar hexagonal mesophase Col$_h$ of **78** (Figure 5).

| d_{obs} [Å][a]	hk[b]	d_{calcd} [Å][a]	Lattice parameter
23.4	(10)	23.5	$a = 27.2$ Å
13.6	(11)	13.6	
11.8	(20)	11.8	

[a] d_{obs} and d_{calcd} denote the observed and the calculated diffraction spacings; [b] hk are the Miller indices of the 2D hexagonal lattice.

are arranged in a perfect hexagon in the small-angle regime (Figure 7).[22]

If it is possible to draw aligned fibers from a Col$_h$ mesophase (for example, by shearing or extrusion), all small-angle reflections related to the 2D hexagonal lattice are located on the equator of the X-ray pattern and the diffuse halo in the wide-angle regime is found on the meridian.[23]

While the reflections in the small-angle regime belong to the large periods of the hexagonal lattice, short distances correlate to the reflections in the wide-angle regime (wide-angle X-ray scattering, WAXS). The broad diffuse halo found for disordered columnar phases such as Col$_{hd}$ in the wide-
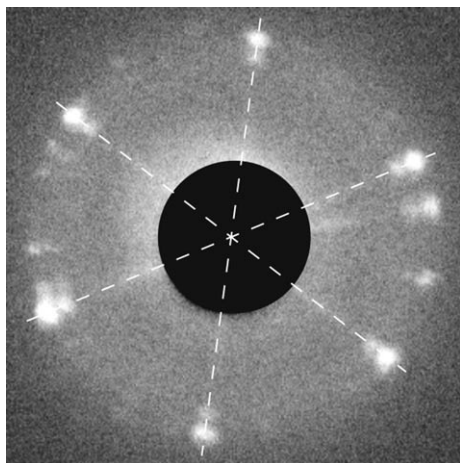
Figure 7. Monodomain sample of a Col_h mesophase of tetraphenylene **77 d**. Six point-shaped reflections are arranged in a perfect hexagon in the small-angle regime.

straight linear defects (Figure 8 d).[27] However, the problem often occurs that only small domains are formed that could not be attributed to a typical texture.

2.2. The columnar rectangular mesophase Col_r

Three different columnar rectangular mesophases Col_r have been identified (Figure 2 b–d).[28] In general the molecules are tilted with respect to the column axis,[29] whereby the cross section, orthogonal to the long axis of a column, is elliptic.

The symmetries of the 2D lattices are specified by three different planar space groups $P2_1/a$, $P2/a$, and $C2/m$,[27,28] belonging to the subset of space groups without any transitional periods in the direction of the principal symmetry axis (that is, the direction of the columns).[30] As a result of the elliptical projection of the molecules in the plane, the symmetry of the Col_r phases deviates from a proper hexag-

angle regime (Figure 4 b) corresponds to the liquidlike order of, for example, the alkyl side chains. Additionally, the diffraction pattern of a Col_{ho} phase shows a second relatively narrow diffuse ring in the wide-angle regime that is related to the regular stacking of the mesogenic cores along the column long axis. In the isotropic melt the hexagonal arrangement of the columns is lost and thus in the small-angle regime a diffuse ring is also observed (Figure 4 c). On the other hand the diffraction pattern of a crystalline phase shows distinct Bragg reflections in both the small-angle and the wide-angle regime (Figure 4 a). In addition to the long-range order of the 2D lattice as in Col_h mesophases, the alkyl side chains are regularly packed and the columns are crystalline.
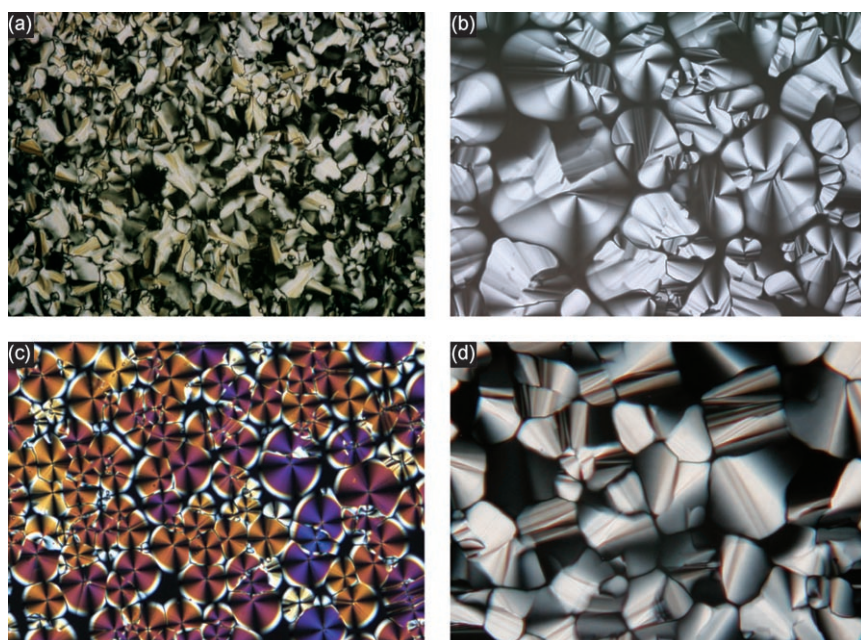
Liquid-crystalline phases are anisotropic fluids which in general are optically birefringent (see 3.2.). In a polarizing microscope (between crossed polarizers) each mesophase shows a typical pattern ("texture"). These textures result from the symmetry-dependent elasticity of the liquid-crystalline phase in combination with defects and the surface conditions of the sample. For Col_h mesophases, conic fan-shaped (pseudofocal conic) and focal textures (Figure 8 a and b, respectively) are characteristic. Mosaic and dendritic textures[24] are not as common. When dendritic textures grow in all directions from one point, "flowerlike" texture are formed.[25] Furthermore, relatively rare spherulitic-like (Figure 8 c) and fingerprint textures[26] are known. It is important to note that these fingerprint textures do not bear analogy to those of cholesteric mesophases, in which the equidistant stripes are related to the periodicity of the chirality-induced helical modulation. On the other hand, fingerprint textures of columnar hexagonal phases can be described as broken focal conics. Textures of an ordered hexagonal columnar mesophase typically exhibit

Figure 8. Textures of Col_h mesophases. a) Fan-shaped focal conic texture (**149**, $R = C_7H_{15}$), b) focal conic texture (**78**, $R = COC_{12}H_{25}$), c) spherulitic-like texture with maltese crosses (**77**, $R = C_{16}H_{33}$). d) The straight linear defects are characteristic for ordered columnar mesophases (**78**, $R = COC_{11}H_{23}$).

onal arrangement. Rectangular phases sometimes are also called pseudohexagonal. However, stronger core–core interactions are needed for the formation of Col_r mesophases than for the formation of hexagonal phases because the cores of one column have to "know" how they must be tilted with respect to the cores of the neighboring columns. Therefore, crossover from columnar rectangular to hexagonal mesophases with increasing side-chain lengths has often been observed.[26,27,31–34]

The 2D X-ray patterns resemble those of a columnar hexagonal mesophase with a diffuse halo in the wide-angle

regime and sharp reflections in the small-angle regime. However, a closer look to the SAXS profiles reveals certain differences (Figure 9). The (10) peak of the Col$_h$ mesophase splits in the (20) and (11) reflection of the Col$_r$ phase. This observation is explained in Figure 10. Here, in a hexagonal
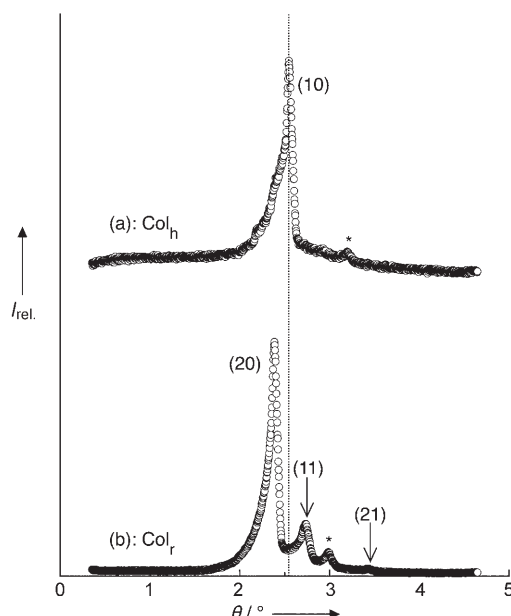
Figure 9. SAXS profiles of a hexagonal (a) and a rectangular columnar mesophase (b) of tetraphenylene **78c**. The (10) reflection of the Col$_h$ phase divides into two peaks of the Col$_r$ phase. The scattering maximum (∗) is a satellite peak of the strong (10) and (20) reflections, respectively, and originates from the parasitic Fe$_{K\alpha}$ radiation.
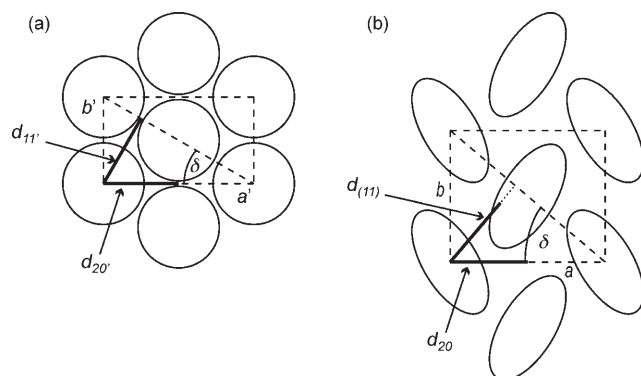
Figure 10. Symmetry breakdown at the transition from a hexagonal (a) to a rectangular columnar phase (b). For better clarification the rectangle in (b) is shown in a disproportionate way. Normally the lattice of a rectangular mesophase is closer to that of a hexagonal columnar phase.

lattice a rectangular unit cell with the lattice constants a' and b' is shown (Figure 10a). Since $\delta = 30°$ in a hexagonal arrangement, $b' = a'/\sqrt{3}$, and thus $d_{11'} = d_{20'}$, since for a rectangular lattice, Equation (3) is valid.

$$\frac{1}{d_{hkl}^2} = \frac{h^2}{a^2} + \frac{k^2}{b^2} \tag{3}$$

As soon as the lattice deviates from perfect hexagonal symmetry, that is, $\delta \neq 30°$ (Figure 10b), the degeneracy of d_{11} and d_{20} is broken and two separate reflections appear in the small-angle regime.

The indexation of a columnar rectangular mesophase and the determination of the lattice structure (space group) are complex and often not completely unambiguous. As can be seen from the reflection conditions given in Table 2, the clear

Table 2: Reflection conditions of the three space groups of columnar rectangular mesophases.[35]

Space group	Reflection conditions	
P2$_1$/a	hk:	–
	h0:	$h = 2n$[a]
	0k:	$k = 2n$
P2/a	hk:	–
	0k:	$k = 2n$
C2m	hk:	$h + k = 2n$

[a] n is an integer.

discrimination between the different lattice structures requires the observation of a large number of peaks in the X-ray pattern. Since only a quite limited number of reflections are actually observed, in practice an unequivocal determination of the symmetry is questionable. Furthermore, it can be helpful to consider the lattice constants a and b, which can be calculated from Equation (3), in relation to the molecular dimensions obtained, for example, by molecular modeling.

Two-dimensional X-ray patterns of aligned samples can be most helpful to further clarify the symmetry of rectangular phases. The angle in the azimuthal scattering directions of adjacent small-angle reflections deviates from 60° from that expected for a perfect six-fold symmetry (cf. Col$_h$ mesophase). Donnio et al. interpreted the origin of this arrangement of the Bragg spots.[22] Moreover, Billard et al.[36] and Morale et al.[31] give further examples of X-ray analyses of columnar rectangular mesophases.

As a result of the minor differences in the structures, textures known for Col$_h$ phases (Figure 8) can also be observed for Col$_r$ phases. However, broken fan-shaped and mosaic textures are more common for columnar rectangular mesophases than for columnar hexagonal ones.

2.3. The columnar oblique mesophase Col$_{ob}$

Figure 2e shows the arrangement of the columns in a columnar oblique mesophase, in which the tilted columns are represented by elliptic cross sections. The symmetry of this 2D lattice corresponds to the space group P_1. Examples for columnar oblique mesophases are rare because strong core–core interactions are required.

Since P_1 is a primitive planar space group, there are no reflection conditions and therefore all peaks (hk) are allowed. In Table 3, an example from literature is given for the

© 2007 Wiley-VCH Verlag GmbH & Co. KGaA, Weinheim

Table 3: *d* Spacings and lattice parameter for a columnar oblique mesophase Col$_{ob}$ (from [CoCl$_2$(L$_2$)])[31]

d_{obs} [Å][a]	I[b]	hk[c]	d_{calcd} [Å][a]	Lattice parameter
17.8	vs	(20)	17.8	$a = 35.7$ Å
16.75	vs	(11)	16.75	$b = 18.4$ Å
15.9	vs	(11)	15.9	$\gamma = 86.4°$
10.2	s	(31)	10.3	
9.65	m	(31)	9.7	
7.55	m	(32)	7.5	
7.3	w	(51)	7.1	

L = 2,6-Bis[3′,4′,5′,-tri(octyloxy)phenyliminomethyl]pyridine. [a] d_{obs} and d_{calcd} denote the observed and calculated diffraction spacings; [b] intensity of the diffraction signal (vs: very strong, s: strong, m: medium, w: weak); [c] indexation in the 2D oblique lattice.

reflections actually observed for a Col$_{ob}$ mesophase. Beside fan-shaped textures,[37] spiral textures are characteristic for Col$_{ob}$ phases.[27,31]

2.4. The discotic nematic mesophase N$_D$

In a discotic nematic mesophase, the flat molecules possess full translational and rotational freedom around their short axis, whereas their long axes (spanning the plan of the discotic mesogen) orient, on average, parallel to a general plane (Figure 11 b). Nematic phases are fluid,
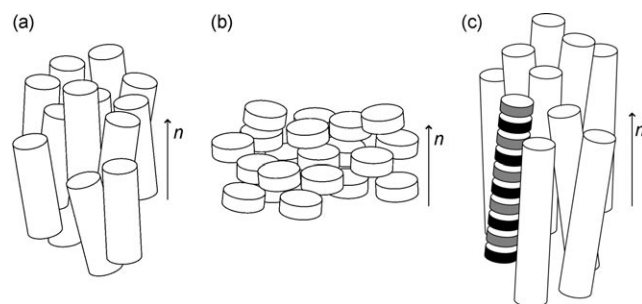

Figure 11. Different types of nematic phases: a) nematic phase N of calamitic mesogens, b) discotic nematic phase N$_D$, and c) columnar nematic mesophase N$_C$ induced by the charge-transfer interactions between a disk-shaped donor (black) and an electron acceptor (gray). The respective building blocks of the phase (disk-shaped molecules or columns) are long-range orientationally ordered with no longe-range translational order, so that all phases have the same symmetry.

whereas the Col$_h$, Col$_r$, and Col$_{ob}$ liquid-crystalline phases normally have a rather waxy consistency. N$_D$ mesophases typically show the Schlieren texture,[38] similar to that of a nematic phase of calamitic molecules. However, the discotic nematic phase is optically negative, which clearly contrasts with the optically positive nematic phase of calamitic liquid crystals (see also Section 3.2.).

The diffraction profile of a N$_D$ phase resembles that of an isotropic phase (cf. Figure 4c). The wide-angle diffraction peak is related to the lateral distance between the cores, while the small-angle diffraction peak is attributed to the diameter of the core.

When the molecules are chiral[39] or a chiral dopant is added,[40] the resulting chiral nematic mesophase, called the cholesteric phase N$_D$*, shows a modulated structure—a twisted nematic phase, which is illustrated in Figure 12. The director **n** is continuously twisted along the *z* axis with the pitch *P* of the helical structure, which is equal to one complete turn of the local director by 2π.
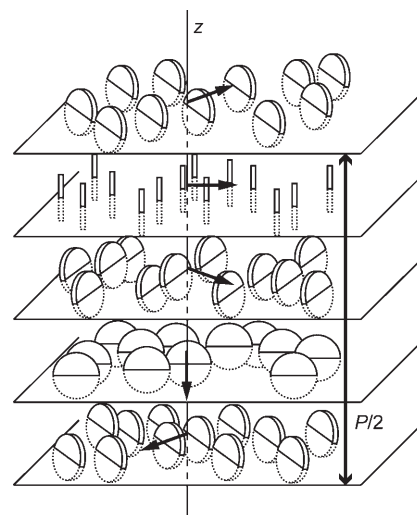
Figure 12. The cholesteric mesophase N$_D$*: the director **n** is periodic along the helix axis *z* with the pitch *P* of the helical structure, equal to a turn of the local director by 2π. Reproduced from Ref. [40].

Similar to the textures of cholesteric phases of calamitic molecules, oily streaks, fingerprint, and polygonal textures[40] can be observed for N$_D$* phases.

2.5. The columnar nematic mesophase N$_C$

When the electron donor, for example, alkynylbenzene **7d** is doped with an electron acceptor, for example, 2,4,7-trinitrofluorenone (TNF) (Scheme 3, Scheme 4),[15,41] ordered columns are formed as a result of the charge-transfer interaction. If the difference between the different lengths of the side chains is large enough, the arrangement of the columns in a 2D lattice (for example, hexagonal or rectangular) is disturbed. Therefore, the columns show only orientational order to each other and form a columnar nematic mesophase N$_C$ (Figure 11c). The columns can be regarded as building blocks of the N$_C$ phase instead of single molecules (as in the nematic phases of calamitic mesogens). Since all these nematic phases (N, N$_D$, N$_C$) have the same symmetry, the similar characteristic textures are observed. As a result, the N$_C$ mesophase shows Schlieren textures,[15,42] which, because of the formation of charge-transfer complexes, exhibit deep colors.

An X-ray pattern of a columnar nematic phase (Figure 13)[15] shows relative sharp reflections in the wide-angle regime that correspond to the regular stacking of the donor and acceptor molecules on top of each other. The
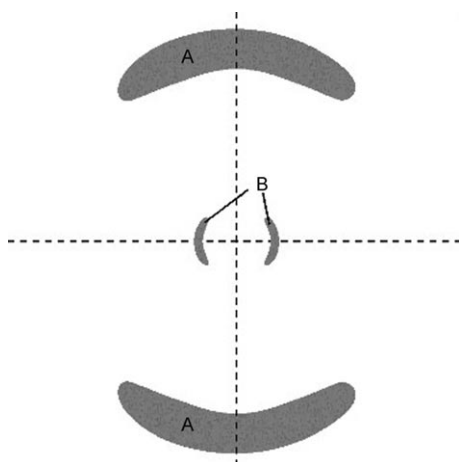
Figure 13. X-ray pattern of a columnar nematic mesophase: A) relatively sharp reflection in the wide-angle regime caused by the long-range intracolumnar ordering, B) diffuse reflections attributable to the liquidlike arrangement of the columns.

reflections in the small-angle regime are rather diffuse and broadly related to the liquidlike arrangement of the columns.

In a 2D diffraction pattern of an aligned N_C sample, the small-angle reflections are normal to the reflections in the wide-angle regime. Therefore the columns are orientated more or less parallel and have only short-range positional order, which is characteristic for a nematic mesophase.

2.6. The lamellar mesophase D_L

As the word "lamellar" implies, in a D_L mesophase the molecules are arranged in layers similar to calamitic mesogens in smectic phases.[43] Also, the textures of the lamellar mesophase are similar to the textures of calamitic smectic phases. Typically, broken fanlike textures with large domains (Figure 14) can be observed for D_L phases.

The structure of the lamellar mesophase has not yet been completely clarified. A suggestion by Sakashita et al.[44] is shown in Figure 15.
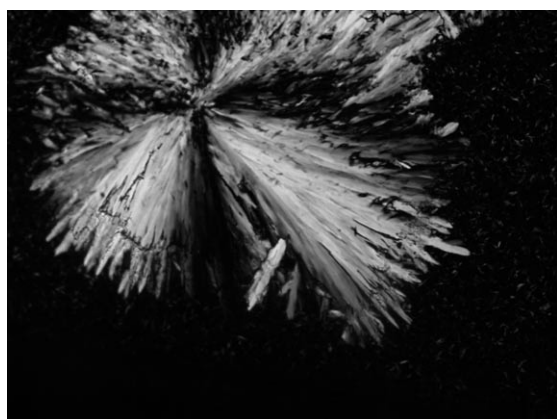

Figure 14. Broken fanlike texture of a lamellar mesophase of tetraphenylene **77e**.
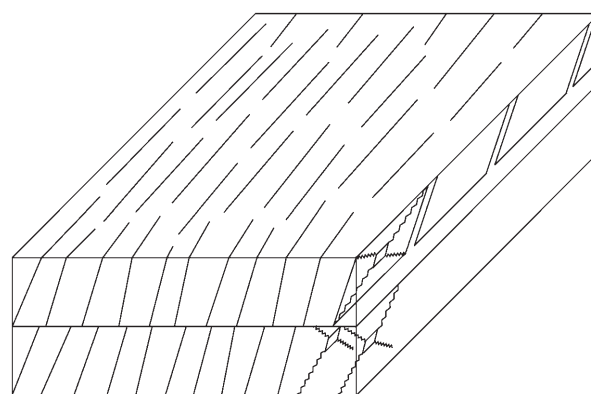
Figure 15. Structure of the lamellar D_L phase proposed by Sakashita et al. Reproduced from Ref. [44].

In a 2D diffraction pattern of an orientated sample, Sakashita et al. observed only one diffraction maximum and its corresponding higher order peaks in the equatorial direction; Figure 16 shows this behavior for the crown ether
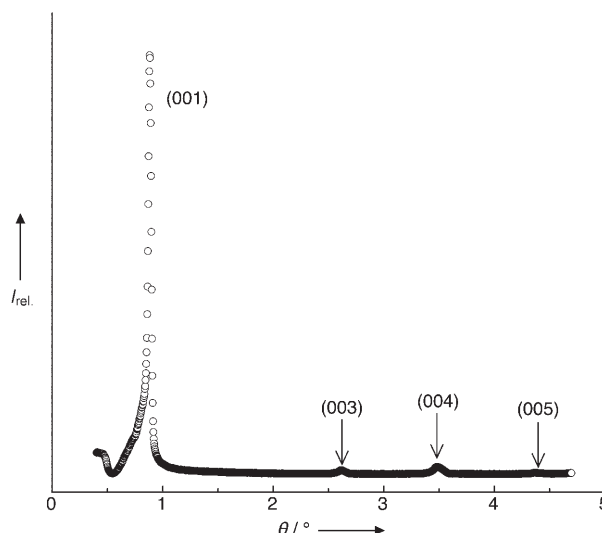
Figure 16. X-ray scattering profile of a lamellar (smectic) mesophase of the *ortho*-terphenyl crown ether **150c**. Only one diffraction maximum and its corresponding higher order peaks are observed, related to pure 1D translational order. Example taken from Ref. [45].

150c.[45] This observation indicates a layer structure, whereby the interlayer spacing is comparable to the molecule length. However, the diffraction pattern exhibits fine peaks along the vertical direction that suggests that there is also some (layer) structure normal to the first named layers. The lines that connect the points of the highest intensity of the peaks, which lie along the horizontal and the vertical direction, do not cross each other perpendicularly. Therefore, it was deduced that the molecular plane is tilted against the layer normal by about 5° (Figure 15). Furthermore, no columnar structure in a D_L mesophase was observed, and the molecules possess a liquidlike order in the layers. Thus the structure of the

© 2007 Wiley-VCH Verlag GmbH & Co. KGaA, Weinheim

lamellar mesophase deduced by Sakashita et al. is very similar to that of a SmC phase of calamitic mesogens.

Méry et al. presented a further lamello-columnar mesophase, in which the molecules of [1]benzothieno[3,2-*b*] [1]benzothiophene-2,7-dicarboxylate were proposed to assemble in microcolumns made of alternatively crossed molecules within the smectic layers.[46]

3. Physical properties of columnar mesogens

3.1. Electrical conductivity

As a result of the assembly of discotic aromatic mesogens into columnar stacks with typical intercore distances of about 3.5 Å, an overlap of the π*–π* LUMOs (lowest-unoccupied molecular orbitals) should be possible, which would lead to a conduction band for charge transport along the column axis (Figure 17).
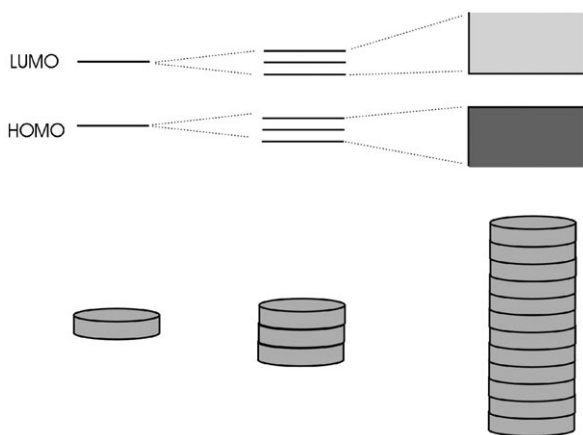

Figure 17. Electronic band formation from a single molecule (left) to the column (right).

The columns would form molecular wires with conductive channels surrounded by insulating peripheral chains,[47] so that the columnar liquid crystal may display photoconductivity. Model systems for conductivity studies were based on triphenylene derivatives, which do not usually possess intrinsic charges.[48] To investigate the charge transport along the columns, charges were created by doping or through photogeneration. Vaughan et al.[49] doped **44b** with iodine, which increased the conductivity by several orders of magnitude. Boden et al. used **35b** with AlCl₃,[50,51] which transformed the insulating **35b** into a p-doped semiconductor, in which the conduction along the columns was three orders of magnitude greater than in the perpendicular direction. This result clearly indicates the high anisotropy of conduction in the columnar phase and the columnar phase can be considered a practical one-dimensional conductor along the columnar axis.

For studying charge transport in discotic liquid crystals, the time-of-flight (TOF) technique, which relies on charge photogeneration, is most widely used. Charges are generated by light irradiation of discotic films in a typical sandwich-cell

configuration (Figure 18). A light pulse with a defined wavelength and a short duration is sent, so that the absorption and the following charge generation occurs in a very thin layer at only the first interface. An electric field is applied to induce
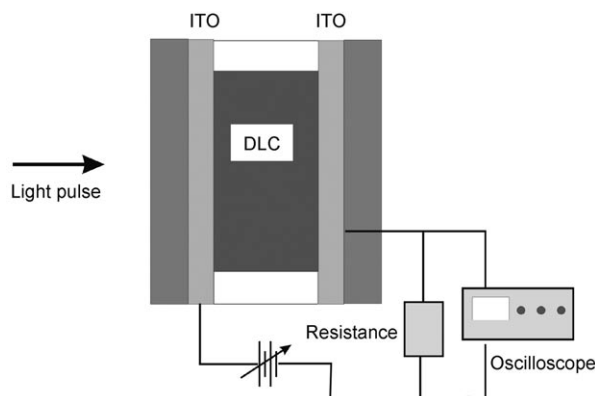
Figure 18. Setup of the TOF experiments.

a drift of the charges. Depending on the polarity of the applied field, holes or electrons will move across the sample, thus inducing a transient current, which is recorded in an external circuit, and allowing the deduction of the type of charge carriers involved. The time that these charges take to travel between the electrodes allows the mobility μ to be estimated. In fact, μ depends on the applied voltage V and transit time t_t according to Equation (4), where v is the drift velocity, d is the film thickness, and E is the applied electric field.

$$\mu = \frac{v}{E} = \frac{d^2}{Vt_t} \tag{4}$$

The disadvantage of the TOF method is that monodomains with the columns aligned perpendicular to the electrodes (homeotropic alignment) are required. Any defect in the path has a strong effect on the mobility, so the values can underestimate the true transport potential of the material. Discotics that do not align accordingly might be impossible to investigate with the TOF method.

Transport in triphenylenes was modeled by Haarer and co-workers.[52] Despite the remarkable results in terms of mobility because of the high degree of order in the columns, the transport seems not to be described by a bandlike model but rather by a hopping process, in which the charges stay in one site until they jump to the next. A 1D hopping model was used that was based on a Gaussian distribution in the energy levels involved in the conduction (for example, the HOMOs, the highest-occupied molecular orbitals) and dependent on the disorder and on a "jump rate" between adjacent sites. This rate is a function of the hopping distance (taken as the intermolecular distance) and temperature. By using a Monte Carlo simulation, the photocurrent was predicted, and from this the mobility was deduced. The dependence of the electric conductivity on the field and the temperature were derived from this model, and this dependence agrees with the

measured temperature dependence of the mobility in the triphenylene dimer **46b** in its glassy phase (Scheme 18). For higher temperatures, however, other factors, such as the variation of the order parameter with the temperature and thermal activation effects, should be taken into account in the model.

When samples cannot be properly aligned, the pulse-radiolysis time-resolved microwave conductivity technique (PR-TRMC) has been used.[53] A schematic illustration of the PR-TRMC technique (Figure 19) indicates the two main stages of creation of the charges and detection of the conductivity.
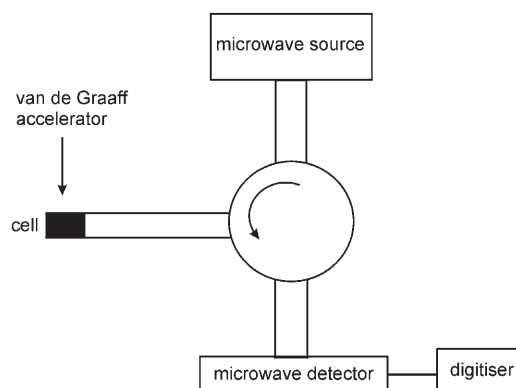
Figure 19. Simplified setup of the PR-TRMC experiments, reproduced from Ref. [53].

Charges are uniformly created in the whole sample by irradiation by a high-energy electron pulse from a Van de Graaff accelerator. The detection mechanism is based on the use of microwaves sent to the sample that propagate through the sample and at the opposite side, reflect back. The observed change in power of the reflected microwaves is connected to the induced change in conductivity in the material. This change is in turn related to the charge mobility μ_i and the induced charge-carrier concentration N_i in the sample [Eq. (5)].

$$\Delta\sigma(t) = e \sum [N_i(t)\mu_i] \qquad (5)$$

Van de Craats et al.[54] compared TOF and PR-TRMC techniques investigating the conductivity of **47b** as function of temperature. The times of the process with PR-TRMC are in the nanosecond range, which allows the monitoring of the conduction in stacks of a few molecules even if it is not possible to distinguish the sign of the charge carriers. Moreover, PR-TRMC is advantageous because no electrodes are needed, the samples do not require uniform alignment (as already mentioned), and, unlike TOF, it is possible to obtain mobility values even in the crystalline state.

The effect of the type and size of the core is investigated by PR-TRMC with a comparative study of the mobility of five families differing in the core (triphenylene, porphyrin, azocarboxyldiimidoperylene, phthalocyanine, hexa-*peri*-hexabenzocoronene; Scheme 1 and 22).[55] Data of derivatives

with various peripherally substituted alkyl chains for each family were presented. The peripheral chains influence the phase-transition temperatures from crystalline to liquid crystal as well as from liquid crystal to isotropic. For phthalocyanine and triphenylene, the chains have very little influence on the mobility in the mesophase. In contrast, the element that connects the core to the chains plays an important role. If oxygen is used as the linking atom, a mobility lower than with direct coupling (for example, through a methylene moiety) or through a sulfur atom results. This decrease in conductivity is attributed to the fact that the oxygen atom is less bulky and thus allows higher mobility, which in turn gives higher intracolumnar disorder, detrimental for charge transport. As a general finding, the bigger the core size, the higher the mobility—probably due to better π-orbital overlap and/or higher intermolecular forces that increase the columnar stability. For all the compounds studied, the highest mobility values were measured in the crystalline phase,[54] but this phase is not attractive because of the formation of domains with subsequent creation of charge traps at the domain boundaries. In contrast, liquid-crystalline phases avoid this limitation through the formation of columns and possessing the unique feature of self-annealing of defects. The values measured with the PR-TRMC technique can be useful to optimize the desired molecular structure, and to determine which structure gives the highest mobility within few molecular stacks. In macroscopic samples measuring with DC fields, these values could be expected only in case of a well ordered monodomain. Notably, while molecules with big cores have higher stability and conductivity, they are often more difficult to process, which can be cumbersome for applications where macroscopically aligned films are needed (see Section 5 for applications).[56]

A quantum-chemical approach was used to correlate structure with properties,[57] considering four molecular structures (triphenylene, hexaazatriphenylene, hexaazatri-naphthylene and hexabenzocoronene; Scheme 1 and 37). The proposed model is based on a hopping mechanism, which describes the rate of charge hopping from one site to the nearest in terms of the molecular reorganization energy and of the intermolecular transfer integral. On studying the reorganization energy, first its reduction was found when the size of the core was increased. Second, while alkylthio chains only slightly affect the energy, the alkoxy chains decrease the energy, thus adversely affecting the charge transport. Another indicator of the efficiency of transport is the intermolecular transfer integral that is related to the electronic coupling between molecules. The impact of the possible movements that occurred, such as molecular rotation, variation of the intermolecular distance, and translations were evaluated. Although small variations of distance do not have a great effect, rotations do have an effect, independent of the core size, with the complication that the change as a function of the angle is not really predictable. This makes it impossible to estimate the effect of rotation from just the molecular structure. However, in case of bigger molecules, the effect of translational movements is smaller. The theory predicted that transport occurs predominantly by holes, in agreement with the common experimental finding. On the

other hand, for hexaazatrinaphthylene derivatives, a substantial electron transport as well as a charge-carrier mobility of an order of magnitude higher than in triphenylene was predicted.

3.2. Optical properties

Liquid crystals (LCs) are optically anisotropic media whose properties, as the name suggests, depend on the direction in the medium. The optical properties of a material can be visualized using a geometrical representation of the dielectric tensor, known as the index ellipsoid. The intercepts of the ellipsoid surface with its three principal axes give the principal refractive indices of the medium. If the system is isotropic, that is, the properties are independent of direction, the index ellipsoid becomes a sphere. The most common liquid-crystalline phases have one optic axis (they are optically uniaxial), with two principal refractive indices n_o and n_e (the ordinary and the extraordinary refractive index, respectively). The index ellipsoid in this case is an ellipsoid of revolution. Moreover, liquid crystals are most often uniaxial positive, which indicates that the value of n_o (the refractive index of the light propagating along the optic axis) is lower than that of n_e (the refractive index of the light propagating perpendicular, but with polarization parallel, to the optic axis). Many discotic LC phases, like the nematic and the columnar phases, are optically uniaxial, but with negative anisotropy, that is, $n_o > n_e$, which makes the index ellipsoid oblate (Figure 20). This property has been fundamental for the application of discotic films as optical compensators for LC displays (see section 5). The magnitude of the optical anisotropy $\Delta n = n_\parallel - n_\perp$ is generally lower for discotics than calamitics. Experimental values are scarce, but some reports give values in the range of -0.08 to -0.04.[58]
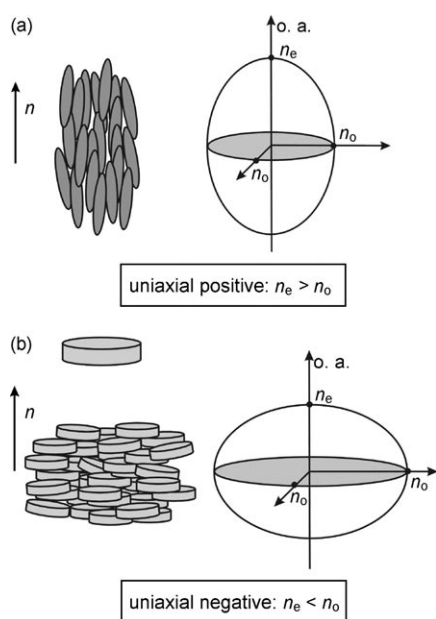
Figure 20. Index ellipsoids for uniaxial positive (a) and negative (b) liquid crystals.

4. Classes of compounds used for columnar liquid crystals

As molecular shape is an important factor in determining whether certain molecules will self-assemble into liquid-crystalline phases, molecules may be usefully classified according to their shape as calamitic or columnar (discotic) mesogens, as long as no additional interactions (such as hydrogen bonds or tethering into dimers, oligomers, or dendrimers) are present.[59] Most columnar LCs typically consist of a rigid central core (planar, pyramidal, conical, or a similar geometry; Scheme 1), surrounded by several flexible groups.[60]
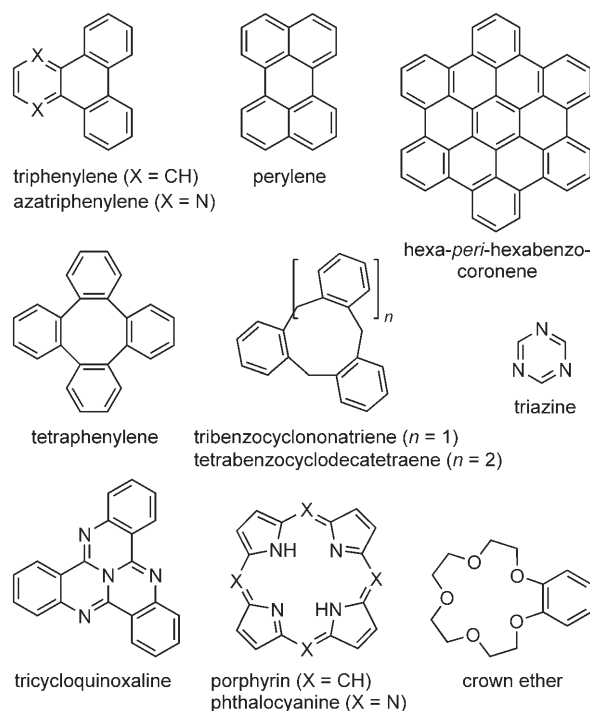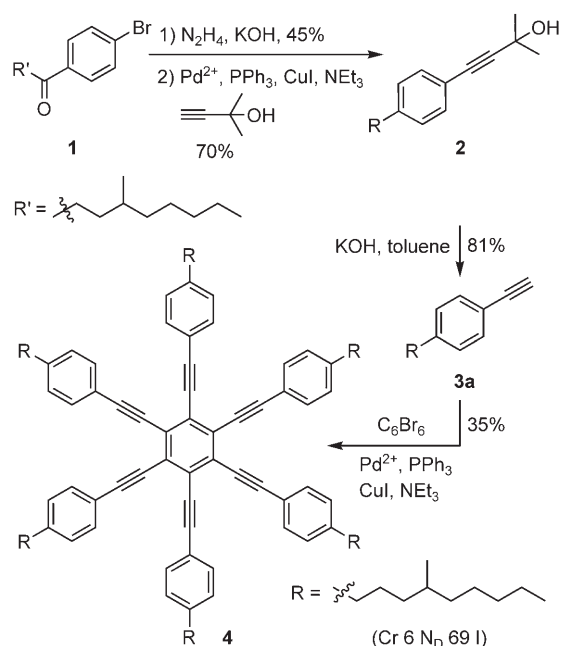

Scheme 1. Some selected core units for columnar liquid crystals.

4.1. Benzene derivatives

Since the seminal findings by Chandrasekhar et al. that hexaesters of benzene display columnar mesophases,[3] mesogenic benzene derivatives have been developed into different areas. The most common columnar benzene derivatives are hexa- and 1,3,5-trisubstituted benzenes.

In an attempt to overcome the problem of the viewing angle for twisted and supertwisted nematic LC displays, Kumar et al. prepared the hexaalkynylbenzene derivative **4**[61] from the 4-bromophenyl ketone **1** by Wolff–Kishner reduction and subsequent Pd-catalyzed coupling with 1,1-dimethylpropargylic alcohol to give the alkynol **2**, which underwent base-induced fragmentation to the phenylacetylene derivative **3a**. Sonogashira coupling of **3a** with hexabromobenzene finally yielded hexakis[4-(4-methylnonanyl)phenylethynyl]benzene (**4**), which indeed displayed the desired nematic discotic phase at ambient temperature (Scheme 2).[62]

Angew. Chem. Int. Ed. **2007**, *46*, 4832–4887

© 2007 Wiley-VCH Verlag GmbH & Co. KGaA, Weinheim

www.angewandte.org **4843**

Scheme 2.

When the symmetry of such compounds is reduced by replacing one alkynyl substituent with an ether moiety, systems such as **7** were obtained, which display both nematic discotic and hexagonal columnar mesophases depending on the side chain (Scheme 3).[63]

While alkyl- and alkoxy-substituted derivatives **7a** and **7b** form nematic discotic phases, a hexagonal columnar disordered mesophase was found for the thioether **7c**. The
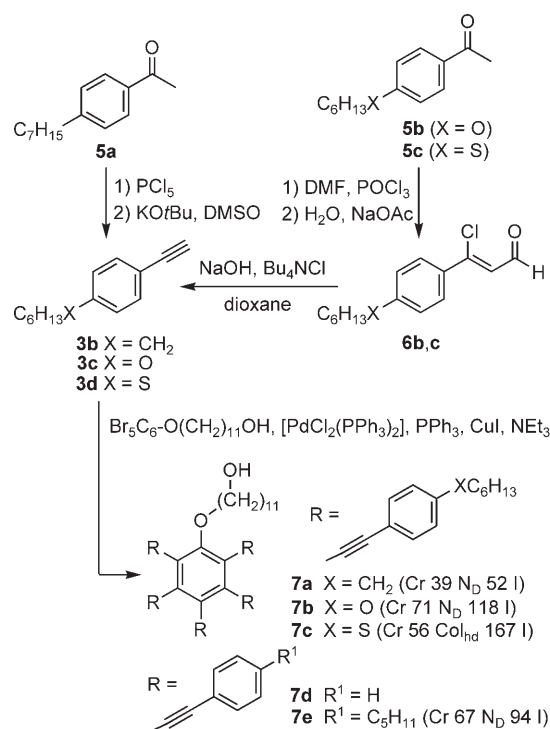
Scheme 3.

terminal hydroxy group in pentaalkynylbenzenes **7a–c** allows further tethering to a polyacrylate backbone.[63] Picken and co-workers also studied the change of the mesophase behavior of pentaalkynylbenzenes **7** by charge-transfer interactions. When **7b** was doped with the electron acceptor TNF (Scheme 4) a nematic discotic phase was still produced, while the corresponding 1:1 complex of **7b** and 2,4,7-trinitrofluoren-9-ylidenemalonitrile (TNF-DCM) formed columnar plastic (Col$_p$),[64] hexagonal columnar and nematic discotic phases.
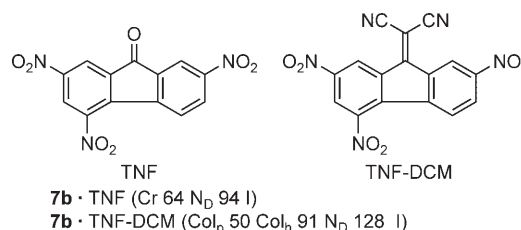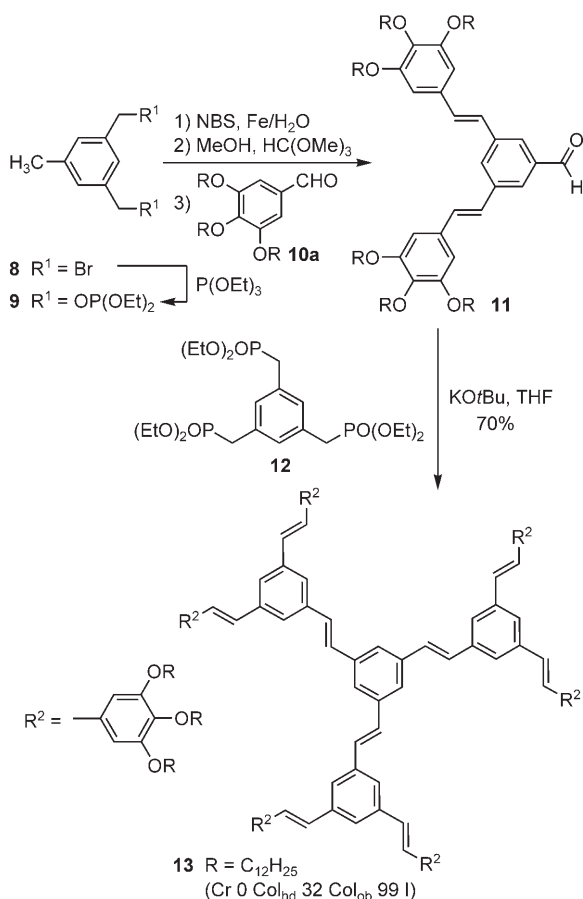

Scheme 4.

Ichimura and co-workers have successfully applied photo-patterned discotic LC films of pentakis(arylethynyl)benzene **7e** to elucidate orientational behavior (Scheme 3). Polarized photoluminescence measurements of these systems provided information on the aggregation and spatial orientation at a microscopic level.[65] System **7e** also represents a building block for the formation of star-shaped dendrimers as shown by Janietz and co-workers.[66]

Stilbenoid compounds play an increasingly prominent role in materials science and are already used as optical brighteners and laser dyes. These compounds might be potentially interesting for light-emitting diodes, photoresists, photoconductive devices, imaging and optical switching techniques, and nonlinear optics (NLO).[67] However, a major limitation with respect to their application is their decomposition by [2+2] photocycloaddition and photopolymerization reactions. To circumvent this problem, Meier, Lehmann, and co-workers investigated a series of stilbenoid dendrimers such as **13** (Scheme 5).[68] The convergent synthesis used the triphosphonate **12** as the core and dendron **11** that were finally linked together through a threefold Wittig–Horner olefination to give the all-*E*-configured second-generation dendrimer **13**. This synthetic strategy also gave access to higher generation stilbenoid dendrimers. Compound **13** displayed a hexagonal columnar mesophase at ambient temperature and a columnar oblique phase at elevated temperatures. By using temperature-dependent ^{2}H NMR studies of selectively deuterated dendrimers such as **13**, Lehmann et al. found that molecular motion is a necessary condition for photooligomerization. Thus, the suppression of molecular motion is a prerequisite for a successful application of these materials.[68d]

Several groups have explored the structural motif of D_{3h}-symmetrical star-shaped columnar liquid crystals based on either trimesic acid or phloroglucinol. For example, Chang et al. synthesized compound **17** to stabilize columnar structures in a polymer network through 1,4-photopolymerization of
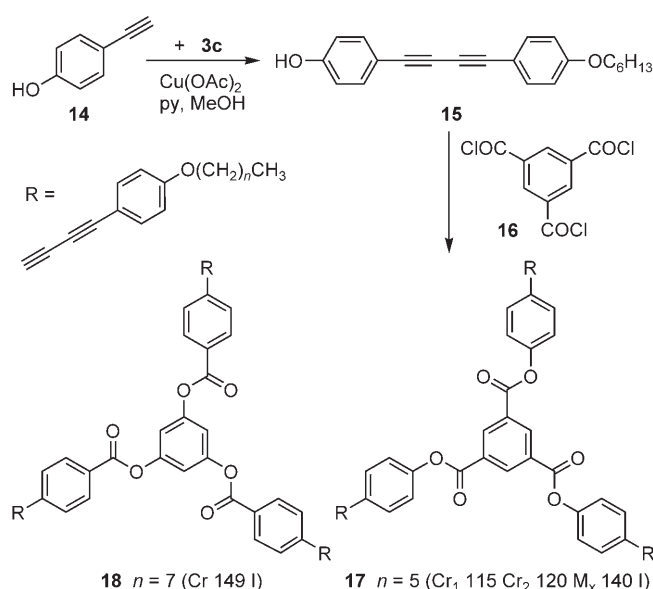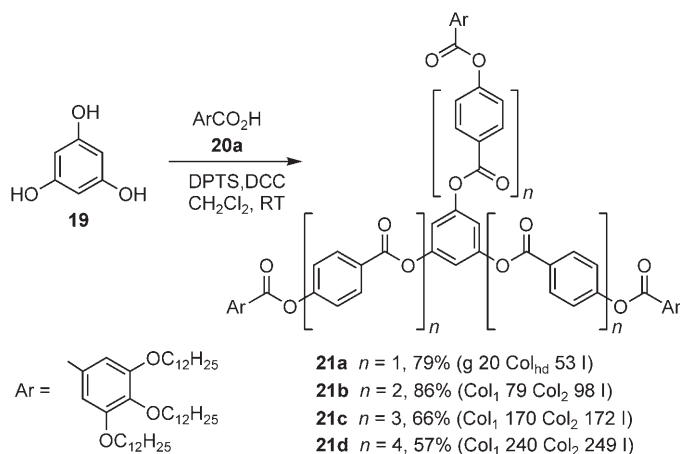
Scheme 5. NBS = N-bromosuccinimide.

Scheme 6. M_x denotes an unknown mesophase. py = pyridine.

21a $n = 1$, 79% (g 20 Col$_{hd}$ 53 I)
21b $n = 2$, 86% (Col$_1$ 79 Col$_2$ 98 I)
21c $n = 3$, 66% (Col$_1$ 170 Col$_2$ 172 I)
21d $n = 4$, 57% (Col$_1$ 240 Col$_2$ 249 I)

Scheme 7. DPTS = 4-(dimethylamino)pyridinium 4-toluenesulfonate, DCC = N,N'-dicyclohexylcarbodiimide.

diacetylenes. 4-hydroxyphenylacetylene (**14**) and 1-ethynyl-4-(hexyloxy)benzene (**3c**) were coupled using Cu(OAc)$_2$ to yield the diacetylene precursor **15**, which was treated with benzenetricarbonyl trichloride **16** to give the benzene tricarboxylates **17** with pendant diacetylenic groups (Scheme 6).[69] The phloroglucinol analogue **18**, however, was nonmesogenic in contrast to **17**.

Lehmann et al. prepared phloroglucinol-derived mesogens **21** as nonconventional columnar liquid crystals which possess an E-shaped conformation (in the columnar mesophase) rather than a star-shaped conformation to avoid empty space in the columnar mesophase (Scheme 7).[70] The monotropic columnar mesophase of star-shaped mesogen **21a** can serve as a template for crystal growth.[71] Real-time AFM measurements revealed that mesophase-assisted crystallization can be viewed as 1D growth, whereby the growing crystalline phase preserves the orientation of the "parent" mesophase. Crystal growth occurs along the tracks of the columnar axes. This control of the crystal structure by the mesophase template should allow for the tailoring of crystalline morphologies at the scale of individual columnar diameters.

The existence of both thermotropic and lyotropic mesomorphism in disk-shaped compounds is rather unusual. However, the latter can be stabilized by hydrogen bonds as
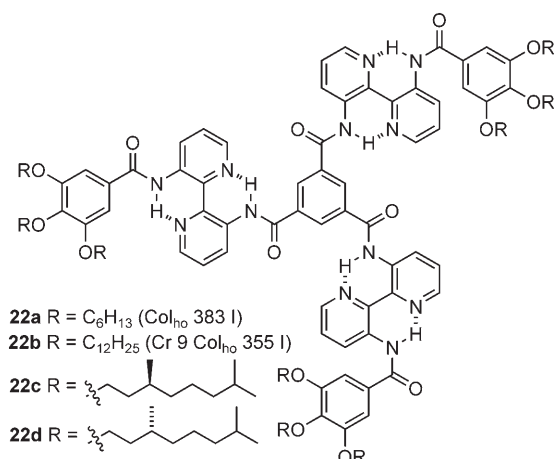
was shown by Meijer and co-workers for **22a**, which was based on 3,3'-di(acylamino)-2,2'-bipyridine (Scheme 8).[72,73]

Between glass plates, the lyotropic solutions adopt a uniaxial, planar orientation. In an electric field, the columns can be switched to a homeotropic alignment, and such voltage-induced formation of large monodomains might be useful for 1D charge transport of ions.[72] The corresponding chiral derivatives **22c** and **22d** with dihydrocitronellol side chains self-assemble into a dynamic chiral helix in apolar solvents (Figure 21).[74] By detailed CD spectroscopy, Meijer and co-workers were able to demonstrate the "majority-rules" effect: a slight excess of one enantiomer leads to a strong bias toward the helical sense, preferred by the major enantiomer, in such a noncovalently bound aggregate. Comparison of the experimental data with the calculation yields a mismatch penalty, that is, the free-energy penalty on a monomer present in a helix of its nonpreferred screw sense

22a R = C$_6$H$_{13}$ (Col$_{ho}$ 383 l)
22b R = C$_{12}$H$_{25}$ (Cr 9 Col$_{ho}$ 355 l)
22c R =
22d R =

Scheme 8.

1) H$_2$SO$_4$
2) HNO$_3$, H$_2$SO$_4$ → **19** X = H
23 X = NO$_2$
20b R = C$_{10}$H$_{21}$

R^1 =

NEt$_3$, THF

24 (Cr 47 Col$_h$ 94 l)   **25** (Cr −11 Col$_h$ 54 l)

Scheme 9.
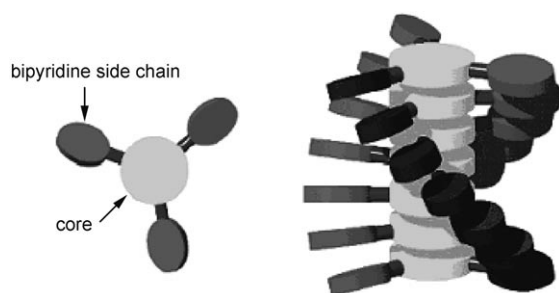
Figure 21. The helical orientation of the amides **22 c,d**. Reproduced from Ref. [74].

Figure 22. The stacking of **25** in the Col$_h$ mesophase.[75]
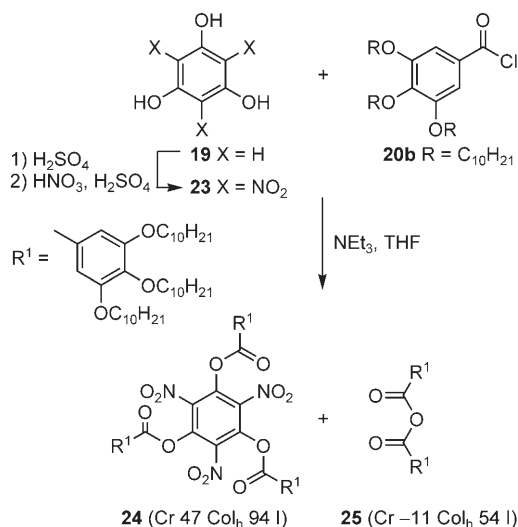
(0.94 KJ mol^{-1}), which is almost a factor of eight lower than the penalty on a helix reversal (7.8 KJ mol^{-1}).

Second-order materials with NLO effects are required for high-performance electrooptic modulators, frequency doublers, and holographic memories. One approach towards NLO properties uses octopolar systems with a D_{3h} symmetry such as 1,3,5-trihydroxy-2,4,6-trinitrobenzene (**23**), which was synthesized by the nitration of phloroglycinol (**19**; Scheme 9).[75]
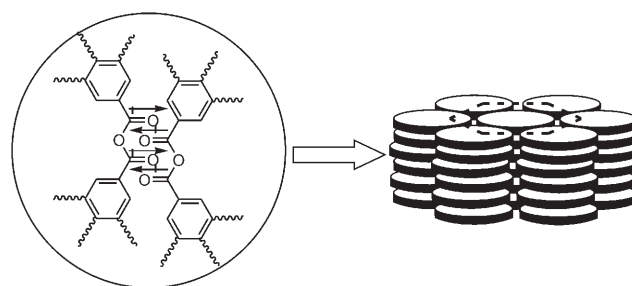
Compound **23** was esterified with the gallic acid chloride **20b** to give **24** and the anhydride **25** as a byproduct. Surprisingly, **25** was also found to be mesomorphic and its Col$_h$ mesophase might be explained as shown in Figure 22.

The observed second-order polarizability β_{333} of **24** was similar to the value observed for the parent system **23**, which demonstrates that it can be combined with mesogenic side chains without any loss of NLO activity.

Organic molecules for polyelectrochromic materials and multielectron redox catalysts should exhibit multiple-electron transfer and significant absorption in the visible range. In this respect, the use of azulenes as redox-active chromophores is interesting because their electrochemical reduction is strongly facilitated by the formation of the cyclopentadienide subunit. Ito et al. recently reported hexakis(6-octyl-2-azulenyl)benzene (**31**) that displays a complex polymorphism with several hexagonal columnar mesophases (Scheme 10).[76]
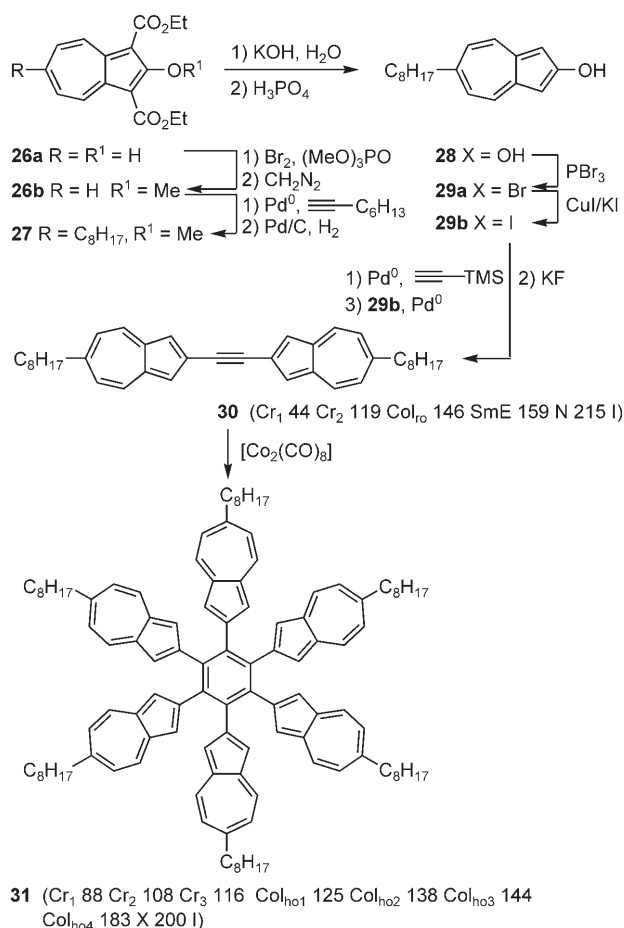
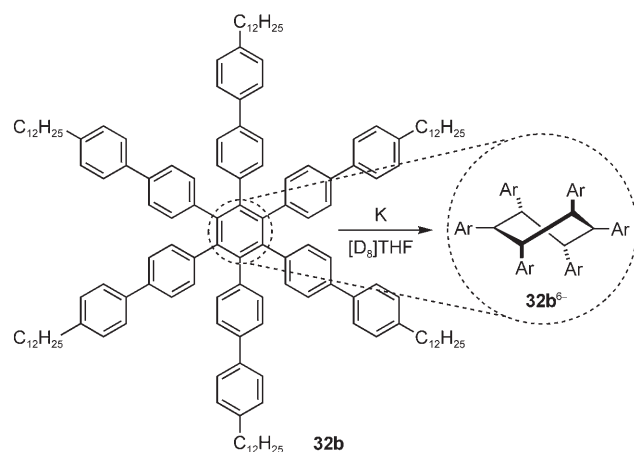The synthetic sequence to **31** consists of the bromination of azulene diester **26 a**, followed by Sonogashira coupling with 1-octyne, and subsequent catalytic hydrogenation of the C≡C bond to give **27**. Saponification and decarboxylation yielded **28**, which was converted with PBr$_3$ into 2-bromo-6-octylazu-lene (**29 a**). Sonogashira coupling with trimethylsilylacetylene, deprotection, and Sonogashira coupling with 2-iodo-6-oct-ylazulene (**29 b**) afforded bis(6-octyl-2-azulenyl)acetylene (**30**), which displays a rectangular ordered columnar meso-phase along with a smectic E (SmE)[77] and a nematic mesophase, despite its linear shape. Compound **30** was converted into the desired hexasubstituted benzene deriva-tive **31** by a [2+2+2] cycloaddition induced by [Co$_2$(CO)$_8$]. A reversible reduction wave at −2.01 V for the product indicated a one-step multiple-electron transfer to produce an anionic species **31**$^{6-}$.[76b]

It should be mentioned that Rabinovitz and co-workers determined by variable-temperature NMR a remarkable distortion of symmetry on reduction of hexa(4-dodecylbiphe-nylyl)benzene (**32 b**) with alkali metals, which led to a twisted conformation of the central benzene ring in the hexaanion **32 b**$^{6-}$ (Scheme 11).[78] The activation enthalpies for pseudo-rotation of the twist form and the phenylene rotation were 16.3 kcal mol^{-1} and 8.1 kcal mol^{-1}, respectively.

31 (Cr$_1$ 88 Cr$_2$ 108 Cr$_3$ 116 Col$_{ho1}$ 125 Col$_{ho2}$ 138 Col$_{ho3}$ 144 Col$_{ho4}$ 183 X 200 I)
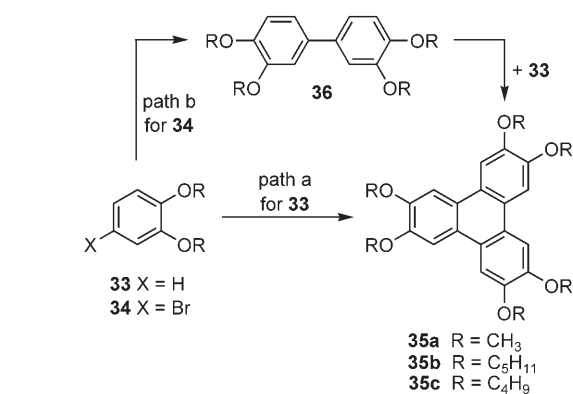
Scheme 10.
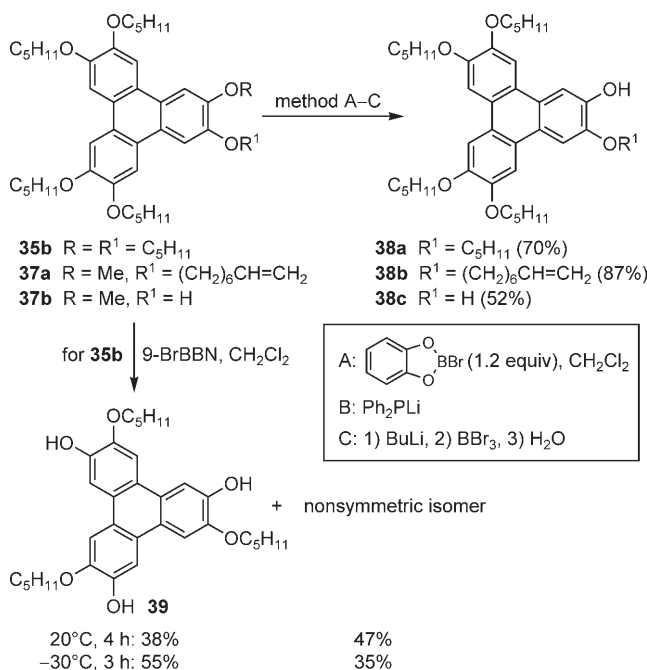

Scheme 11.

4.2. Triphenylene derivatives

Triphenylenes are one of the most extensively investigated classes of columnar liquid crystals.[60a,79,80] The "working horse" of LC chemists are symmetrical hexakis-(alkyloxy)triphenylenes **35**, which were obtained either by oxidative trimerization of 1,2-dialkoxybenzene **33**[81–86] (Scheme 12, Path a) or alternatively by the "biphenyl

Scheme 12. Preparation of triphenylenes **35**.

route", that is, by oxidative cocyclization of dialkoxybenzene **33** and tetraalkoxybiphenyl **36** with FeCl$_3$ in CH$_2$Cl$_2$ (Path b).[87] The latter route was conveniently available by the base-induced biaryl coupling of the bromide **34** as was shown by the research group of Laschat.[88,89]

While HBr/HOAc completely demethylated hexakis-(methoxy)triphenylene **35a** to the corresponding hexahy-droxytriphenylene, which can be further modified by alkyla-tion or arylation,[90] procedures were developed to obtain selectively mono-, di-, or trihydroxytriphenylenes for subse-quent functionalization (Scheme 13).

Seminal contributions came from Ringsdorf and co-workers,[91a] who reported the demethylation of triphenylene **37a** with Ph$_2$PLi to give the monohydroxy derivative **38b**, while the 2,3-dihydroxy-functionalized triphenylene **38c** is accessible from **37b** by cleavage of the methoxy group with BBr$_3$ by means of intramolecular assistance.[91a] Treatment of hexakis(pentyloxy)triphenylene **35b** with the hindered Lewis
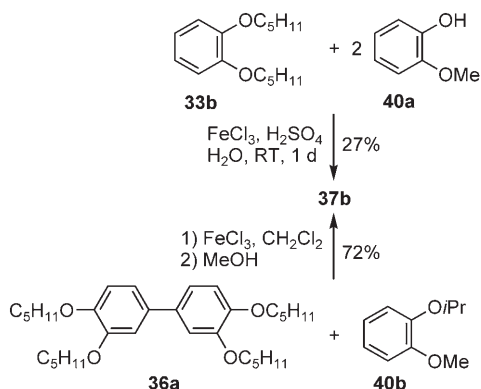

Scheme 13. 9-BrBBN = 9-bromo-9-borabicyclo[3.3.1]nonane.

acid 9-bromo-BBN gave a mixture of the C_3-symmetric trihydroxytripentyloxytriphenylene **39** and its nonsymmetric counterpart. The product ratio was reverted in favor of the C_3-symmetric derivative **39** by simply lowering the reaction temperature to $-30\,°C.$[92] Kumar and Manickam further improved the yield of **39** by using 3.6 equivalents of the highly selective *B*-bromocatecholborane in $CH_2Cl_2.$[93] Only 1.2 equivalents of *B*-bromocatecholborane were needed to selectively cleave one pentyl group in **35b** to give monohydroxytriphenylene **38a** in good yield. Reacting compound **35b** with BBr_3 also leads to selective removal of one pentyl group.[91b]
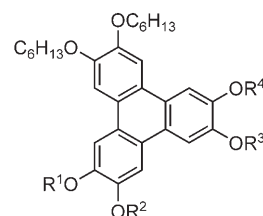
Monohydroxytriphenylenes such as **37b** are available by direct $FeCl_3$-mediated cocyclization of guaiacol (**40a**) and dipentyloxybenzene (**33b**) in a ratio of 2:1[89] or alternatively by the method reported by Bushby and Lu,[94] which involved aryl oxidative coupling of isopropoxyguaiacol **40b** and the biphenyl **36a** with $FeCl_3$ followed by MeOH quenching (Scheme 14).[95]

35d $R^1=R^2=R^3=R^4=C_6H_{13}$ (Cr 68 Col$_h$ 97 I)
41a $R^1=R^2=R^3=C_6H_{13}$, $R^4=C_8H_{17}$ (Cr 55 Col$_h$ 91 I)
41b $R^1=R^2=R^3=C_6H_{13}$, $R^4=C_{10}H_{21}$ (Cr 45 Col$_h$ 72 I)
41c $R^1=R^2=R^3=C_6H_{13}$, $R^4=C_{12}H_{25}$ (Cr 46 Col$_h$ 51 I)
41d $R^1=R^2=C_6H_{13}$, $R^3=R^4=C_8H_{17}$ (Cr 47 Col$_h$ 84 I)
41e $R^1=R^2=C_6H_{13}$, $R^3=R^4=C_{10}H_{21}$ (Cr 58 Col$_h$ 74 I)
41f $R^1=R^2=C_8H_{17}$, $R^3=R^4=C_{12}H_{25}$ (Cr 39 Col$_h$ 75 I)
41g $R^1=R^2=C_{10}H_{21}$, $R^3=R^4=C_{12}H_{25}$ (Cr 43 Col$_h$ 51 I)

Scheme 15.

Scheme 14.

43a $R^*=$ (Col$_h$ 267 I)
43b $R^*=$ (Col$_h$ 244 I)
43c $R^*=$ (Col$_h$ 112 I)
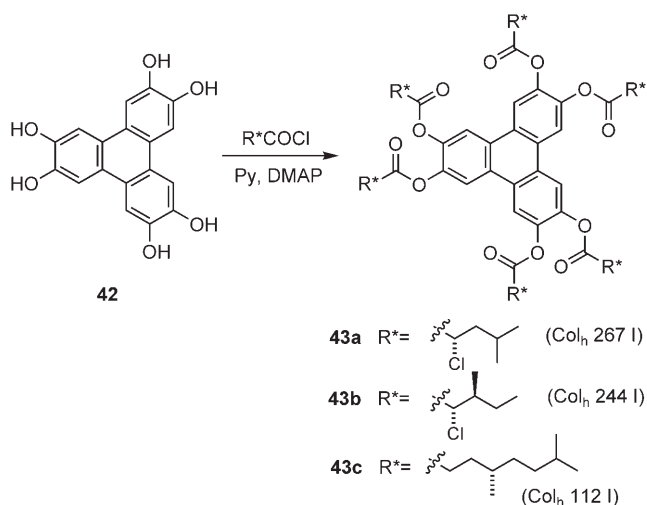
Scheme 16. DMAP = 4-dimethylaminopyridine.

As a result of their high photoconductivity, hexaalkoxytriphenylenes are of significant interest as fast photoconductors for applications in xerography and laser printing.[96] However, the relatively high melting point of symmetrical hexakis(alkoxy)triphenylenes limits their application. Therefore, several series of unsymmetrical alkoxytriphenylenes **41** have been prepared and their mesomorphism studied by the research groups of Kelly,[97] and of Marcelis and Zuilhof[98] (Scheme 15). The results in Scheme 15 show a subtle balance between combination of different chain lengths and melting or clearing points, respectively, but the melting points indeed could be lowered close to ambient temperature while keeping the clearing temperature sufficiently high (for example, **41f**).

Since the seminal finding of ferroelectrically switchable chiral columnar liquid crystals by Bock and Helfrich,[99] a large number of studies have been devoted to the preparation of chiral triphenylene derivatives and the investigation of their mesophase behavior and ferroelectric properties.[100] Esterification of **42** with chiral carboxylic acids resulted in chiral triphenylene esters **43** which still display hexagonal columnar mesophases (Scheme 16).[101] On mixing of the nematic discotic phase of hexakis[(4-nonylphenyl)ethynyl]-benzene (**4**, $R = C_9H_{19}$, Cr 67 N_D 83 I) with chiral **43**, induction

of a chiral nematic discotic phase N_D^* was observed. When the D_6 symmetry of **43** is further reduced by replacing one to three ester moieties by *n*-alkoxy chains, contact preparation did not show any chiral induction in the host nematic discotic phase.[101]

Chiral triphenylenes do not necessarily result in helical mesophases. Grubbs and co-workers studied hexakis(dihydrocitronellyloxy)triphenylene **35e** (Scheme 17).[102]

While the neat compound displays a hexagonal columnar mesophase with only $20\,°C$ mesophase width, the corresponding charge-transfer complex of **35e** with hexakisfluorotriphe-

35e R = (Cr 19 Col$_{hd}$ 36 I)
35f R = ($Cr_1 -132\ Cr_2 -36$ I)
35g R = OC_8H_{17}
44a R = F (Cr 109 I)
44b R = $S(CH_2)_5CH_3$
44c R = $C_6H_4(CH_2)_8CH_3$
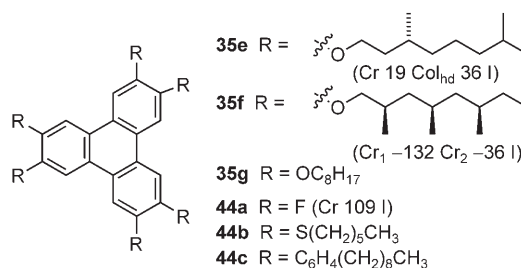
Scheme 17.

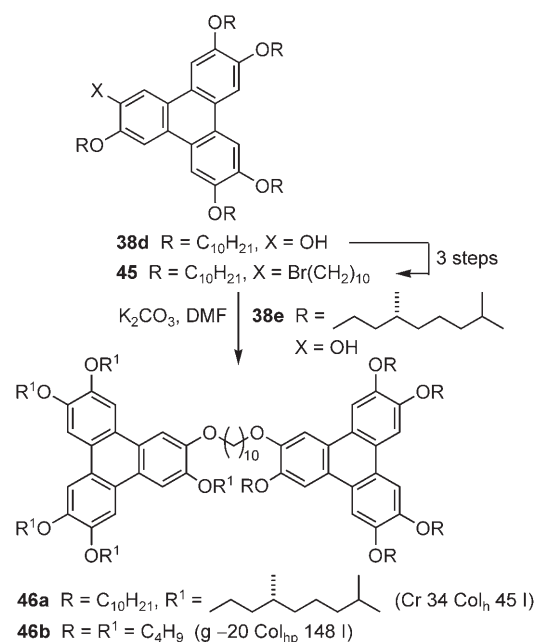nylene **44a** has an extended mesophase width up to 104 °C (Col$_{hd1}$ 21 Col$_{hd2}$ 104 I). In contrast, the chiral triphenylene **35f** with highly methyl-branched alkoxy chains was non-mesomorphic.[103] Nevertheless **35f** was completely miscible with hexakis(octyloxy)triphenylene **35g** and the (1:1) mixture formed a columnar mesophase (Cr 47 Col 67 I). Adam and co-workers measured the charge mobility in the mesophase of **35b** (Scheme 12), which is easily aligned homeotropically in a sandwich cell, to detect holes and electrons. A quasi-intrinsic transport for holes and a multiple shallow transport for electrons were found.[104] The electron mobility of 0.001 cm^{2}V^{-1}s^{-1} was lower than that of holes. A much higher hole mobility of 0.1 cm^{2}V^{-1}s^{-1} was measured with TOF[105] in the helical columnar phase of **44b**, independent of the temperature within the phase and of the applied electric field. Measurements reveal a very low mobility in the isotropic phase where no columnar order is present, a step-like increase when the columnar structure formed in the hexagonal columnar phase and a further abrupt increase after the transition into the helical phase, which reflects the increase in molecular order of these subsequent phases. Transient photocurrents decreased with increasing chain length of the triphenylene. Kato and co-workers[106] succeeded in the enhancement of the hole mobility of triphenylene **35d** (Scheme 15) by a factor of three by gelation with hydrogen-bonded fibers made of peptide derivatives.[107] Compound **35d** and a mixture of **35d** and triphenylene **44c** were investigated with respect to quantum efficiency of the photogeneration of charge carriers.[108] From the DC photocurrent, Bushby, Boden, and co-workers deduced the generation efficiency of the photocarriers based on the relation between the current and quantum efficiency, and on the probability that recombination does not occur. The addition of **44c** to **35d** largely improved the hole mobility of pure **35d**, but the efficiency of the pure **35d** was drastically reduced. The photocharge was also found to be produced exclusively because of **35d**.
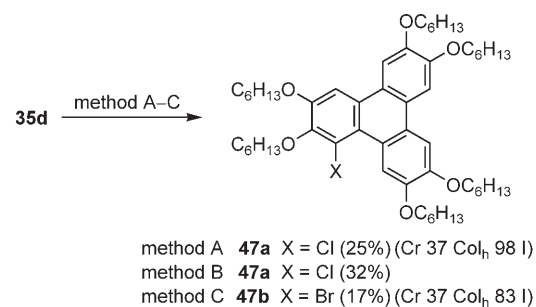
By tethering the achiral triphenylene **38d** to a chiral monohydroxytriphenylene **38e**, the achiral-chiral twin **46a** was obtained (Scheme 18). Compound **46a** gave intermediate phase-transition temperatures between those of hexadecyloxytriphenylene (Cr 58 Col$_h$ 69 I) and the chiral analogue **35e**. Again no chiral nematic discotic phase was detected.[109]

A completely different approach to chiral triphenylenes was almost simultaneously reported by the research groups of Bushby[110] and Praefcke.[111] From semiempirical calculations, it became evident that suitable α-substitution of the triphenylene moiety converts it from a planar into a propellerlike geometry. Halogen substituents were chosen as particularly promising candidates (Scheme 19).

The reaction of hexakis(hexyloxy)triphenylene **35d** with ICl to the chloro derivative **47a** was accompanied by formation of di- and trichloro-substituted byproducts (Scheme 19, Method A). An alternative route used sulfuryl chloride in the presence of AlCl$_3$ (Method B). Bromination was realized by treatment of **35d** with bromine at subambient temperatures (Method C). Although direct proof of the molecular chirality has not been achieved until now, both compounds **47a** and **47b**, and the corresponding fluoro-,


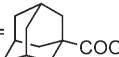**Scheme 18.** Col$_{hp}$ = hexagonal plastic.

method A **47a** X = Cl (25%) (Cr 37 Col$_h$ 98 I)
method B **47a** X = Cl (32%)
method C **47b** X = Br (17%) (Cr 37 Col$_h$ 83 I)

Scheme 19. Method A: ICl (1.5 equiv), CH$_2$Cl$_2$, RT, 20 min; Method B: SO$_2$Cl$_2$, AlCl$_3$, 1,2-C$_6$H$_4$Cl$_2$, RT, 4 days; Method C: Br$_2$, CCl$_4$, 0°C, RT, 4 days.

nitro-, and amino-derivatives displayed hexagonal columnar mesophases.

Also the modification of mesophase behavior of triphenylenes by substituents, additives, charge-transfer interactions, and pressure has been studied. Some general trends were observed regarding substituent effects. The introduction of additional alkoxy groups (for example, **48a**) results in a pronounced decrease of the melting temperature as compared to the D_{6h}-symmetrical analogue (Scheme 20).[112] Kettner and Wendorff reported that replacement of one alkoxy group by an ester function (**48b,c**) destabilized the mesophase when the steric bulkiness and polarity of the ester moiety were increased.[113] For the adamantoate **48d**, an additional plastic columnar phase was characterized[114] that shows promising charge-carrier mobilities greater than 10^{-2} cm^{2}V^{-1}s^{-1}, which makes this type of compounds attractive as organic photoconductors and organic light-emitting diodes (OLEDs). Brandl and Wendorff anticipated that the charge-carrier mobility might be increased by increasing the pressure as a result of decreased intracolumnar distances.[115] The induced decrease of molecular distances of 6% for
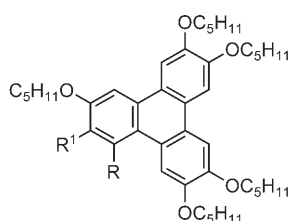
48a R=R¹=OC₅H₁₁ (Cr 22 Col 65 I)
48b R=H, R¹=C₄H₉COO (Cr 47 Colₕ 178 I)
48c R=H, R¹=naphthoyl-O (Cr 103 Colₕ 158 I)
48d R=H, R¹= [structure] COO (Colₙₚ 135 Colₕₒ 186 I)
48e R=H, R¹=Br (g −47 Colₓ 14 Colₕ 163 I)
48f R=H, R¹=CN (Cr 51 Colₓ 85 Colₕ 226 I)

Scheme 20.

pressures up to 17 kbar is too small to modify the electronic structure and thus optoelectronic properties. In contrast, as was independently found by the research groups of Ringsdorf,[116] Kumar[117] and Bushby,[118] strongly electron-withdrawing substituents such as bromo- or cyano (for example, **48e** and **48f**) not only stabilize the mesophase, but also increase the fluorescence quantum yields, important for the development of optoelectronic devices. However, most known triphenylenes have only poor fluorescence efficiencies as a result of their high symmetry.
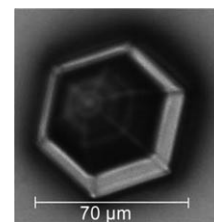
A very different solution to this problem was presented by Shinkai and co-workers, who attached 2-hydroxy-*N*-alkylacetoamide side chains to the triphenylene core. The resulting compound **49** (Scheme 21) immediately forms an organogel on mixing with cyclohexane (2.7 wt/vol%).[119] The organogel represents a rectangular columnar mesophase and exhibits unusual fluorescence emission that results from the unique eclipsed overlap of the triphenylene moieties.

While charge-transfer interactions are well known to stabilize columnar mesophases,[120,121] Luz and co-workers

49

eclipsed overlap   staggered overlap
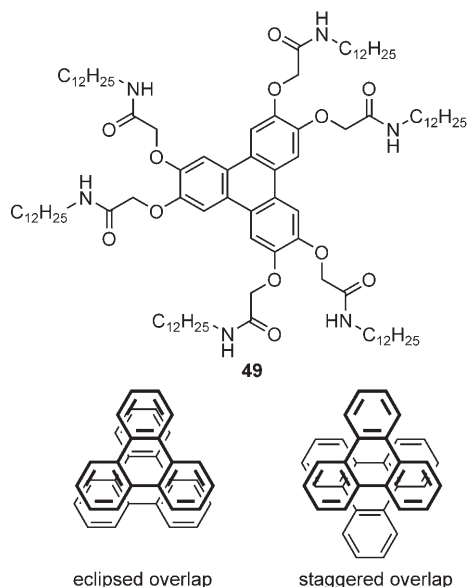
Scheme 21.

reported the induction and stabilization of triphenylene-based columnar mesophases by trifluoroacetic acid.[122] In the study of eutectic mixtures of triphenylenes that display highly ordered phases with nondiscotic compounds such as 3,4,3′,4′-tetrakisbutyloxybiphenyl, Brandl and Wendorff found that the mutual arrangement of the columns and the intracolumnar order are unaffected by the dilution of the discotic compound, whereas the phase morphology and kinetics of phase separation change significantly with dilution. Rod-shaped discotic domains with a hexagonal cross-sectional area are formed (Figure 23) and the rods grow linearly as a function of time.[123]
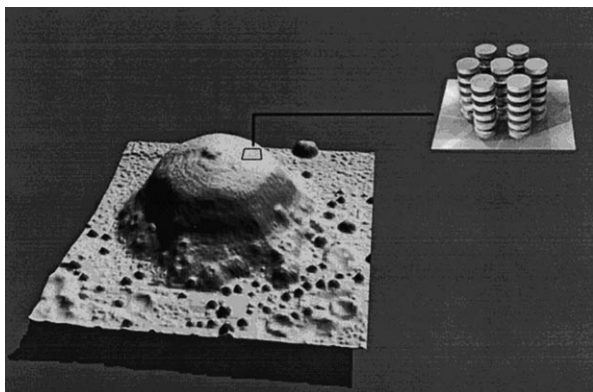
Along with the mesophase behavior, the important properties of alignment on surfaces, the molecular motion, and the photoconductivity have been studied in detail. Boden, Bushby, and co-workers studied self-assembled monolayers (SAMs) of a pentahexyloxytriphenylene-based LC with an ethyleneoxythiol side chain on a gold surface.[124] Thickness measurements of these SAMs indicated an "edge on" attachment of the triphenylene moieties with the columnar director lying parallel to the surface. The structure and conformation of the triphenylene **35b** (Scheme 12), which was spin-coated on amorphous carbon, were determined by electron diffraction, high-resolution electron microscopy, and computer simulations.[125] A surprising outcome of these studies was that the triphenylene core is not perpendicular to the column but tilted by 9°. Bai and co-workers investigated the arrangement of SAMs of hexaalkyloxytriphenylenes with various chain lengths on highly ordered pyrolytic graphite (HOPG) by scanning tunneling microscopy (STM).[126] The molecular superlattices strongly depend on the chain lengths. With C₁₂ chains, the molecular interaction dominates the crystallization, and the whole arrangement contains threefold symmetry. With C₁₄ chains, part of the alkyl chains form a highly packed structure. With C₁₆ chains, the alkyl moiety directs the intermolecular ordering and the molecules lose their symmetry.

The alignment on surfaces can be controlled by different parameters.[127] For example, host–guest complexes of penta-pentyloxytriphenylene-2-yl-cyclohexanoate and the chromophore tris[(*E*)-4-pyridinyl-4-styrenyl]amine on a polyimide-coated glass surface resulted in a dewetting-induced formation of hexagonal microstructures, which can be visualized by AFM (Figure 24).[128]

Photoalignment is another technique used to obtain discotic LCs with a preferred orientation. Poor thermal stability of the molecular ordering of the aligning layer was overcome by Ichimura et al.,[129] who studied the photoalignment of hexakis(4-octyloxybenzoyloxy)triphenylene on a poly[4-(4-cyanophenylazo)phenylmethacrylate] as the photo-aligning film (Figure 25). Irradiation with oblique nonpolarized light resulted in a 3D photoreorientation of the longitudinal axis of the

Figure 23. Phase morphology for a 1:1 mixture of pentabutoxytriphenylene-2-yl-(1-adamantenoylmethanoate) and tetrakisbutoxybiphenyl. Reproduced from Ref. [123].

Figure 24. AFM image of a hexagon and a scheme showing the orientation of the discotic columns. The diameter and the height of such a hexagon are typically of the order of 10 μm and 1 μm, respectively. The original film thickness (80–200 nm) is thus smaller than the height of the hexagon. In contrast to the original unannealed film, the columns are oriented parallel to the surface. Reproduced from Ref. [128].
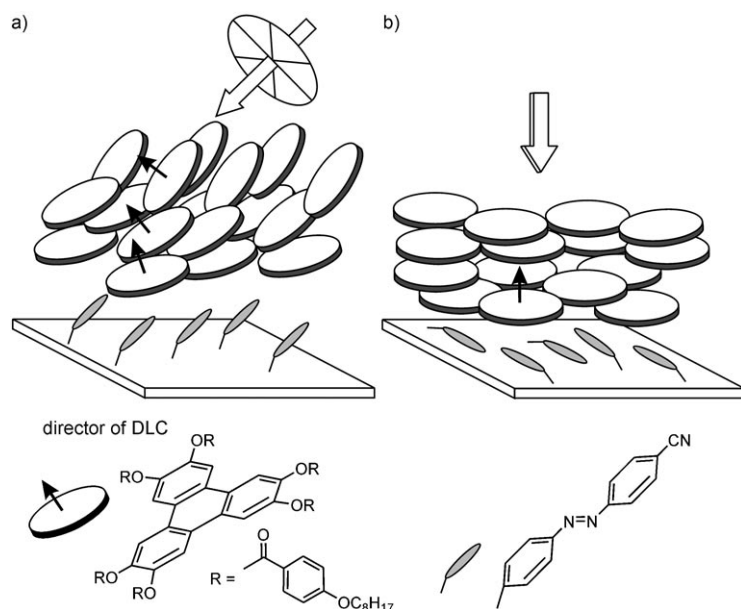
Figure 25. a) Tilted and b) homeotropic alignment of discotic triphenylene mesogens (disks) in the N_D phase on a thin film with *para*-cyanoazobenzene residues (rods) exposed to irradiation with oblique nonpolarized and linearly polarized light.[129]

E isomer of azobenzene towards the direction of the incident light to minimize their light absorption. This reorientation induced an overall change of the director of the triphenylenes. Irradiation with linearly polarized light, however, resulted in a homeotropic alignment with an orientational director of the columnar liquid crystal perpendicular to the substrate plane, similar to the cases for a nonirradiated film of the poly[4-(4-cyanophenylazo)phenylmethacrylate] or a hydrophobic silica plate. This procedure may open up ways to fabricate optical compensatory sheets for twisted nematic LC displays.

Shimizu and co-workers reported the alignment change of LC domains of **35 d** (Scheme 15) by vibrational excitation of

the aromatic C=C stretching band at 1615 cm^{-1} with a free-electron laser.[130] Spontaneous homeotropic alignment in a hexagonal columnar mesophase was achieved by introducing perfluoromethylene groups into the peripheral chain of triphenylenes.[131] Spiess, Ringsdorf, and co-workers[132] studied the molecular motion of hexaheptyloxytriphenylene, a corresponding dimer and a main-chain polymer, as well as their charge-transfer complexes with TNF, by means of ^{2}H NMR spectroscopy. Fast rotation of the disks around their column axis takes place in the monomer, and is quenched in the dimer and the polymer. In the charge-transfer complex with the triphenylene monomer, almost all the electron-acceptor molecules stack in the columns, even at temperatures close to the clearing temperature, while for the dimer and the polymer, a significant fraction of the TNF molecules exhibit isotropic motion.

4.3. Perylene derivatives

Perylene-derived pigments are important technical dyes, although their applications are hampered by their low solubility.[133] This limitation, however, was overcome by the introduction of functional groups such as carboxylic acids.[134] The first attempt towards liquid-crystalline perylene derivatives was published by the research group of Müllen.[135] Suzuki coupling of the naphthylbromide **50a** with the corresponding boronic acid **50b** gave the 4,4′-disubstituted binaphthyl **51**. Subsequent reductive coupling yielded the perylenes **52**, which underwent smooth Diels–Alder reactions with *N*-alkyl-3,5-dioxotriazole **53** to give the perylene bisimides **54a** and **54b** in good yields (Scheme 22).

Surprisingly, even perylene **54a**, which contains short alkyl chains and has a low aspect ratio, displays a broad mesophase. Solid-state ^{2}H NMR spectra of selectively deuterated derivatives of **54**

54a R = R^1 = C$_5$H$_{11}$ (Cr 27 Col 319 I)
**54b** R = C$_{18}$H$_{37}$, R^1 = C$_5$H$_{11}$ (Cr 69 Col 261 I)
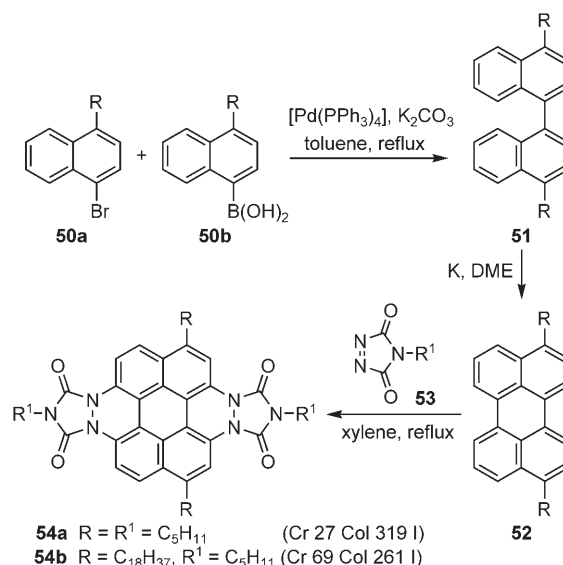
Scheme 22.

revealed the nonplanarity of the triazole unit and the dynamic behavior of the *N*-alkyl chains.[135b]

A different approach was pursued by Würthner et al.,[136] who prepared columnar perylene bisimides **57** by condensation of perylene tetracarboxylic acid dianhydrides **55** with 3,4,5-tridodecyloxyaniline (**56**) in the presence of a Lewis acid (Scheme 23).


57a R = H (Col_hd 373 I)

57b R = (Col_hd 346 I)

57c R = (Cr 243 I)
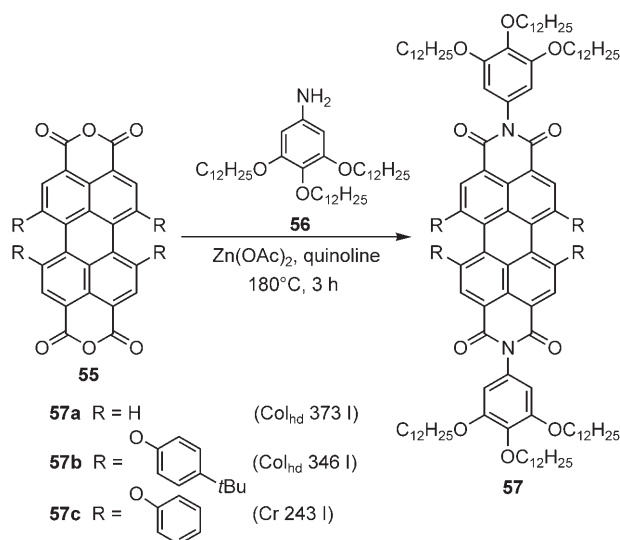
Scheme 23.

The mesomorphic properties of **57** depend on the substituents in the bay region of the perylene core. In solution, the derivatives **57** form fluorescent J-type aggregates, that is, absorption and emission maxima are red-shifted with respect to the isolated chromophore, and no quenching of fluorescence occurs in the aggregate, which makes these compounds useful as polarizers and electroluminescent devices. The AFM image of thin-film spin-coated solution of analogues of **57** (in which the dodecyloxy groups are replaced with dodecyl chains) onto HOPG shows the formation of 1D nanoaggregates, in which the columns are oriented coplanar to the HOPG surface.[137]

As a result of their electronic properties, perylene bisimides are well suited as n-type semiconductors. Therefore, Zuilhof, Sudhölter, and co-workers studied the architecture and charge-carrier mobilities of perylene bisimide **58a** (Scheme 24).[138]

According to X-ray diffraction data, **58a** is highly ordered in the two mesophases that are both smectic and columnar discotic in nature. A charge-carrier mobility of $0.11 \, cm^2 V^{-1} s^{-1}$ in the mesophase was detected by PR-TRMC (see Section 3.1), thus making compound **58a** a promising candidate for electron-transporting materials in photovoltaic devices. Perylene bisimide **58b**, with alkyl chains that bear an internal *Z* alkene, displays a lamello-columnar mesophase (L_col).[139] However, on mixing **58b** with a hexagonal columnar phthalocyanine derivative (1:3 mixture), only a very broad hexagonal columnar mesophase is observed, with a 260°C phase width, thus demonstrating the miscibility of disk- and lathlike mesogens.[139] Méry et al.
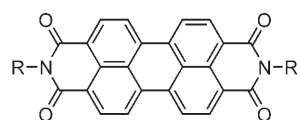
58a R = $C_{18}H_{37}$ (Cr_1 111 Cr_2 141 Cr_3 180 S_{x1} 216 S_{x2} 312 I)

58b R = $H_{16}C_8$ C_8H_{17} (Cr 178 L_col 292 I)

58c R = $CH(CH_2CH_3)_2$
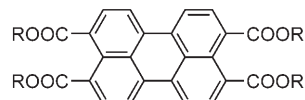
59a R = C_2H_5 (Cr_1 134 Cr_2 150 Cr_3 244 Col_h 313 I)

59b R = C_3H_7 (Cr 193 Col_h 287 I)

59c R = C_8H_{17} (Cr 62 Col_h 132 I)

Scheme 24.

observed exceptionally high charge-carrier mobilities for smectic thiophene and anthracene derivatives.[46,140] Also tetra(*n*-alkyloxycarbonyl)perylenes are mesomorphic. Bock, Kitzerow, and co-workers found that even tetraethylperylenetetracarboxylate (**59a**) displays a columnar mesophase that is stable over a temperature range of 70 K.[141] The orientation of **59a** in the mesophase correlates very well with the crystal packing in the solid state.[142a] From UV/Vis photoelectron emission spectra, STM spectroscopy, and cyclic voltammetry, a HOMO–LUMO gap of 2.3 eV was calculated, thus making **59a** suitable as an electron-transfer layer in OLEDs. Mixing various perylenecarboxylates **59** with short alkyl side chains leads to formation of columnar liquid-crystalline glasses which are stable at room temperature and show electroluminescence.[142b]

4.4. Hexa-peri-hexabenzocoronene derivatives

The interesting physical properties of graphite, for example, electric conductivity, have motivated many researchers to investigate polyaromatic hydrocarbons as graphite model systems.[143] However, their low solubility and poor processibility severely hampered detailed studies. This situation has dramatically changed since the pioneering studies by Müllen and co-workers on liquid-crystalline hexa-*peri*-hexabenzocoronenes (HBCs) such as **63a**[144] (Scheme 25).[145]

The synthesis of **63a** started with a Sandmeyer reaction of 4-alkylaniline **60** to the iodide **61a**. Subsequent Sonogashira coupling, deprotection of the silyl group, and a second Sonogashira coupling with iodide **61a** yielded 4,4′-dialkyltolane **62a**, which was cyclotrimerized under $[Co_2(CO)_8]$ catalysis to the hexaphenylbenzene **32a**. The key step was an oxidative cyclodehydrogenation of **32a** in the presence of AlCl_3 to give the hexaalkyl-substituted HBC derivative **63a**, which displayed an extremely broad columnar mesophase with a phase width of 339°C. The corresponding hexaalkyltriphenylenes, however, are nonmesomorphic. One possible reason for this different behavior might be that larger disks can form columns with substantial overlap of the aromatic regions more easily than the smaller ones. Thus, the HBCs exhibit extremely broad columnar mesophases, yet are less
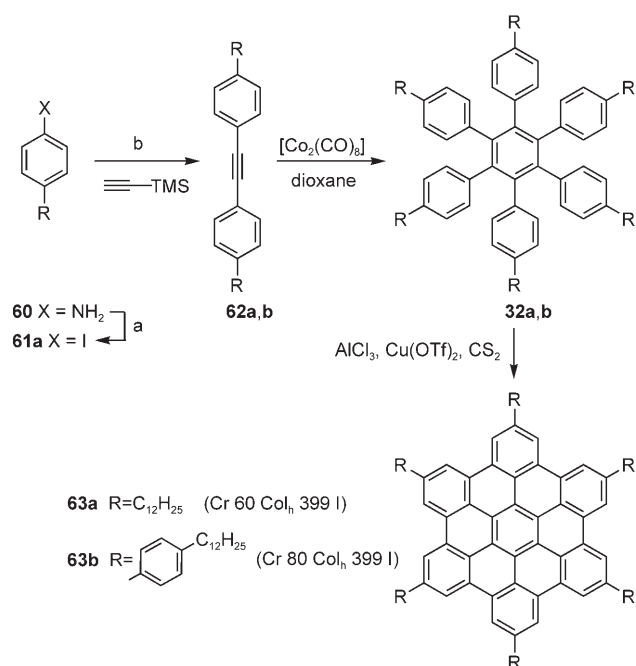
Scheme 25. Reagents and conditions: a) 1. $C_5H_{11}NO_2$; 2. KI. b) 1. [PdCl$_2$(PPh$_3$)$_2$], CuI, PPh$_3$, piperidine; 2. KF, DMF; 3. [Pd(PPh$_3$)$_4$], CuI, piperidine. Tf = trifluoromethylsulfonyl, TMS = trimethylsilyl.

ordered within the columns than conventional triphenylenes (Figure 26).[144]
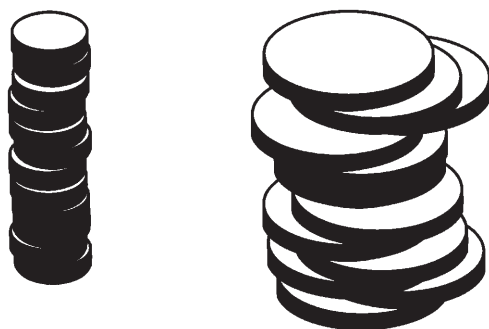
**Figure 26.** Stacks of small and large disks.[144] To obtain strong π–π interactions, the stacking of small disks requires substantially higher orders as compared to large disks.

Based on an X-ray single-crystal study of an unsubstituted HBC by Krüger and co-workers,[146] a so-called "herringbone" pattern and an interplanar distance of 0.342 nm was assumed for the mesophase.[147] The major degree of freedom was found to be due to axial rotation. As high molecular mobility decreases the overall charge-carrier mobility, **63b** with 4-alkylphenyl substituents was prepared by a twofold Kumada coupling to alkyne **62b**, [2+2+2] trimerization to the hexaphenylbenzene **32b**, and final cyclization of **32b** in the presence of FeCl$_3$ in nitromethane/CH$_2$Cl$_2$ instead of AlCl$_3$/Cu(OTf)$_2$ in CS$_2$.[148] Double-quantum ^{1}H solid-state NMR spectroscopy indeed revealed an improved inter- and intra-columnar order of the alkylphenyl HBC **63b** as compared to **63a**.

Although the cobalt-mediated alkyne trimerization and subsequent Lewis acid catalyzed cyclization provides a convenient entry to highly symmetrical HBCs, a practical route to unsymmetrical HBCs was developed by Müllen and co-workers (Scheme 26).[149] The synthesis of unsymmetrical
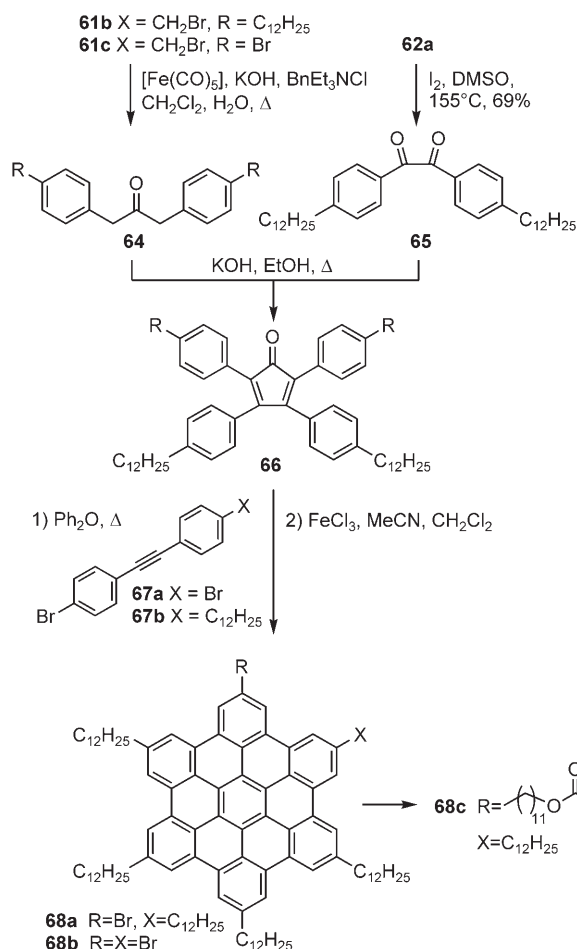
Scheme 26. Bn = Benzyl.

HBCs commenced with the preparation of diarylacetones **64** from benzylbromides **61b** and **61c**, and 1,2-diketone **65** (obtainable by iodine oxidation of tolane derivative **62a**). Diarylacetones **64** underwent base-catalyzed aldol condensation with **65** to give the tetraarylcyclopentadienones **66**, which were heated with the bromotolanes **67**, and subsequently treated with FeCl$_3$ to give the unsymmetrical HBCs **68a** and **68b**. The bromo substituent in **68a** was particularly useful for the introduction of further functional groups such as ethers, amines, esters, and nitriles.[149] Scheme 26 shows the acrylate-containing unsymmetrical HBC **68c**, which is accessible from bromo HBCs such as **68a**.[150] The HBC **68c** (Cr 75–100 Col$_h$ 140–180 polymer) was polymerized by simply heating the columnar mesophase above 100 °C, while maintaining the columnar structure in the polymer, as was proven by X-ray powder diffraction.

Chirality was introduced in symmetrical HBCs by several approaches. For example, phase chirality was found for the hexaalkynyl HBC **63c** (Scheme 27).[151]

63c R= ⬡—≡—C_6H_4-4-($OC_{12}H_{25}$)   (Col_{hh} 86 Col_h)

63d R= [dihydrocitronellyl chain]   (Cr 96 Col^*_{ho} 430 I)

63e R= [branched alkyl chain]   (Cr 81 Col_{ho} 420 I)

63f R= [branched alkyl chain]₃   (Cr −36 Col_{ho} 231 I)

63g R= [pentaphenyl with H substituent]

63h R= [pentaphenyl with $C_{12}H_{25}$ substituent]

63i R= [$C_{12}H_{25}$ / $C_{10}H_{21}$ branched chain]

63j R= [chain]C_8F_{17} (Cr_1 122 Cr_2 138 Cr_3 180 Col_r 300 decomp)

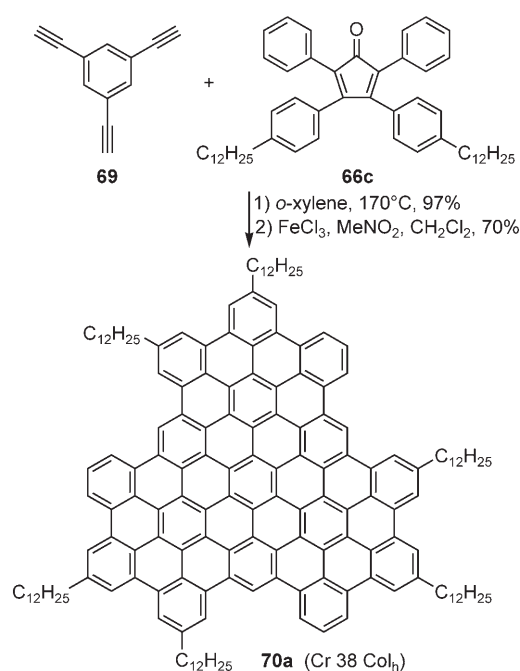**63k** R= ⬡—C_8F_{17} (Cr_1 227 Cr_2 236 SmA 300 decomp)

63l R= [chain]C_8H_{17} (Cr 124 Col_h 300 I)

63m R= [chain]$C_{12}H_{25}$ (Cr_1 52 Cr_2 109 Col_h 250 decomp)

Scheme 27.

1) o-xylene, 170°C, 97%
2) $FeCl_3$, $MeNO_2$, CH_2Cl_2, 70%

70a (Cr 38 Col_h)

Scheme 28.

The presence of a novel helical plastic phase at room temperature is attributed to the rigid diphenylacetylene arms that have a large empty wedge that can be filled efficiently when discs are rotated successively by 15°. In contrast, from a THF solution, **63c** forms nanoribbons (21 nm wide, 3.8 nm high) on HOPG.[151] The introduction of a dihydrocitronellyl moiety leads to the chiral HBC derivative **63d**, which displayed a helical superstructure within the hexagonal columnar mesophase[152] as confirmed by CD spectroscopy. The corresponding racemic analogue **63e** enters the columnar mesophase at lower temperature.

Different strategies are amenable to improve electronic and optoelectronic properties of HBCs towards applications in solar cells and field-effect transistors (FETs). For example, the size of the graphite subunit might be enlarged. Such superphenalenes **70** or extended HBCs, accessible from the thermal Diels-Alder reaction of 1,3,5-trisalkynylbenzene **69** and tetracyclone **66c** followed by cycloaromatization in the presence of $FeCl_3$ (Scheme 28),[153] have been investigated also by Müllen and co-workers.[154]

The aggregation behavior of extended HBCs such as **63g–i** (Scheme 27) in solution could be easily controlled by the bulkiness of the dendrimer subunit.[155] While compound **63g** dimerizes in solution, **63h** does not form any aggregates. To improve the long-range self-assembly of HBCs, dovetailed alkyl substituents were attached to the HBC core (for example, in **63i**) by Müllen and co-workers.[156] Well-ordered spherulite textures with a diameter of 200 µm (Figure 27) were observed, which indicates an exceptionally long-range self-assembly.
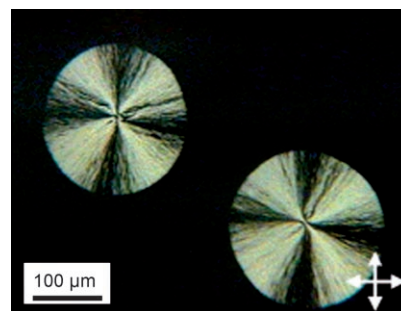
Figure 27. POM image of **63i** during isothermal crystallization at 35°C. Reproduced from Ref. [156].

Jenny and co-workers anticipated that HBCs with perfluoroalkylated chains constitute an insulating "mantle" around the central π-stacked aryl moiety and thus facilitate their self-organization into single dispersed columns.[157] The perfluoroalkylated chains increased the rigidity of the molecule and resulted in an increased melting temperature for **63j** (Scheme 27) as compared to the nonfluorinated counterpart **63l**. Incorporation of a phenyl spacer gave a fluorinated HBC **63k**, which was claimed to have a biaxial smectic A mesophase instead of a columnar mesophase (Figure 28). The

Figure 28. Mesomorphic structure (SmA) of **63k** and **63j**.[157]

raised transition temperatures are explained by the existence of much longer columnar aggregates, which compensate for the reduced lateral interactions.

The combined properties of wide mesophase range, high thermal stability and 1D charge-carrier mobility make alkyl-substituted HBCs promising candidates as vectorial charge-transport layers in xerography, electrophotography, or as nanowires in molecular electronic devices. Warman, Müllen, and co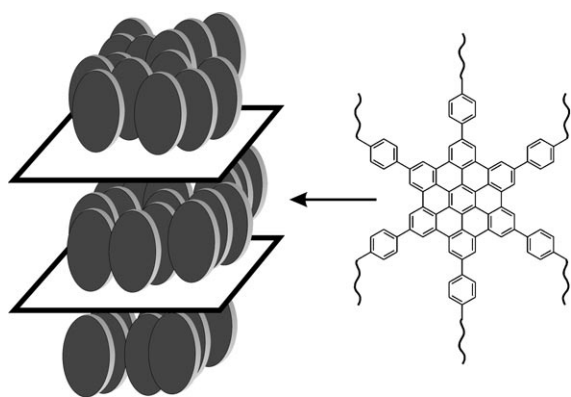-workers studied the charge-carrier mobilities of a series of HBCs by PR-TRMC.[158,159] The mobility in the crystalline phase of the homologues **63a,l,m** (Scheme 25 and 27) increases with the longer chains to values of the order of $1\ cm^2V^{-1}s^{-1}$, while in the mesophase there is little variation. For HBC **63a**, an intramolecular mobility $\Sigma\mu_{1D} = 0.38\ cm^2V^{-1}s^{-1}$ at 110 °C was found. Derivative **63m** showed a mobility of $0.13\ cm^2V^{-1}s^{-1}$ in the Col$_h$ phase. Incorporation of a phenyl ring into the side chain resulted in increased mobilities, as expressed by $\Sigma\mu_{1D} = 0.46\ cm^2V^{-1}s^{-1}$ at 192 °C for **63b** (Scheme 25).[159]

Watson, Müllen, Bard, and co-workers synthesized a hexakisphytyl HBC **63f** (Scheme 27), which shows a hexagonal ordered mesophase between −36 and 231 °C.[160] From photoconductivity measurements, two orientation of the molecular columns were proposed, in which the columns are either parallel to the ITO layer or perpendicular with a slight tilt (Figure 29).
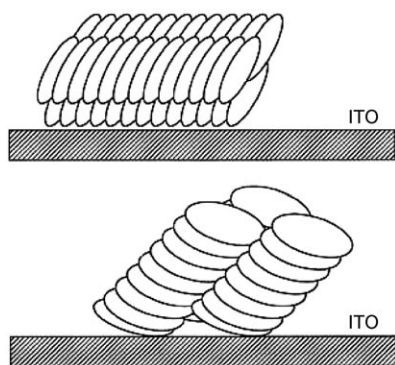

Figure 29. Proposed limiting orientations of the molecular columns of **63f** relative to the electrode surface. Reproduced from Ref. [160].

The optical and charge-transport properties of a variety of polycyclic aromatic hydrocarbons (PAH), including HBCs and superphenalenes **70** were investigated.[161] The highest intramolecular mobility was measured for the superphenalene with C_7H_{15} chains, which showed $\Sigma\mu_{1D} = 1.26\ cm^2V^{-1}s^{-1}$ in the columnar mesophase. The experimental results also revealed that a larger size of the aromatic core does not necessarily mean high charge-carrier mobility. For a PAH with 132 carbon atoms in the core unit, the $\Sigma\mu_{1D}$ was much less than for the superphenalene **70** with 96 carbon atoms. In a more recent study, Warman, Müllen, and co-workers reported that the decay time of the conductivity depends exponentially on the effective diameter of the discotic molecules.[162] Thus, the chain lengths have an important influence on the decay time.

Nuckolls and co-workers presented a contorted HBC derivative **71**, whose aromatic core is nonplanar as a result of the steric congestion of the proximal C−H bonds (Figure 30).[11] Nevertheless, **71** possesses a columnar meso-phase and displays a charge-carrier mobility $\Sigma\mu_{1D} = 0.02\ cm^2V^{-1}s^{-1}$, which allows its successful application in a field-effect transistor.
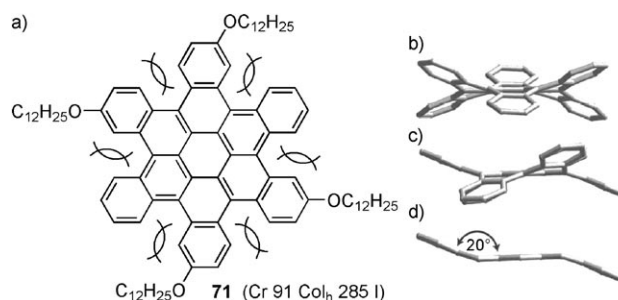
Figure 30. Compound **71** and side view of its crystal structure.[11]

Processibility, alignment, and formation of thin films are major issues with regards to possible applications. It has been independently shown by the research groups of Müllen and Bjørnholm[163] and Tsukruk[164] that HBCs with amphiphilic side chains easily form Langmuir Blodgett (LB) films. Bunk, Friend, et al. reported the fabrication of HBC **63e** films by crystallization from solution onto friction-transferred poly(-tetrafluoroethylene) (PTFE) layers, and thus the alignment is induced by the PTFE layer.[165,166] Recently, Tracz, Müllen, and co-workers developed a zone-casting technique, which allowed the alignment of HBC **63a** on untreated glass by solution processing (Figure 31).[167,168] These thin films (15 nm), which are composed of uniaxially aligned exceptionally long columns with single-crystalline-like order over several centimeters have been used for FETs.

Müllen, Warman, and co-workers were also able to induce thermal switching of the optical anisotropy of a macroscopically aligned film of the HBC derivative **63b** through a change in the intracolumnar tilt angle (Figure 32).[169,170] This phenomenon is quite useful for optical data-storage media. The advantage over the previously reported mechanism for switching the optical properties of columnar LCs is that the columnar arrangement remains intact and therefore their
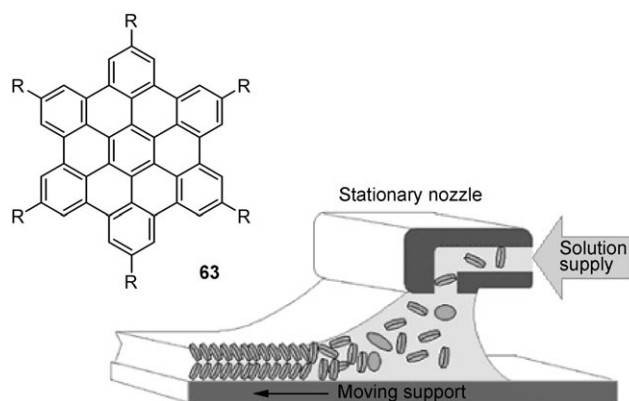
Figure 31. Setup of the zone-casting process. The disks represent the HBC molecules.[167, 168]
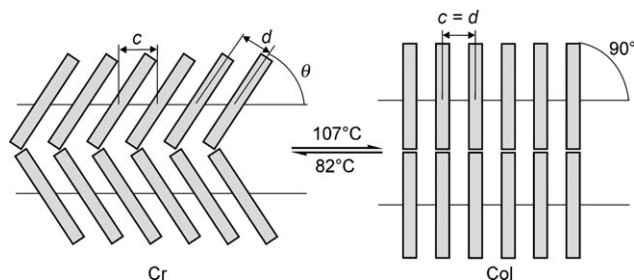
Figure 32. The columnar arrangement in crystalline phase at room temperature.[169]

excellent semiconductive properties could be exploited along with their unique optical behavior.

4.5. Tribenzocyclononatriene, tetrabenzocyclododecatetraene, metacyclophane, and tetraphenylene derivatives

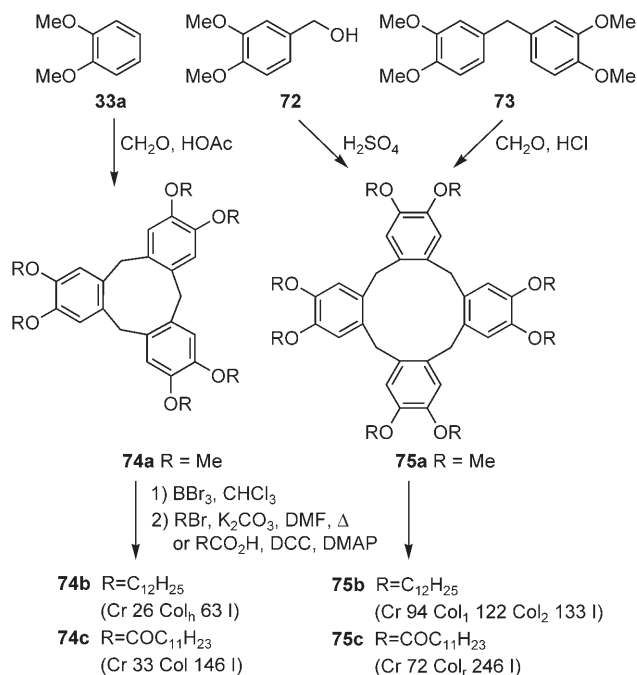Although structurally different at first glance, the tribenzocyclononatrienes, tetrabenzocyclododecatetraenes, metacyclophanes, and tetraphenylenes share some common features. They are nonplanar and adopt either a cone-shaped, crown-shaped, or saddle-shaped conformation depending on the ring size and the substituents. In particular, the cone-shaped conformation is very interesting for possible applications because the resulting mesophases are potentially ferroelectric or antiferroelectric (Figure 33).[171] Furthermore, the different conformations exist in a dynamic equilibrium and several of these compounds are able to form host–guest complexes.

Most of liquid-crystalline tribenzocyclononatrienes and tetrabenzocyclododecatetraenes have been explored by the research groups of Luz and Zimmermann,[172] Malthête,[173] Percec,[174] and Tschierske and Pelzl.[175, 176] As shown in Scheme 29, the tribenzocyclononatrienes (cyclotriveratrylenes) **74** are obtained by the acid-catalyzed condensation of veratrol (**33a**) and formaldehyde, while the synthesis of the tetrabenzocyclododecatetraenes (cyclotetraveratrylenes) **75** is preferably carried out with 3,4-dimethoxybenzyl alcohol (**72**) rather than 3,3′,4,4′-tetramethoxydiphenylmethane (**73**).
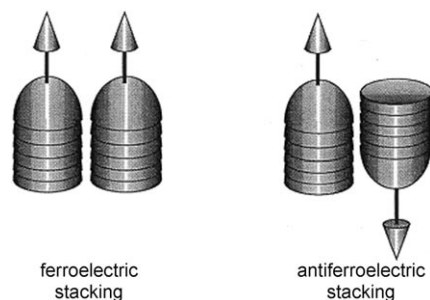
Figure 33. Parallel (ferroelectric) and antiparallel (antiferroelectric) packing of columns of bowl-shaped molecules. Reproduced from Ref. [171].

74a R = Me **75a** R = Me

1) BBr₃, CHCl₃
2) RBr, K₂CO₃, DMF, Δ
   or RCO₂H, DCC, DMAP

74b R=C₁₂H₂₅
(Cr 26 Colₕ 63 I)

74c R=COC₁₁H₂₃
(Cr 33 Col 146 I)

75b R=C₁₂H₂₅
(Cr 94 Col₁ 122 Col₂ 133 I)

75c R=COC₁₁H₂₃
(Cr 72 Colᵣ 246 I)

Scheme 29.

After BBr₃-induced demethylation, the hydroxy groups were either submitted to etherification or esterification to give the compounds **74b,c** and **75b,c**. It should be noted that the mesophase width of the columnar phase dramatically increases when going from the ethers **74b**, **75b** to the corresponding esters **74c**, **75c**. In addition, the tetrabenzocyclododecatetraenes **75b,c** display much higher melting and clearing points than the corresponding tribenzocyclononatrienes **74b,c**.[172b, 177]

Laschat and co-workers identified octamethoxytetraphenylene **77a** as the most suitable key building block for liquid-crystalline tetraphenylenes (Scheme 30).[178, 179]

The synthesis started from 4-bromoveratrol (**34**) via the biphenyl **76**, which was treated sequentially with *n*BuLi, ZnBr₂, and CuCl₂ at subambient temperatures to give the octamethoxytetraphenylene **77a**.[178] Demethylation with BBr₃ yielded the octahydroxy derivative **77b**, which turned out to be very sensitive to oxidation. Thus, the yields of both the ethers **77c–e** and esters **78c–e**[179] are compromised by the
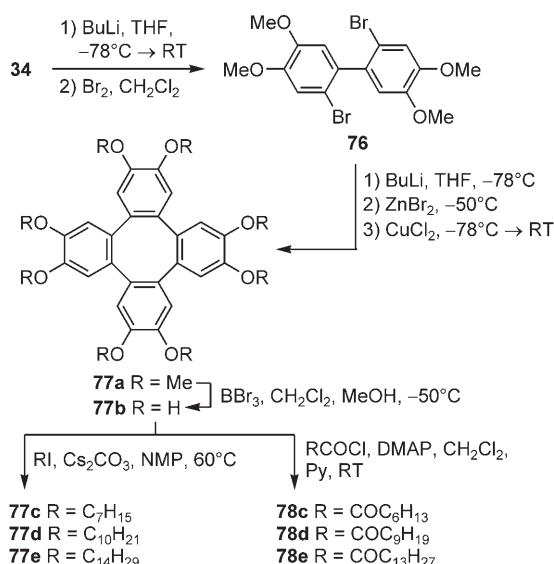
Scheme 30. NMP = N-methylpyrrolidone

rapid oxidation of **77b**. Ethers **77c–e** and esters **78c–e** differed remarkably in their mesomorphic properties. In the series of ethers **77**, compounds with a C_7–C_{12} alkyl chain display enantiotropic hexagonal columnar mesophases, those with longer alkyl chains (C_{13}–C_{16}) display smectic mesophases.[173] In contrast, esters **78** with a minimum chain length of C_7 exhibit columnar mesophases.[179]

Luz, Zimmermann, and co-workers studied the dynamic behavior of nonasubstituted tribenzocyclononatrienes **74d** (Scheme 31).[180] This compound exhibited a special form of mesomorphism, in which the crown and the saddle conformer exhibit (two) different columnar mesophases. The clearing temperature of the crown conformer is much higher than that of the saddle isomer, which demonstrates the thermodynamic stability of the crown conformer. The saddle conformer slowly transforms into the crown mesophase apparently by sublimation. The ^{13}C MAS NMR spectra show that the molecules in the crown mesophase reorient about the column axis, whereas
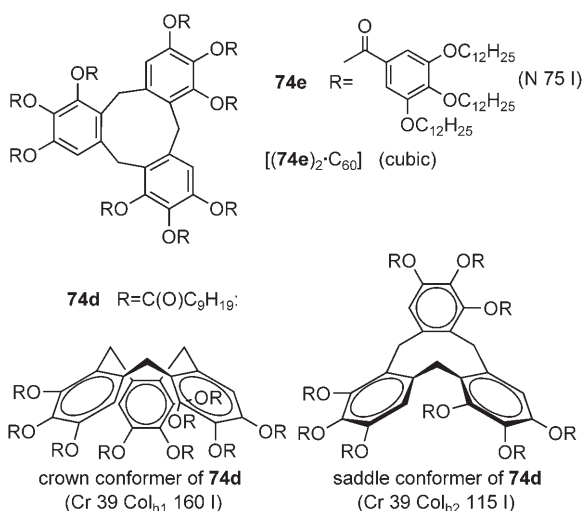
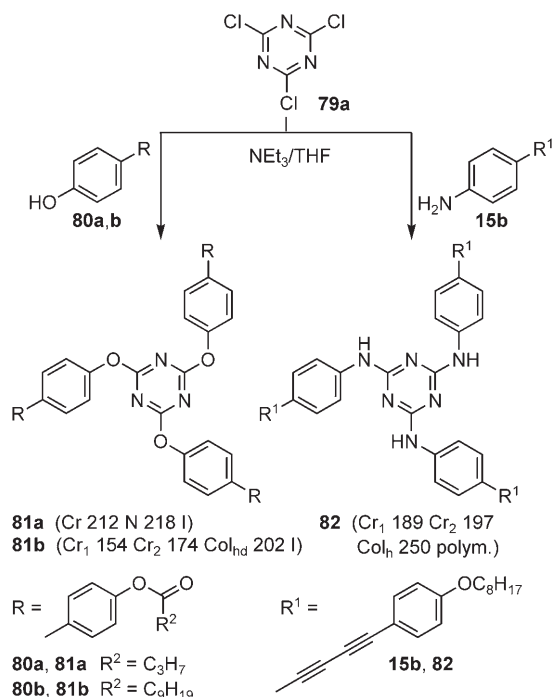in the saddle mesophase they are static. Nierengarten and co-workers synthesized the hexagallic ester **74e** which formed a nematic mesophase (Scheme 31).[181] However, on complexation of **74e** with 0.5 equivalents of fullerene C_{60}, a cubic mesophase was detected. In contrast to the mesomorphic (2:1) complex, a (1:1) complex was observed by UV/Vis titration in solution and an association constant $K_a = 330 \, \text{M}^{-1}$ was determined.

4.6. Triazine derivatives

Most organic semiconductors reported so far exhibit p-type (electron-rich) characteristics. However, for the fabrication of real "plastic electronics" such as bipolar transistors, p–n junction diodes or complementary circuits, both p- and n-type (electron-deficient) materials are needed.[182] For this purpose electron-poor heteroaromatics are of particular interest; for example, triazine might be a useful core unit. However, previous studies by the research groups of Lattermann,[183] Mormann,[184] and Mahlstedt[185] indicated that the substituents in the periphery have a strong influence on the mesomorphism of triazines.

C_3-symmetrical triazines **81** were prepared by treatment of cyanuric chloride (**79a**) with biphenyl derivatives **80** (Scheme 32).[186] Whereas compound **81a** formed only a nematic phase, the corresponding derivative **81b** exhibited a smectic mesophase which coexisted with a hexagonal columnar mesophase. The mosaic texture pointed to a smectic phase; X-ray analysis, however, supported the Col_{hd} phase. Chang prepared the polymerizable C_3-symmetrical triazine derivative **82** also starting from **79a** (Scheme 32).[187] On heating at 250 °C or UV irradiation, the hexagonal mesophase polymerized into an ordered solid.

74e R= (N 75 I)

[(**74e**)$_2$·C_{60}] (cubic)

74d R=C(O)C$_9$H$_{19}$:

crown conformer of **74d**
(Cr 39 Col$_{h1}$ 160 I)

saddle conformer of **74d**
(Cr 39 Col$_{h2}$ 115 I)

Scheme 31.

81a (Cr 212 N 218 I)
81b (Cr$_1$ 154 Cr$_2$ 174 Col$_{hd}$ 202 I)

82 (Cr$_1$ 189 Cr$_2$ 197 Col$_h$ 250 polym.)

R =

80a, 81a R^2 = C$_3$H$_7$
80b, 81b R^2 = C$_9$H$_{19}$

R^1 =

15b, 82

Scheme 32.

Triazines are octupolar molecules and thus should be useful for NLO applications. Octupolar NLO molecules have several advantages over traditional dipolar NLO molecules, in that they lack permanent dipole moments so are better able to adopt a noncentrosymmetric packing in the solid state compared to dipolar molecules. Also, where the β value reaches a maximum and thus declines with increasing bond-length alternation for dipolar molecules, β increases steadily with the extent of the charge transfer in octupolar molecules. To achieve macroscopic orientation, liquid-crystalline triamines would be perfectly suited.

Kim and co-workers reported a novel approach to both achiral and chiral triazines **85** by the Suzuki coupling of **79a** with boronic acid **84** (Scheme 33).[188] While the achiral
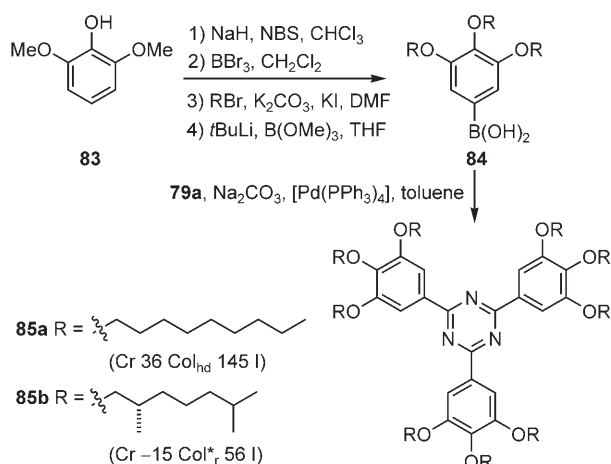
Scheme 33.

triazine **85a** displayed a hexagonal columnar mesophase, the chiral triazine **85b** exhibited a chiral rectangular columnar mesophase, in which the columns form a helix as illustrated in Figure 34. In CD spectra, no circular dichroism was observed
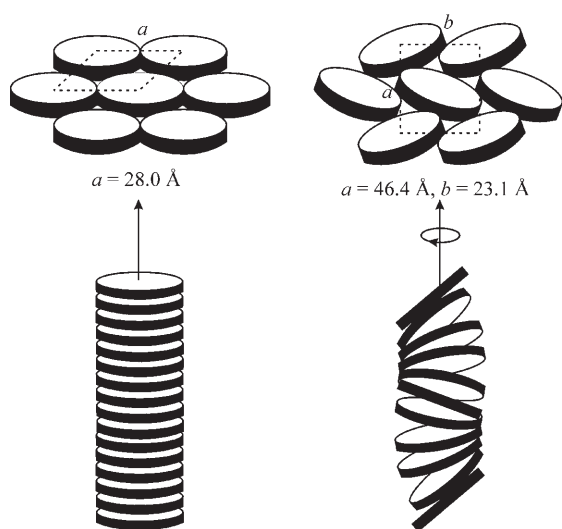
Figure 34. Idealized representation of the Col$_h$ mesophase of **85a** and the Col*$_r$ mesophase with a left-handed helix of **85b**.[188]

with a solution of **85b**. Circular dichroism of a film of **85b** supported the proposal that its optical activity is not derived from the stereogenic center of the alkyl tails, but rather from the helical arrangement of the molecules induced by the chiral tails. Reduction of the symmetry of **85**, for example, by replacing a nitrogen atom by a CH moiety, resulted in lamellar columnar mesophases.[189]

Recently the research group of Oriol and Serrano reported very interesting phosphorus analogues of triazine, that is, cyclotriphosphazenes **88** (Scheme 34),[190] in which
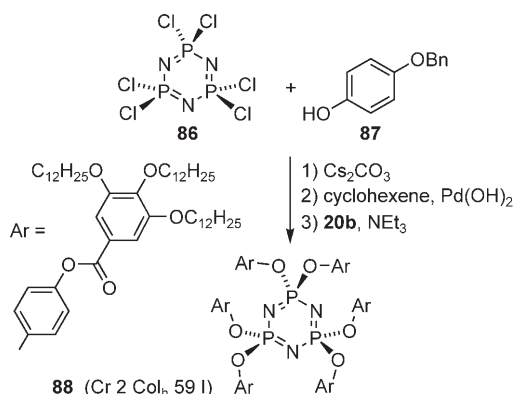
Scheme 34.

columnar mesophases are stable even at subambient temperatures. The phosphazenes are very promising because of their synthetic versatility, remarkable chemical stability, optical transparency from near-infrared to about 210–190 nm in the ultraviolet spectrum, and low flammability.

4.7. Azatriphenylene and tricycloquinoxaline derivatives

The logical extension of triazines towards n-type materials are the azatriphenylenes and tricycloquinoxalines. Surprisingly, this issue has been studied only very recently with seminal contributions from the research groups of Ohta[191] and Keinan.[192] On the way to porphyrin complexes, Ohta observed a broad hexagonal columnar mesophase for the diazatriphenylene **92a**, which was obtained from the benzil derivative **89a** by acid-catalyzed condensation with diamino-malodinitrile **90** followed by Lewis acid mediated cyclization (Scheme 35).[191] Even unsymmetrical systems such as **92b** displayed columnar mesophases.[193] Replacing the nitrile groups in **92a** by a hydrogen atom or an additional annelated benzene ring gave nonmesomorphic compounds.[194] The electronic properties of the electron-withdrawing nitrile groups seem to be responsible for the mesogenic behavior as they may enhance the π–π interactions between the aromatic cores that would stabilize the mesophase.

Condensation of phenanthrene-9,10-dione **93** with methyl 3,4-diaminobenzoate (**94a**) or 3,4-diaminobenzoic acid (**94b**) yielded the extended azatriphenylenes **95** (Scheme 36).[195] Surprisingly, a carboxylic acid instead of the ester group in **95** changed the mesophase from a hexagonal ordered columnar to a rectangular ordered and a nematic phase. In

Scheme 35.

92a R = R¹ = C₁₀H₂₁
(Cr 72 Col_ho 254 I)
92b R = C₁₀H₂₁, R¹ = C₆H₁₃
(Cr 38 Col_ho 216 I)

93 R = C₁₀H₂₁

95a X = Me (Cr 98 Col_ho 136 I)
95b X = H (Cr 122 Col_ro 196 N 209 I)
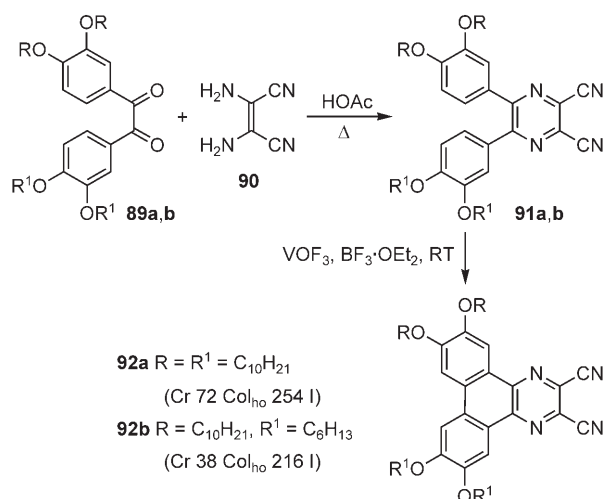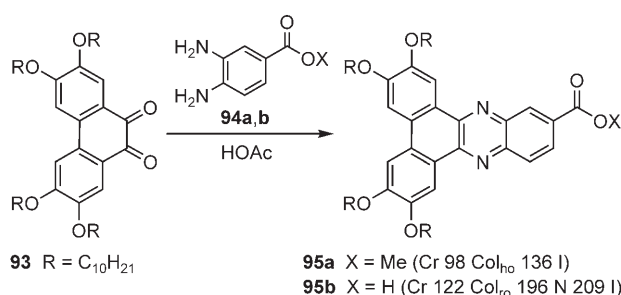
Scheme 36.

addition, both melting and clearing points and the stability of the mesophase were varied. This behavior could be explained by the formation of hydrogen-bonded dimers (Figure 35) which are better suited for a rectangular lattice as compared to the hexagonal lattice.

Figure 35. Simplified arrangement of the disk-shaped ester **95 a** and of the dimers of the acid **95 b**.

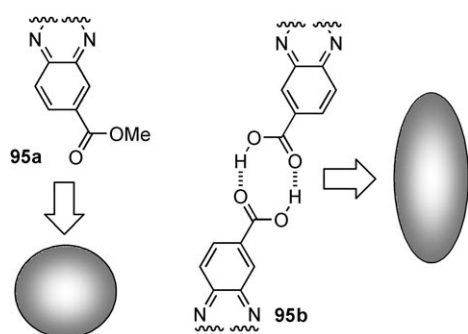While C_3-symmetrical triazatrinaphthylenes have only been studied with regard to 2D self-assembly on HOPG,[196] the hexaazatrinaphthylenes **98** were shown by Lehmann, Geerts, and co-workers to behave as π-deficient discotic mesogens, thus displaying rectangular and hexagonal columnar mesophases (Scheme 37).[197] The charge-carrier mobility

98a R = C₆H₁₃ (Cr 205 Col_hd)
98b R = C₁₀H₂₁ (Cr 113 Col_rd0 134 Col_rd1 181 Col_rd2 222 Col_hd)
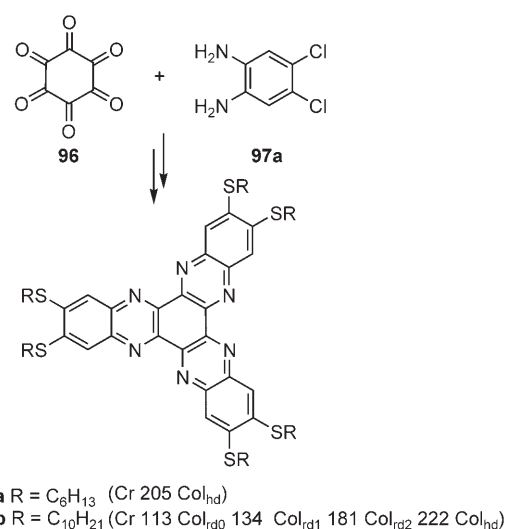
Scheme 37.

was found to be strongly dependent on the nature of the side chain (the sum of the hole and electron mobilities $\Sigma\mu_{1D}$ $< 0.01\ cm^2 V^{-1} s^{-1}$ for **98a**, and $\Sigma\mu_{1D} = 0.32\ cm^2 V^{-1} s^{-1}$ for **98b**). The combination of a low reduction potential (-1.09 V), which should facilitate electron injection, and high charge-carrier mobilities make these compounds good electron transporters. However, the transition temperatures are currently too high for practical use.

Based on their previous results with photoconducting thioether-substituted tricycloquinoxalines, Keinan and co-workers investigated the corresponding alkoxy-substituted analogues **101** (Scheme 38).[192] First 4,5-dimethoxy-2-nitro-benzaldehyde (**99**) was reduced with tin in acetic acid to give the oxazoline **100**. The latter was further condensed to give the C_3-symmetrical target compounds **101a** and **101b** with a hexagonal columnar mesophase. Later Boden, Bushby, et al. synthesized hexakis[2-(2-methoxyethoxy)ethoxy]tricycloqui-nazoline **101c**, which not only has a very broad columnar mesophase, but also facilitates n-doping with potassium metal because of the electron-poor/π-deficient nature of the core and the complexing ability of the diethylenoxy side chains

101a R = C₃H₇
(Cr₁ 237 Cr₂ 286 Col_h 306 I)
101b R = C₅H₁₁
(Cr₁ 144 Cr₂ 188 Col_h 301 I)
101c R = (CH₂CH₂O)₂Me
(Cr 77 Col_h 233 I)
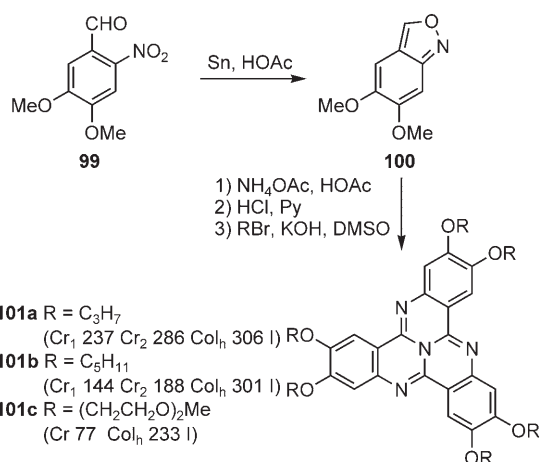
Scheme 38.

toward K^+ counterions.[198] In the Col_h phase, the conductivity increases from $\sigma = 6.073 \times 10^{-8}\,S\,m^{-1}$ by five orders of magnitude on doping with potassium to give $\sigma = 1.058 \times 10^{-3}\,S\,m^{-1}$ at 160°C. Furthermore, for **101c**, both hole and electron transport were observed, and a electron mobility $\mu_e < 4.5 \times 10^{-4}\,cm^2\,V^{-1}\,s^{-1}$ was determined by TOF experiments.

4.8. Phthalocyanine and porphyrin derivatives

Porphyrins and phthalocyanines are interesting materials because their physical and chemical properties can be tuned both by the substituents in the periphery and by the central metal ion. One of the main advantages of mesomorphic phthalocyanines[199] over many other discotic macrocycles is their strong absorption in the visible and NIR regions. However, for possible applications, the long-time stability of the mesophase as well as easy alignment is highly desirable.[200] Drenth and co-workers prepared phthalocyanines **103** by the cyclocondensation of dinitriles **102** (Scheme 39).[201a]
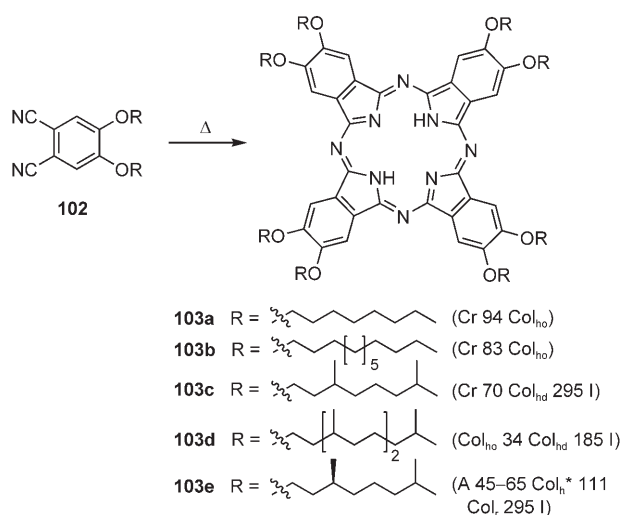
Scheme 39. A = amorphous phase.

A comparison of the side chains showed that the phthalocyanines **103c,d** with branched alkoxy chains display more phase transition than **103a,b** with unbranched side chains. Thus, the introduction of branching points in the alkoxy chain reduces the melting transition to such an extent that a stable mesophase was observed even at room temperature.[201a] If the metal-free phthalocyanine **103e** bears chiral aliphatic tails derived from (S)-citronellol, a novel chiral columnar mesophase Col_h^* was observed at room temperature, and an achiral rectangular columnar mesophase Col_r was observed at elevated temperature.[196b] Three different helical arrangements of **103e** in the chiral mesophase (Figure 36) were discussed by Nolte and co-workers.[201c] In the first, the phthalocyanine rings are arranged in a spiral staircase-like manner (a); in the second, the rings are positioned on top of each other, but the staggering angle between the neighboring molecules is nearly constant and always the same direction (b); in the third, the normal of the
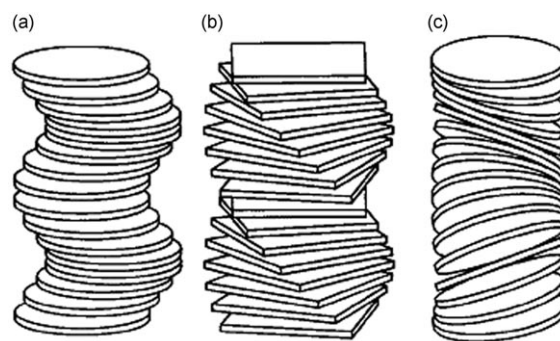

Figure 36. Possible helical arrangements of **103e**, represented as disks (a and c) and as a square (b). Reproduced from Ref. [201c]

plane of each phthalocyanine ring is tilted and gradually rotating along the stacking axis (c). Although X-ray analysis and CD results support an arrangement of **103e** as depicted in Figure 36c, the second arrangement (b) could not completely ruled out. To resolve this problem, **103e** was complexed with $Si(OH)_2$ and the resulting dihydroxy(phthalocyaninato)silicon polymerized. The CD spectra of the monomer **103e** and its polymer are completely different. The phthalocyanine rings in the polymer are suggested to arrange in a left-handed helix, that is in agreement with the structure in Figure 36b. This novel type of main-chain chirality in a polymer was termed "shish kebab" chirality"[201c] and might prove useful for nonlinear optical materials and optical switches.

Ino et al.[202] measured the hole mobility in 1,4,8,11,15,18,22,25-octaoctylphthalocyanine (**103** with C_8H_{17} instead of OR; Scheme 39) in the rectangular and hexagonal columnar phases, as well as in the isotropic phase by using the TOF technique because of the good long-range homeotropic alignment of the columns. In agreement with the expected higher charge mobility for molecules with a bigger core, a high mobility of $0.2\,cm^2\,V^{-1}\,s^{-1}$ was found in the rectangular columnar phase, with a decrease to about $0.1\,cm^2\,V^{-1}\,s^{-1}$ in the lower-order hexagonal phase.

Nolte, Rabe, and co-workers studied the self-assembly of the crown ether phthalocyanine **104** at the gel–graphite interface by using STM (Figure 37).[203] The molecular arrangement comprises two "face-on" phases and one "edge-on" lamellar phase. In organic solvents, **104** forms a gel in which helical fibers are present.

A bis-pocketed porphyrin **107** was prepared by Patel and Suslick[204a] by condensation of dialkyl 5-formylisophthalate **105** with pyrrole (**106**, Scheme 40).[204b] From both homologues, the decyl-substituted compound **107b** displays a hexagonal columnar mesophase even at room temperature.

4.9. Metallomesogens

The discussion of porphyrins and phthalocyanines in Section 4.8 is also true for liquid-crystalline metal complexes, that is, metallomesogens in general. The combination of the unique absorption, emission, fluorescence, and redox properties of the central metal cation with solubility, processibility, mesomorphic properties, and self-assembly of the ligand
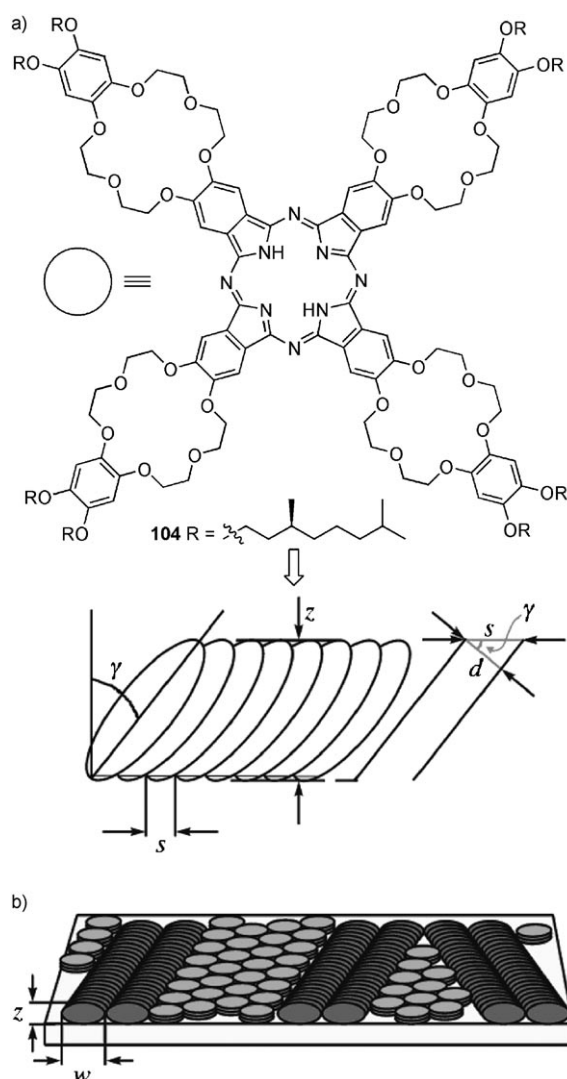
Figure 37. Self-assembled phthalocyanine **104** at the gel-graphite interface.[203]

Scheme 40.

107a R = C$_8$H$_{17}$ (Cr 132 I)
107b R = C$_{10}$H$_{21}$ (Cr −3 Col$_h$ 121 I)

108a X = H, Y = F (Cr 60 Col$_{hd}$ 115 I)
108b X = H, Y = CF$_3$ (Cr 114 Col$_{hd}$ 129 I)
108c X = H, Y = OMe (Cr 78 Col$_{hd}$ 83 I)

Scheme 41.

creates a set of unprecedented materials.[205] With respect to columnar mesomorphism, mainly metal complexes with diketonate, salicylaldimate, glyoximate, phthalocyanine, porphyrin, pyridine, and pyrazole groups have been successfully explored.

Swager and co-workers investigated in detail the chemistry of copper bis-β-diketonate complexes. Surprisingly, even the unsymmetrical systems such as **108** display stable enantiotropic hexagonal columnar mesophases (Scheme 41).[206] Substituent effects of various unsymmetrical copper and palladium β-diketonate complexes **108** were systematically studied by Lai and co-workers.[207] The formation of columnar phases strongly depends on the electronic and/or steric factors of substituents. Whereas bulky substituents (X = Me, Et) seem to favor rectangular columnar mesophases, electron-withdrawing substituents (X = Cl, Br, CN) induce hexagonal columnar mesophases.

Chiral oxovanadium(IV), copper(II) and palladium(II) diketonates **111**, which are accessible from the mixed aldol
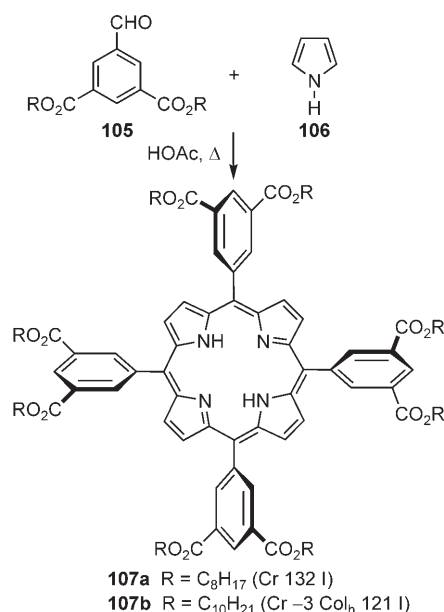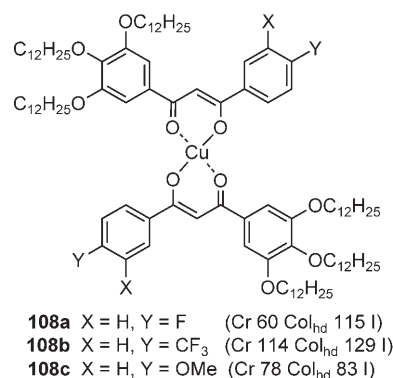
reaction of acetophenone derivative **109a** and gallic ester **20c**, followed by hydrogenolytic removal of the benzyl groups and subsequent esterification with (S)-2-hexyloxypropanoic acid (**110**), show columnar mesophases (Scheme 42).[208] CD data of spin-coated films confirmed a helical arrangement within the columns in the rectangular mesophase. In solution, no CD was observed, which indicates that the optical activity of the complexes does not arise from the individual stereocenters but from the columnar structures in the mesophase. In addition, compounds **111** undergo ferroelectric switching, and by application of an alternating electric field, an electrooptic effect can be observed for the complexes, which results from the strong tilting ($\approx 40°$) of the molecules with respect to the columnar axis.

Xie and co-workers prepared a binuclear discogen **114** based on the β-diketonate structural motif in a two-step procedure (Scheme 43).[209] Complex **114** not only shows two different rectangular columnar mesophases, but also displays reversible monoelectron oxidation at 0.76 V, which indicates a HOMO with high-hole injection ability. Indeed, the conductivity of iodine-doped **114** is raised more than hundredfold
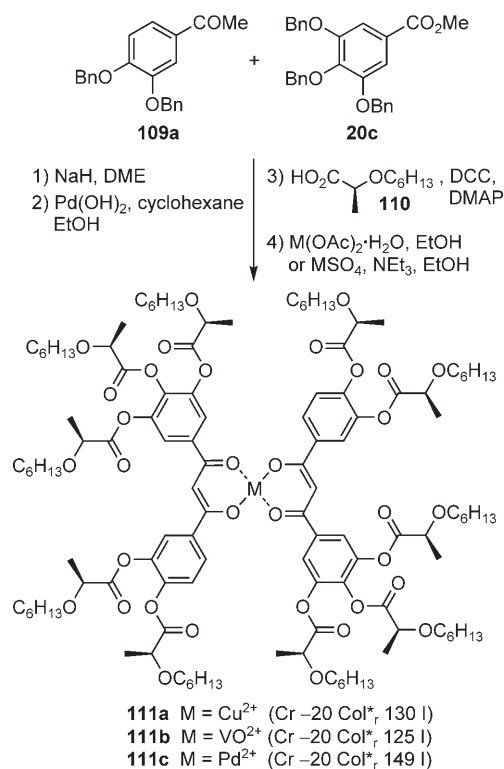
Scheme 42. DME = 1,2-dimethoxyethane.
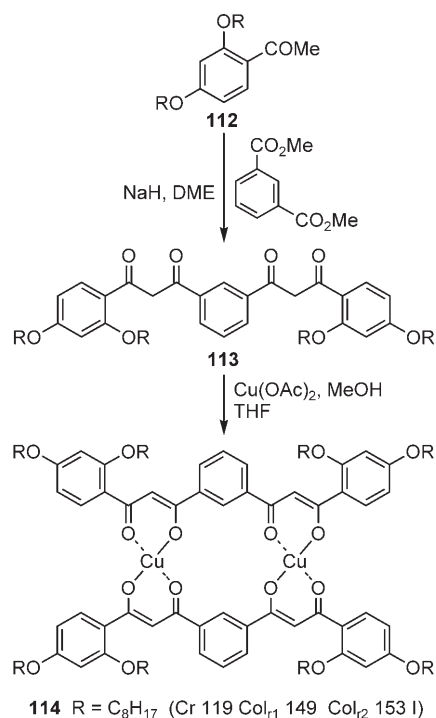
Scheme 43.

(from 10^{-4} to 10^{-6} S cm^{-1}) as compared to the corresponding mononuclear copper diketonate complex. Furthermore, STM revealed an ideal square-planar orientation, which makes these dinuclear complexes well suited for OLEDs.

A logical extension to the β-diketonate complexes are the enaminoketone complexes. The effect of a fluorinated side chain on the mesomorphism of nickel, copper, and oxovanadium complexes **117** with diaminoaryl-bridged enaminoketone ligands (Scheme 44) was studied by Szydlowska et al.[210]
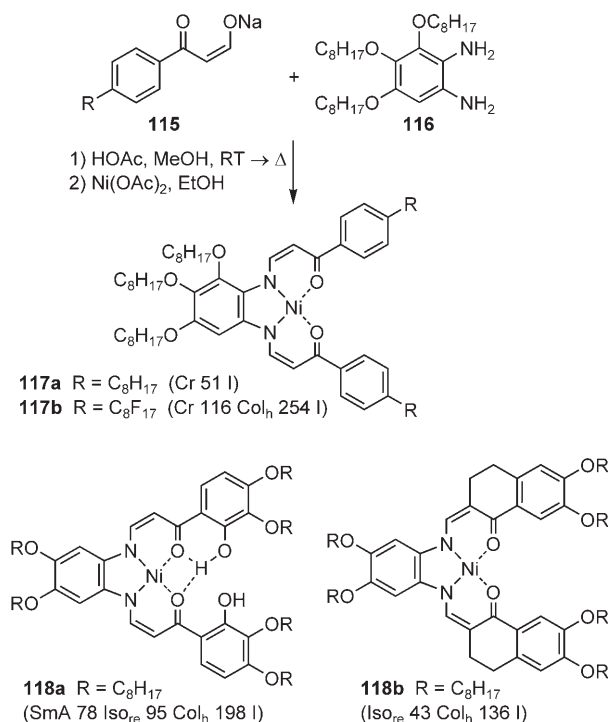
Scheme 44.

Replacing the alkyl chains by perfluorinated chains resulted in a hexagonal columnar phase. The perfluorinated chains are more rigid than their linear alkyl analogues because of higher energy barrier between the *trans* and *gauche* conformations. This rigidity gives more extended and more disklike molecules with stretched side chains that stabilize the Col$_h$ phase. A reentrant isotropic phase (Iso$_{re}$), in which the isotropic phase transforms into a mesophase on heating, is a very rare phenomenon among mesomorphic compounds. Szydlowska and co-workers discovered such reentrant isotropic phases for *cis*-enaminoketone nickel complexes **118 a,b** with additional hydrogen bonds.[211]

Salicylaldimato ligands are electronically related to the enaminoketones and thus should also be suitable for columnar LCs. While the majority of metal salicylaldimato complexes described so far display smectic and nematic mesophases, relatively few columnar mesophases have been published. For example, Serrano and co-workers prepared bis(salicylaldiminate) copper(II) complexes **120** (Scheme 45), which displayed rectangular columnar mesophases.[212] Date and Bruce found that an extension of the mesogenic core leads to hexagonal columnar mesophases.[213]

A mixed copper–lanthanide f–d metallomesogen **121**, which bears a di(salen) core, was reported by Binnemans et al. (Scheme 46).[214]

Ohta et al. found a novel disklike lamellar rectangular mesophase (Col$_{L,rec}$) for bis(diphenylglyoximato)nickel(II)
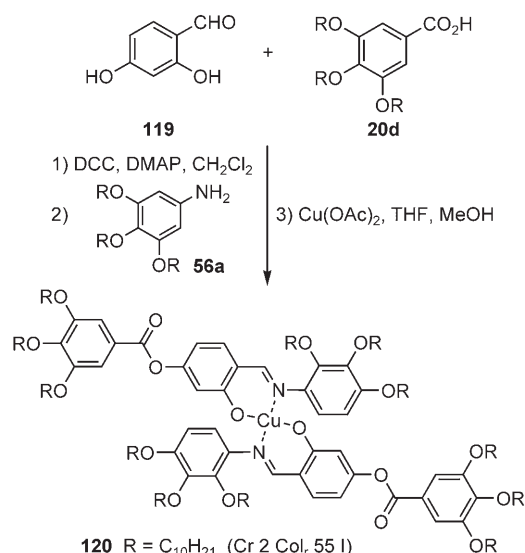
Scheme 45.
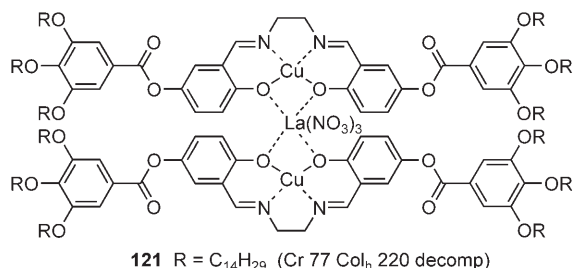
Scheme 46.

complexes **123d** and **123e** (Scheme 47).[215] If further alkyl or alkoxy chains were added to the periphery, hexagonal columnar mesophases resulted.
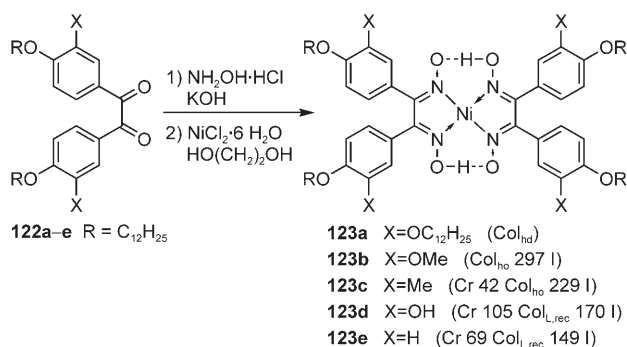
Scheme 47.

Complexes **124** with two different mesogenic ligand systems that employed *ortho*-metalated 2-phenylpyrimidine and a diketonate ligand have been designed by the research groups of Diele and Tschierske (Scheme 48).[216]

Lewis basic nitrogen heterocycles such as pyridine, pyrazole, and 1,3,4-oxadiazole have been used in a variety of columnar metallomesogens. For example, discotic silver
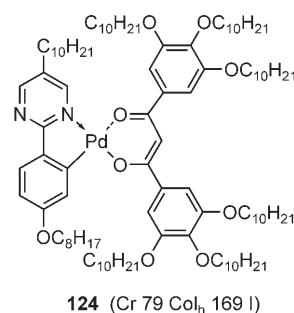
Scheme 48.

pyridine complexes **128** were described by Bruce and co-workers[217] (Scheme 49). Complexes **128** were prepared by base-catalyzed condensation of the imine **125** with 3,5-lutidine (**126**) and subsequent coordination of AgOTf. Even the bent-core pyridine **127** displays columnar mesophases, probably because of an antiperiplanar stacking in the columnar phase (Scheme 49).
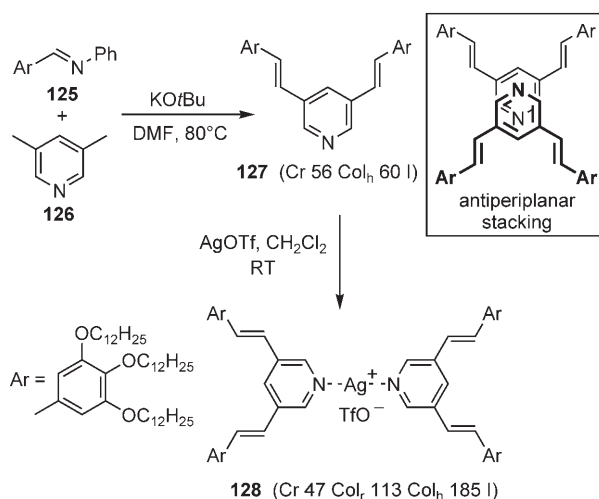
Scheme 49.

Douce, Ziessel, and co-workers prepared the first liquid-crystalline metallohelicate **130**. The bipyridine subunits **129** are nonmesomorphic and the macroscopic ordering was induced by the Cu^{2+} ion (Scheme 50).[218]

It should be noted that the central bipyridine subunit acts as a bridging ligand rather than a chelating ligand. The iminopyridine binding motif can be found in several other metallomesogens, for example **131**,[219] and **132**[220] (Scheme 51).

Pyrazoles have also been introduced as mesogenic subunits in metallomesogens. Serrano and co-workers described trinuclear gold complexes **133** which display hexagonal columnar mesophases (Scheme 52).[221] Noteworthy, luminescent superhelical fibers were obtained on attachment of dendrimer subunits to these "golden triangles" and these fibers were studied by STM.[222] This is one of the rare examples where an achiral building block self-assembles into a helical aggregate.

Scheme 50.

131 R = C₈H₁₇ (Cr 30 Col_h 81 I)

132a–c R = C₁₂H₂₅
132a Ln = Tb (g 160 Cub 171 decomp)
132b Ln = Er (g 150 Col_h 180 Cub 185 decomp)
132c Ln = Yb (g 175 Col_h 195 decomp)

Scheme 51.

133 R = C₁₀H₂₁
(Cr 59 Col_hd 64 I)
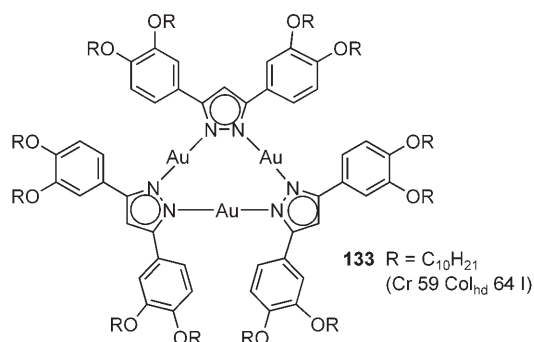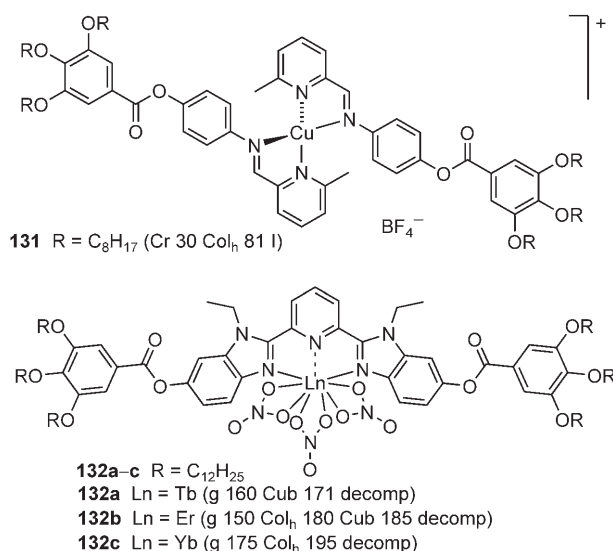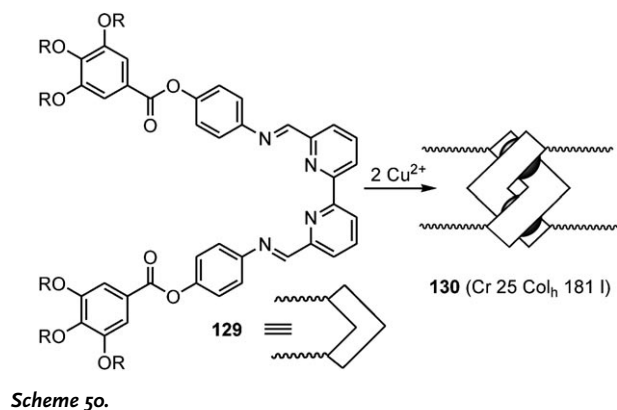
Scheme 52.

Symmetrical pyrazoles are capable of acting as monodentate ligands, as exemplified for the palladium(II) 1,2,3-oxadiazole complex **135**, which was prepared from the hydrazide **134** (Scheme 53).[223]

Either hydrogen bonds or sulfur–sulfur interactions, as in octakis(2-benzyloxyethylsulfanyl)copper(II)phthalocyanine (**137a**), may be used to promote the self-assembly (Scheme 54).[224]

135 R = C₁₀H₂₁
(Cr 1 Col_r 126 I)

Scheme 53.

137a R = (CH₂)₂OBn
(Cr 134 Col_rd 299 decomp)

Scheme 54. DBU = 1,8-diazabicyclo[5.4.0]undec-7-ene.
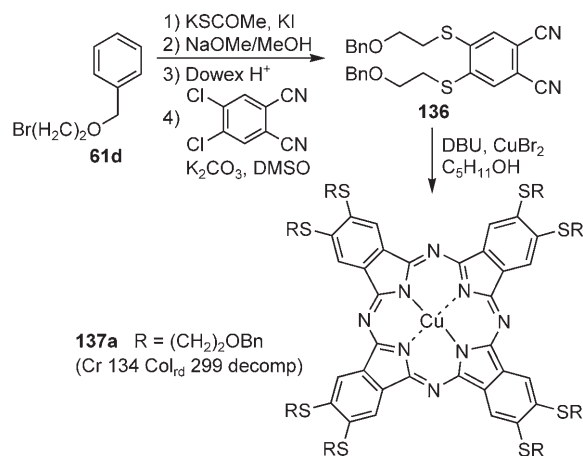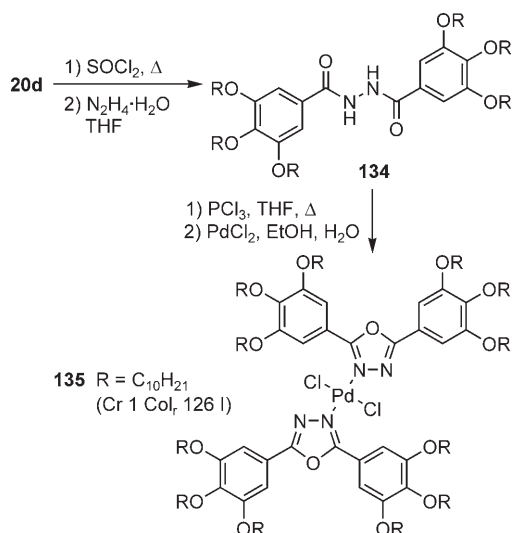
Studies of LB films of these compounds by AFM showed two different column–column spacings on annealing, a behavior that was also found for the polycrystalline material of **137a**. Some very common features of phthalocyanine complexes are their broad mesophase range and the absence of any isotropization under the decomposition temperature, which does not allow the observation of typical textures.[225] Compound **137b** was obtained by cyclocondensation of the dicyano-substituted triphenylene **138b** in the presence of Zn²⁺ (Scheme 55). Magnetic uniaxial alignment of the columnar superstructure of discotic octa(*n*-dodecylthio)porphyrazinecobalt in the centimeter scale was very recently reported by Choi and co-workers.[226]

The coordination of lanthanides to porphyrins gave the square-pyramidal complexes **139a** and **139b**, in which the lanthanide ion lies above the porphyrin plane (Scheme 56).[227] As shown by Simon and co-workers, derivatives of lutetium phthalocyanine display interesting magnetic properties.[228]

Although the chemistry of (η⁶-arene)tricarbonylchromium complexes is well known and some calamitic deriva-

4864   www.angewandte.org

© 2007 Wiley-VCH Verlag GmbH & Co. KGaA, Weinheim

Angew. Chem. Int. Ed. **2007**, *46*, 4832–4887
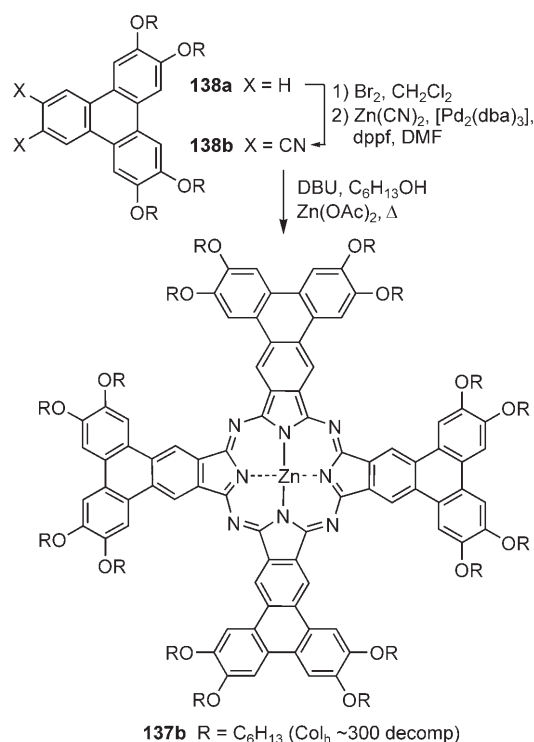
Scheme 55. dba = *trans,trans*-dibenzylideneacetone; dppf = 1,1′-bis(di-phenylphosphanyl)ferrocene.
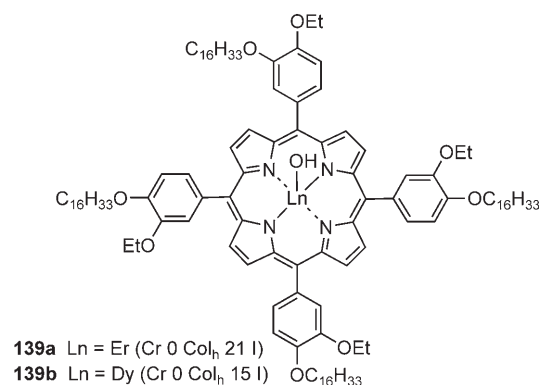
Scheme 56.

tives have been reported,[229] there are few examples of discotic arene chromium complexes. Deschenaux, Levelut, and co-workers reported an interesting change of the mesomorphic properties of compound **143** on complexation with {Cr(CO)$_3$} (Scheme 57).[230]

While the uncomplexed compound **143** displayed a hexagonal columnar mesophase,[231] columnar mesomorphism vanished on complexation with {Cr(CO)$_3$} and a smectic C mesophase was obtained instead. Laschat and co-workers also observed a dramatic effect with (triphenylene)tricarbonyl-chromium complexes **144** (Scheme 58).[232] Whereas complexes **144** with short alkyl chains were nonmesomorphic, the nonyl derivative **144** (R = C$_9$H$_{19}$) displayed a Schlieren texture typical for a nematic discotic phase which was further supported by X-ray diffraction experiments.
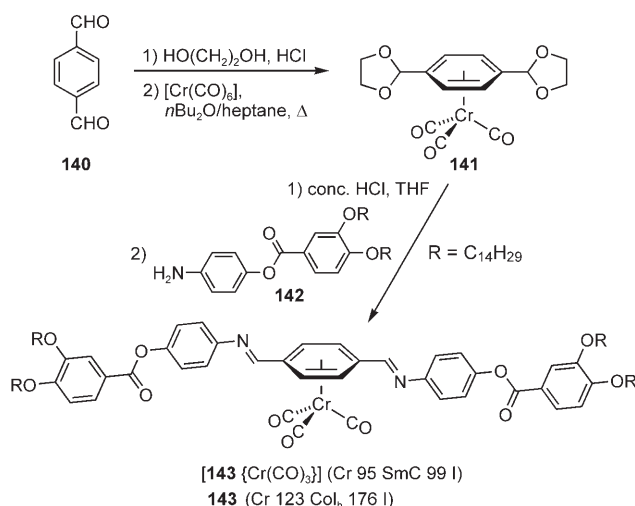
Scheme 57.
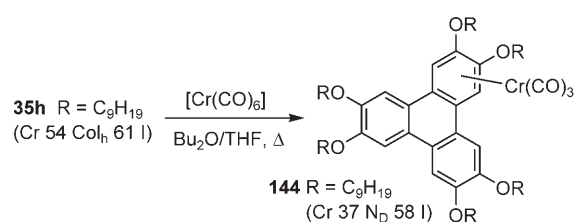
Scheme 58.

4.10. Crown ethers and macrocycles

The combination of crown ethers (or azacrowns) with mesogenic subunits is interesting for several reasons.[60p,233,234] The crown ether unit is able to either modify existing mesophases or induce novel ones because of complexation of metal ions and self-assembly processes. In addition, as a result, the solubility and conductivity are improved. Depending on the particular size of the crown metal ions, the crown ethers can be used as sensors. Three different design strategies have been reported with respect to columnar mesophases.

The first strategy uses rodlike mesogens that were tethered to crown ether units. Typically, most of these molecules form smectic or nematic phases,[235a] and are known as components of liquid-crystalline polymers.[235b] Tschierske and co-workers reported compounds such as **145**, which consist of a rigid calamitic 4,4′-didecyloxy-*para*-terphenyl unit and a crown ether subunit in the lateral position.[235c] For the uncomplexed crown ether **145**, a mono-tropic smectic A and nematic phase were observed (Figure 38).

The situation completely changed on complexation. When **145** was saturated with aqueous 1M alkali metal salts MCl (M = alkali metal), a lyotropic system was obtained. The size of the cation significantly influenced the stability of the induced rectangular columnar mesophases and resulted in different clearing temperatures: the maximum mesophase stability was found for K$^+$ (Figure 38) and the clearing

145
Cr 45 (SmA 13 N 15) I
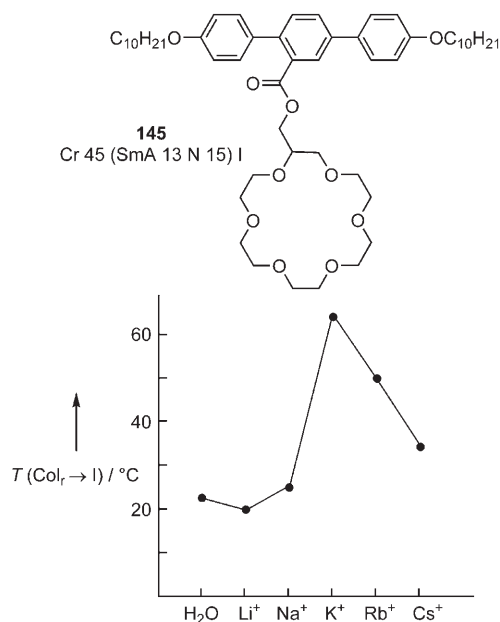
Figure 38. Crown ether **145** and the dependence of clearing temperatures of the mesophase of **145**/1 M MCl/H_2O on the cation M^+.[235c]

temperature also changed depending on the anion (KCl < KBr < KI).

Bruce, Schröder, and co-workers synthesized a 1,4-dithia-7-azacyclononane **146a**, which is tethered terminally rather than laterally to the mesogenic subunit (Scheme 59).[236] This hemiphasmidic compound **146a** forms a hexagonal columnar mesophase. If the three peripheral dodecyloxy chains were replaced by one octyloxy chain as in **146b**, smectic A and nematic mesophases were obtained instead of hexagonal columnar mesophases.[236,237]

146a R = R^1 = $OC_{12}H_{25}$ (Cr 37 Col$_h$ 48 I)
146b R = H, R^1 = OC_8H_{17}
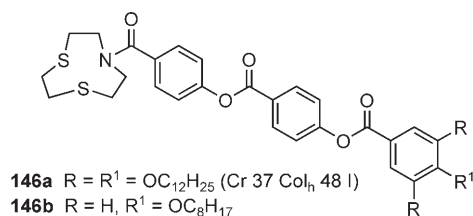
Scheme 59.

The second strategy uses propellerlike mesogens that are tethered to crown ether units. To obtain a columnar LC with a central crown ether core, Laschat and co-workers prepared the dibenzo[18]crown-6 derivatives **149** by a convergent synthesis route (Scheme 60).[238] First, 4-bromo-1,2-dialkoxy-benzenes **34** were converted into the corresponding boronic acids **148**, which, by subsequent Suzuki coupling with the tetrabromide **147b** (obtained by bromination of dibenzo[18]crown-6 **147a**) gave the crown ether derivatives **149**. Even compounds **149** with short alkyloxy chains such as R = C_5H_{11} display hexagonal columnar mesophases. However, a remarkable stabilization of the columnar mesophases was observed on complexation with KI. The benzo crown structural motif with only one *ortho*-terphenyl unit was

147a X = H
147b X = Br
34 Y = Br
148 Y = B(OH)$_2$

[Pd(PPh$_3$)$_4$], Na$_2$CO$_3$
DME/H$_2$O

149 R = $C_{10}H_{21}$ (Cr$_1$ 38 Cr$_2$ 67 Col$_h$ 84 I)
149·KI R = $C_{10}H_{21}$ (Cr 58 Col$_h$ 150 I)
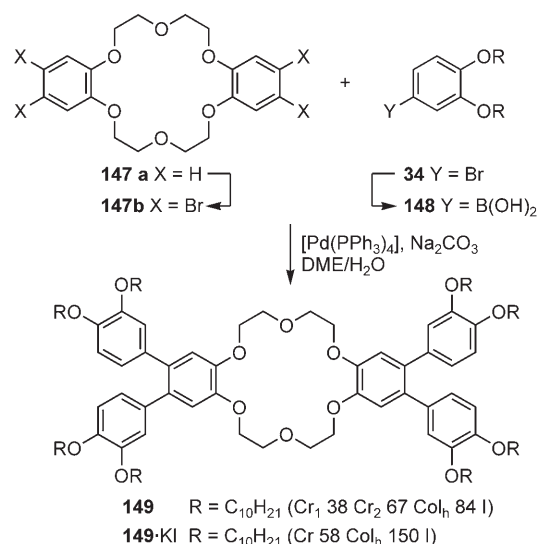
Scheme 60.

further explored[45] to determine whether benzo[15]crown-5 derivatives **150** (Scheme 61) might display columnar mesophases even in the absence of metal salts.

150a R=$C_{10}H_{21}$ (Cr 65 I)
150a·NaI (Cr 43 Col$_r$ 163 I)
**150b** R=$C_{12}H_{25}$ (Cr 40 Sm 71 I)
150b·NaI (Cr 55 Col$_h$ 162 I)
150c R=$C_{14}H_{29}$ (Cr 55 Sm 77 I)
150c·NaI (Cr 43 Col 171 I)
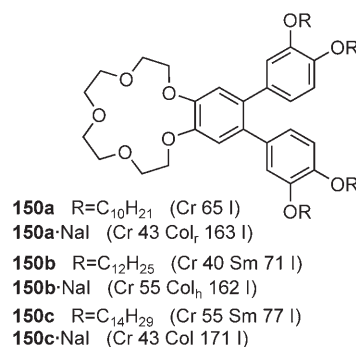
Scheme 61.

Indeed, the metal-free crown ethers **150** were mesomorphic, with a minimum chain length of C_{12}, and a smectic rather than a columnar mesophase was obtained.[45] In contrast, the corresponding NaI complexes display either columnar rectangular phases (chain length of C_{10}) or hexagonal columnar phases (> C_{10}). In agreement with results by Percec et al.,[239] Laschat and co-workers also observed an improved mesophase stability for benzo[15]crown-5 complexes **150·NaI** because of complexation with the Na^+ ion.

The third strategy uses wedge-shaped mesogenic units that were attached to a crown ether head group. Percec et al. reported that complexation with Na^+ or K^+ ions destabilizes the crystalline phase and induces the self-assembly of supramolecular columns, in which the polar crown core forms the center of the column while the nonpolar alkyl chains are radiated towards its periphery, which results in cylindrical ion channels.

These crown ether derivatives were first described by Percec et al.[239] and later explored by the research group of Beginn and Möller.[240] Crown ether **154** was prepared from

methyl 4-(10-undecenyl-1-oxy)benzoate **151**, which was converted in four steps into the tris-methacrylated acid **152**. The latter was finally attached to the (2-hydroxymethyl)benzo[15]crown-5 ether (**153**, Scheme 62).[240a] The wedge-shaped crown ether **154** displayed a columnar mesophase, whose

154

Figure 39. Self-assembly of **154** into columnar superstructures and formation of oriented matrix-fixed supramolecular channels. Reproduced from Ref. [240c].

generated amphiphilic crown ethers, which form planaraligned columnar mesophases upon casting on a warm water surface.[241]

Macrocyclic mesogens based on areno-condensed annulenes are interesting because they are well suited towards aggregation and photodimerization. The research group of Meier prepared a variety of liquid-crystalline annulenes.[242,243] For example, the [12]annulene **158** was available from Arbuzov reaction of the tetrabromide **155**, followed by Horner olefination with **156**, and acetal cleavage to give the resulting tetraaldehyde **157**, which underwent a twofold McMurry reaction (Scheme 63).[243]

Scheme 62.

stability was improved by complexation with NaOTf.[239] The self-assembly of crown **154** was used to design matrix-fixed supramolecular channels, as the amphiphilic compound was found to be an excellent organogelator forming well-defined supramolecular cylindrical fibers. Membranes were prepared from a lyotropic system of **154** in methylacrylate as solvent along with a photoinitiator. Cooling induced the thermoreversible gelation of the mixture as a result of the formation of networks of cylindrical aggregates. Finally, the olefinic terminal groups were copolymerized with the solvent and the aggregates became embedded in a polymer matrix, in which the supramolecular channels were maintained (Figure 39).

The observed differences in the ion-transport rate for Li^+, Na^+, and K^+ ions in the matrix are consistent with a hopping transport mechanism, where the least-interactive Li^+ ion migrates most quickly. Substitution of the methacrylateterminated chains in **154** with semifluorinated alkyl chains

Scheme 63.

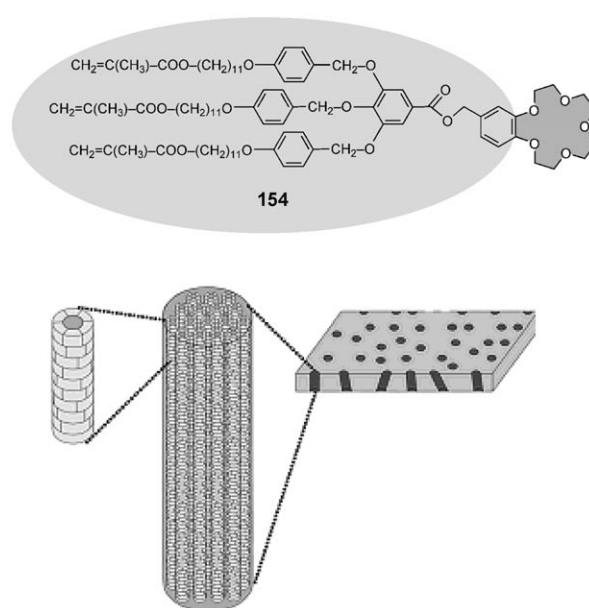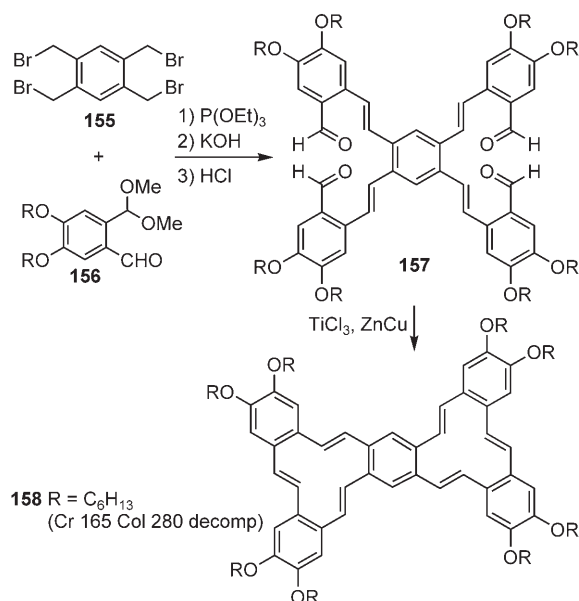Areno-condensed annulenes such as **159a** (Scheme 64) are photoconductors. Above 150°C, an irreversible photo-reaction takes place that leads to the belt cyclophanes **159b** or to a nonspecific cross-linking of the disks.[244] Meier et al. used compounds **159a** and **159b** to study the mechanisms of fluorescence.[242f,g]
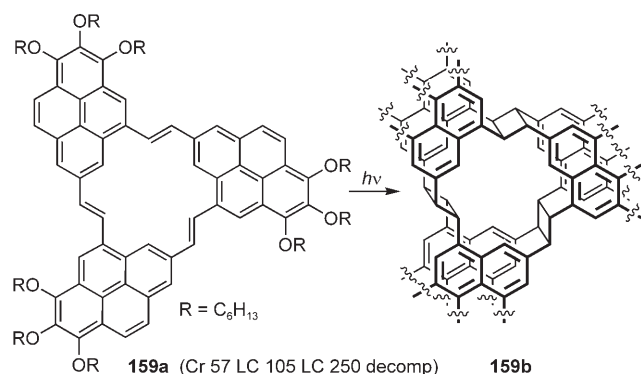
Scheme 64.

In contrast to the annulenes **159,** which can undergo conformational changes, the phenylacetylene macrocycle **160** resists a change in shape (Scheme 65).[245]
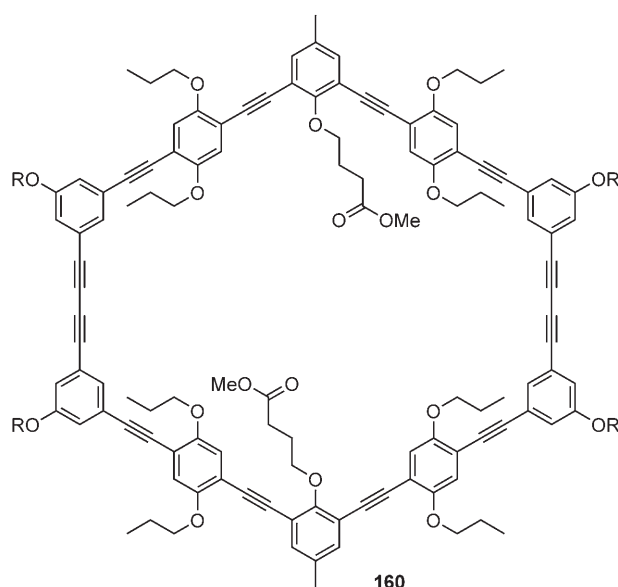
Scheme 65.

Based on seminal work by Zhang and Moore,[246] the research group of Höger demonstrated that the alkoxy chains in these systems are oriented toward the internal volume to avoid empty space and thus result in a discotic LC with an inverted structure as depicted in Figure 40.[245]

Figure 40. Schematic representation of a conventional cyclic molecule and a macrocycle such as **160** with inverted structure. Reproduced from Ref. [245c].

4.11. Columnar mesogens based on hydrogen bonds

The issue of liquid-crystalline aggregates has been covered extensively by a recent review by Kato et al.,[247] and thus, only two examples will be discussed with regard to applications.[248] According to Ivanov and co-workers, the columnar order of hexacarboxamidohexaazatriphenylenes **161** (Scheme 66) is strongly enforced by the amide hydrogen
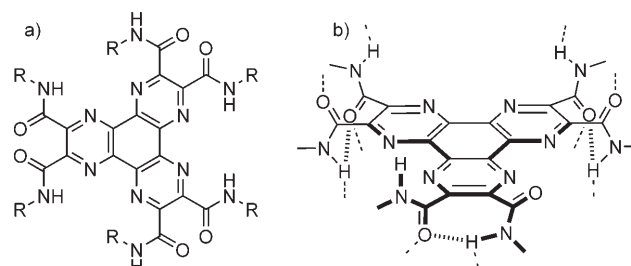
Scheme 66. The structure b illustrates the various possible arrangements of intra- and intermolecular hydrogen bonds.[249]

bonding between the neighboring molecules in the stacks, which helps to preserve the structural order and allows only a small thermal expansion of the intracolumnar distance.[249]

The interdisk distance of 3.18 Å in **161** is the smallest ever found in columnar liquid crystals. The intracolumnar correlation length varies between 120 and 180 Å, and thereby extends over 40–55 disks. PR-TRMC experiments revealed an improved charge-carrier mobility ($\Sigma\mu_{1D} = 0.04$–$0.08\ cm^2\,V^{-1}\,s^{-1}$) as compared to non-hydrogen-bonded triphenylenes. These results make **161** attractive for applications as semiconductor.

Kishikawa et al. synthesized N,N'-bis(3,4,5-trialkyloxyphenyl)ureas such as **162** that exhibited both rectangular and hexagonal phases, in which the molecules in each column were stacked in one direction with strong hydrogen bonds. This result leads to ferroelectric switching of columnar areas even in the absence of any chirality (Scheme 67).[250]
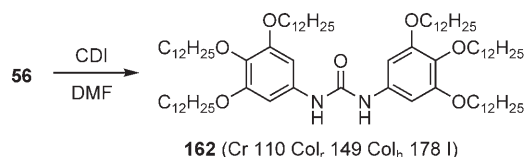
Scheme 67.

4.12. Columnar mesogens based on ionic interactions

Ionic interactions for the stabilization of mesophases have only recently been introduced.[247] The noncovalent strategy is advantageous because the properties might be tuned separately by altering both the cation and the anion. An early example was published by Veber, Levelut, and co-workers who synthesized the dithiolium salt **164a** by condensation of

4-alkoxybenzaldehyde **163** with acetophenone **109b**, and subsequent cyclization with P_4S_{10} (Scheme 68).[251]

164a R = $C_{10}H_{21}$ (Cr 107 Col_r 126 Col_h 144 N_{col} 174 I)
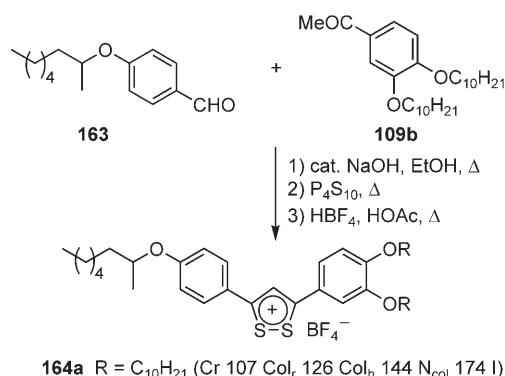
Scheme 68.

Careful temperature-dependent SAXS experiments of derivative **164b** (R = $C_{12}H_{25}$) revealed the presence of three different mesophases: rectangular columnar, hexagonal columnar, and nematic columnar (Figure 41).
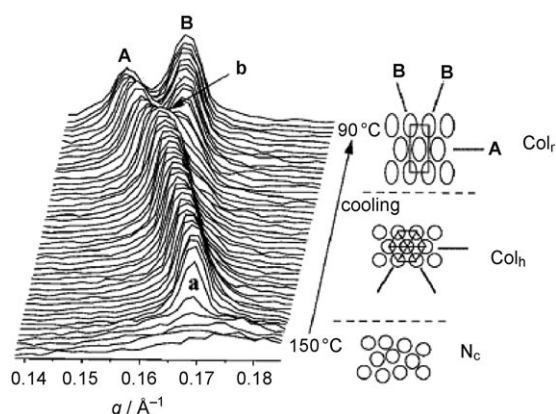
Figure 41. SAXS experiments of **164b**. Intensities of the profile on cooling and the corresponding 2D space groups. The N_c to Col_h and Col_h to Col_r transitions are described by **a** and **b**, respectively.[251]

The supramolecular organization is proposed to arise from the amphipathic feature of the dithiolium salts, which form long columnar aggregates similar to long inverted cylindrical micelles. The arrangement of the columns in a nematic columnar phase at higher temperatures support the supposition that specific interactions are necessary to obtain N_c mesophases (see Section 2.5).

Several groups have investigated a new class of ionic liquids such as **165** and **166** (Scheme 69). Compound **165** exhibited a columnar hexagonal mesophase over a wide temperature range, and Kato and co-workers successfully measured a 1D ionic conductivity.[252] The conductivity parallel to the columnar axis of **165** is much higher than that perpendicular to the axis because the alkyloxyphenyl moieties operate as an insulator. The incorporation of lithium salts led to the enhancement of the ionic conductivity from

165 (Cr 17 Col_h 183 I)
165·LiBF₄ (Cr 17 Col_h 193 I)

166a X=HC≡CCO₂ (Col_r 93 I)
166b X=BF₄ (Cr 37 Col_h 173 I)
166c X=NO₃ (Cr 97 Col_h 140 I)
166d X=Cl (Cr 78 Col_h 114 Cub 165 I)
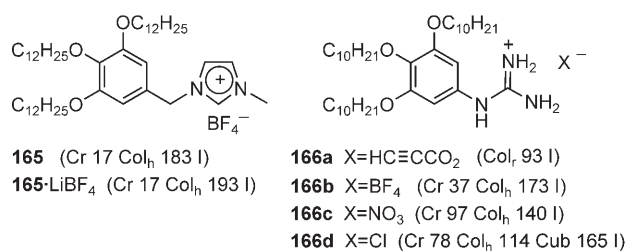
Scheme 69.

$3.1 \times 10^{-5}\,S\,cm^{-1}$ (for **165**) to $7.5 \times 10^{-5}\,S\,cm^{-1}$ (for $LiBF_4$·**165**) at 100°C. Probably the ions are incorporated in the central ionic part of the column.

Kim et al. observed several different self-organized structures for guanidinium salts **166** that depended on the guest anion (Scheme 69).[253] With polyatomic anions such as BF_4^- and NO_3^-, **166** form only columnar hexagonal phases, while **166a**, which contains a cylindrical carboxylate as the guest, has a rectangular phase. The chloride **166d** not only arranges in a columnar, but also a micellar cubic phase. The mesogenic subunit can also be extended to alkoxytriphenylenes that are tethered to pyridinium ions (**167a**),[254] or one (**167b**), or six imidazolium ions (**168**).[255,256] These triphenylene-based salts were found to be mesomorphic and exhibited columnar mesophases (Scheme 70).

167a X = (Cr₁ 76 Cr₂ 96 Col₁ 113 Col₂ 121 I)

167b X =

168 R =

(Cr 47 Col 111 I)
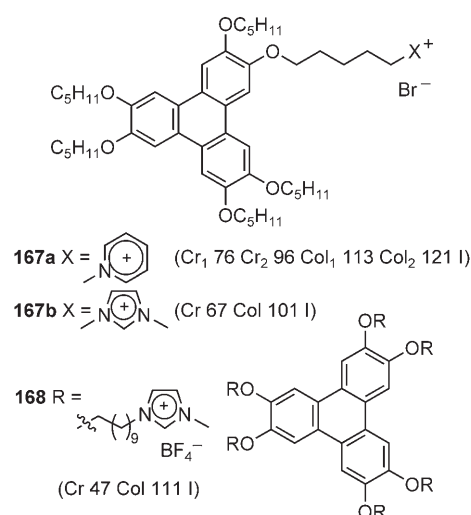
Scheme 70.

The research group of Faul presented an elegant strategy to liquid-crystalline material, in which a water-soluble tricycloquinazoline core is generated by the hydrolysis of the nonionic hexaacetate **169**, itself being a potential mesogen. The intermediate core fragment was then used as a hexaanionic building block for assembly into the liquid-crystalline aggregates **170** using the ionic self-assembly (ISA) technique (Scheme 71).[257] The authors found that the balance between alkyl volume, fragment shape, and number of charges was important for the phase architecture and properties. The transition temperatures can be controlled very easily, thus providing "liquid crystals on demand".

170a R = C_5H_{11} (Cr 185 Col$_h$ 299 I)
170b R = C_9H_{19} (Cr 80 Col$_h$ 237 I)
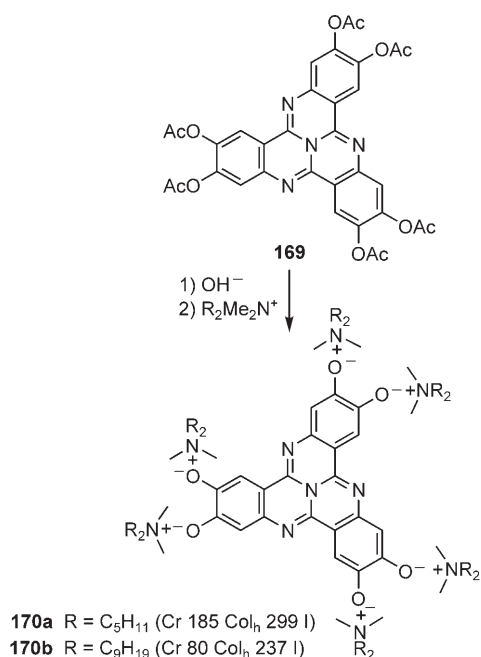
Scheme 71.

This technique can also be applied to metallomesogens.[257] As shown in Scheme 72, Cu^{2+} salts were coordinated with the phenanthroline **171** to yield the Cu^{2+} complex **172**, which undergoes ionic self-assembly with an ammonium salt to give **173**.

171 R = H

172 R = H, X = —
173 R = H, X = $(C_{18}H_{37})_2Me_2N$ ← $(C_{18}H_{37})_2Me_2N^+$
(Col$_{ob}$, Col$_r$)
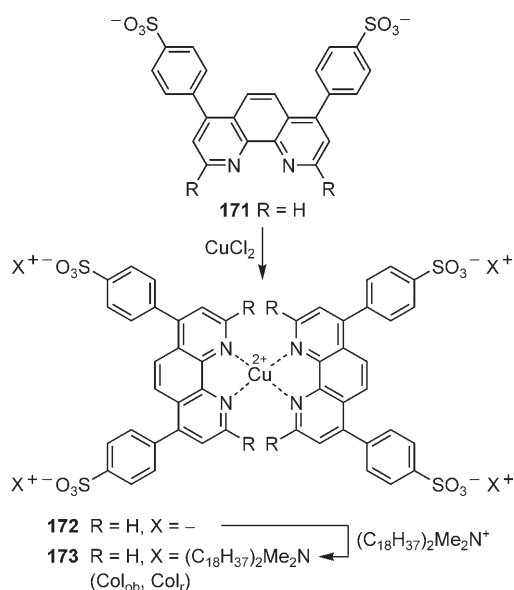
Scheme 72.

4.13. Columnar mesogens based on charge-transfer or donor-acceptor systems

Ringsdorf and Wendorff[258] were the first who studied the behavior of polymeric columnar main-chain and side-chain LCs when mixed with strong nonmesomorphic electron

acceptors such as TNF or TNF-CN (Scheme 4).[259] The electron acceptor not only induces mesophases, but also strongly increases the mesophase stability, as exemplified for mixtures of triphenylenes **37** and TNF.[258] Later studies using the UV/Vis spectroscopy of oriented thin films revealed that the charge transfer occurs through alternating stacks of donors and acceptors,[260] and is also observed in LB films.[261] Recently, Lee and Chang reported the molecular ordering of photoreactive nonmesogenic 1,3,5-triazine **174** into columnar mesophases by charge-transfer (CT) interaction with TNF (Scheme 73).[262]

174 (Cr 64 I)
174·TNF (Col 134 I)
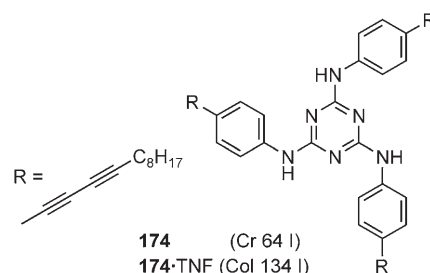
Scheme 73.

Besides TNF and TNF-CN, other electron acceptors have been used in CT complexes. Park et al. studied complementary C_3-symmetric donor-acceptor components based on electron-rich mesogenic hexaalkoxytriphenylenes **35** and electron-poor nonmesogenic tri-*n*-alkylmellitic triimides **175** (Scheme 74).[263]

175a R = C_4H_9
175b R = $C_{10}H_{21}$ (Cr 117 I)

175b·35i (Cr 40 Col$_h$ 136 I)
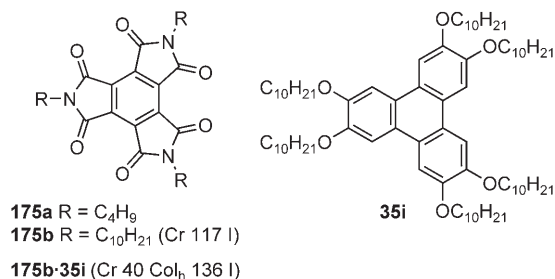
Scheme 74.

An X-ray crystal structure of tri-*n*-butylmellitic triimide **175a** and hexahydroxytriphenylene **42** (Scheme 16) revealed discrete acceptor-donor-acceptor triads with essentially complete overlap of the π faces (Figure 42).

Perfluoroarene–arene interactions, which can also influence the phase behavior of liquid-crystalline materials, are related to the charge-transfer interactions, as was demonstrated by Grubbs and co-workers.[102] A novel method for improving the applicable properties of discotic liquid crystals was recently introduced by the research group of Bushby.[264] Significant enhancement of mesophase ranges was obtained by mixing hexagonal columnar triphenylene **35d** with one equivalent of the large-core polynuclear aromatic compounds **176** (Scheme 75).
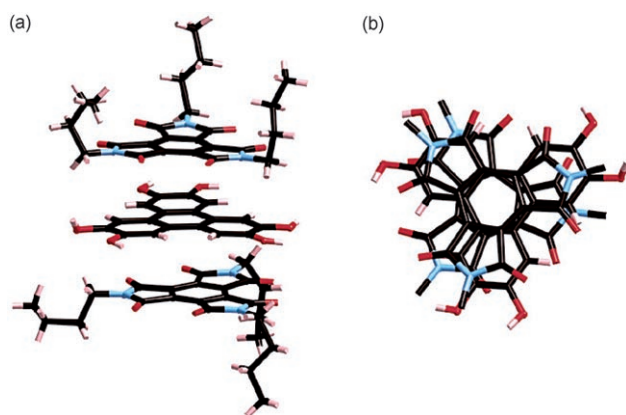
Figure 42. a) Side and b) top view of the acceptor-donor-acceptor triad in the X-ray structure of **175a·42**. Reproduced from Ref. [263].

176a X = N (Cr₁ 71 Cr₂ 81 I)
176b X = CH (Cr 59 I)

35d·176a (Cr 130 Col_h 240 I)
35d·176b (Cr 66 Col_h 155 I)
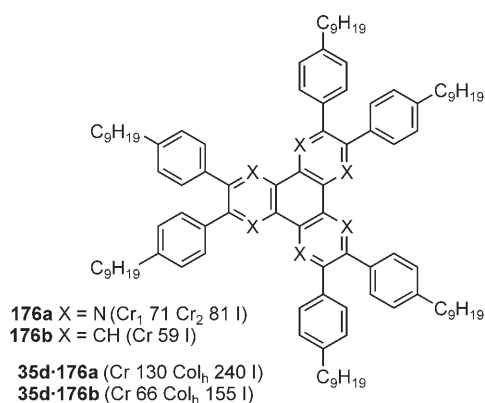
Scheme 75.

The special stability of these novel π-stacked systems arises from a complementary polytopic interaction (CPI), that is, a sum of atom-centered van der Waals and quadrupolar terms.

4.14. Dimers, oligomers, dendrimers, and rod-disk-shaped mesogens

Triphenylene-based columnar liquid-crystalline dimers, oligomers, and polymers have been reviewed recently by Kumar,[80] and therefore the following discussion will be limited to some illustrative examples.[265,266] Mesogenic dimers (twins) or oligomers are formed by tethering two or more mesogenic subunits. If the tether length is chosen correctly and the subunits are identical, the mesophase properties can be improved compared to the corresponding monomer. In contrast, the combination of two different mesogenic subunits or one mesogenic and a nonmesogenic subunit might result in twin materials with novel properties. The same is true for oligomers and dendrimers.

The effect of the spacer length has been studied by Luz and co-workers for a series of homologous dimers **182** (Scheme 76).[267] Tetrahydroxybenzoquinone **177** was first sequentially acylated and, after reduction with SnCl₂/HCl, intermediate **179** was obtained. Acyl transfer of **179** with **181**

182a n = 6   (Cr₁ 75 Cr₂ 116 I)
182b n = 12 (Cr 75 Col_rd 97 I)
182c n = 10 (Cr 128 I)
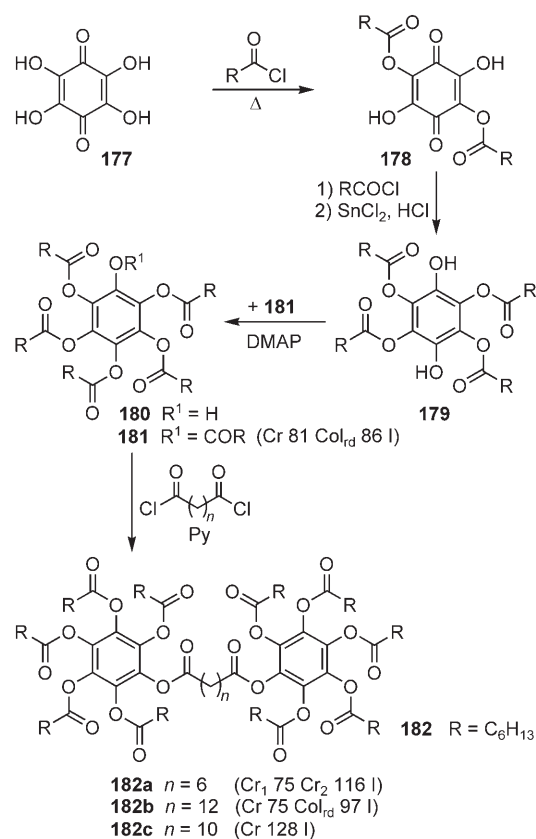
Scheme 76.

gave the monohydroxy compound **180**, which was finally esterified with the α,ω-diacid chloride to the desired twin compounds **182**. In the case of **182a** and **182c** with tether lengths of n = 6 and 10, respectively, the mesophases completely disappeared. However, with a correct tether length (**182b** with n = 12), a rectangular columnar mesophase with an increased temperature range was generated.

The remarkable effect of additional mesogenic subunits on the mesophase stability was found for the tetramer **183a**, which was prepared by fourfold Williamson synthesis (Scheme 77).[89] Compound **183a** displayed a broad hexagonal

183a R = C₇H₁₅, R¹ = Me (g –40 Col_h 80 I)
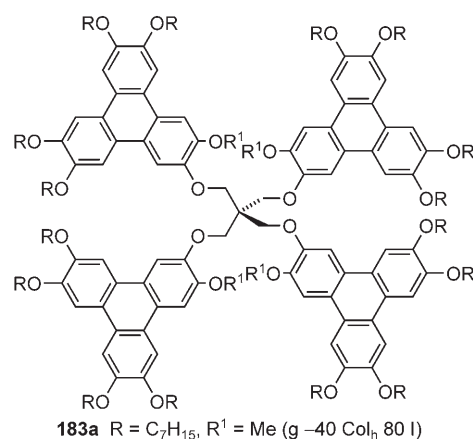
Scheme 77.

columnar mesophase that was stable even at room temperature.

Novel mesophases could be induced, even for symmetrical twin compounds, if rigid tethers are used (Scheme 78).[268] While the monomer **184** displayed a hexagonal columnar mesophase, the twin **185** displayed a nematic discotic mesophase.
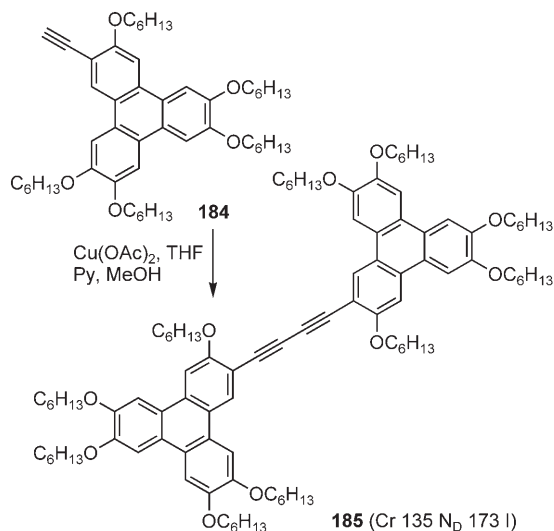
Scheme 78.

Charge-transfer or donor-acceptor twin compounds are especially attractive targets with regard to novel mesomorphic properties. Wendorff, Ringsdorf, and co-workers were among the first who prepared tethered donor-acceptor twins.[269]

Laschat and co-workers prepared the triphenylenes **186**, which were tethered to an anthraquinone moiety, to obtain redox-active liquid-crystalline twin compounds (Scheme 79).[270] Although compound **186** displayed quasi-reversible redox behavior in solution, the mesophase width was quite small, and unfortunately the type of mesophase could not be established. Probably the anthraquinone moiety
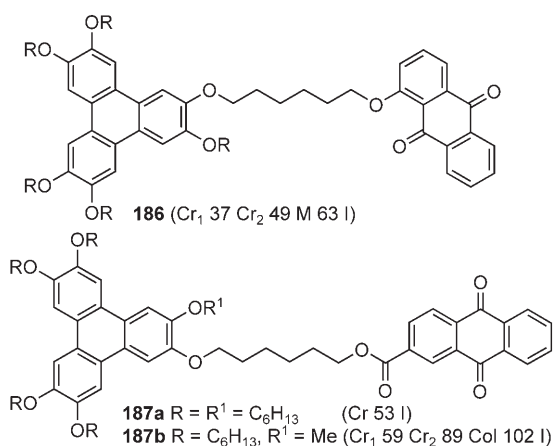
Scheme 79.

disturbs the columnar self-assembly. Almost simultaneously Cooke et al.[271] reported a related system **187** (Scheme 79), which yields a columnar mesophase.

Nonsymmetric donor-acceptor triples **188** with disklike and rodlike characteristics were published by Janietz, Wendorff, and co-workers (Scheme 80).[272] Compound **188** can be used for holographic data storage because of the presence of the chromophoric azo moiety.
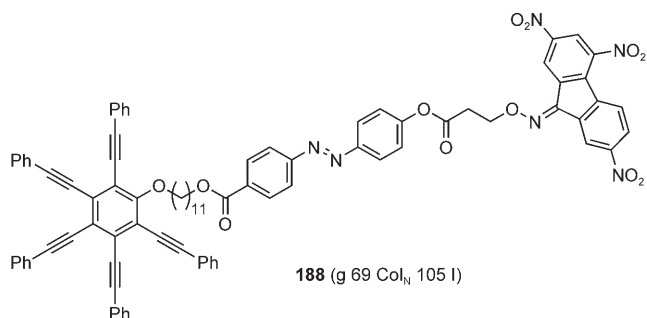
Scheme 80.

The simultaneous supramolecular arrangement of both electron-deficient p-type and electron-rich n-type π-conjugated systems is especially important for organic photovoltaic cells. To this goal, Janssen and co-workers envisioned the preparation of a liquid-crystalline perylene bisimide **189** that is connected to two peripheral oligo(*para*-phenylene vinylene) units (Scheme 81).[273] On photoexcitation of the donor, a
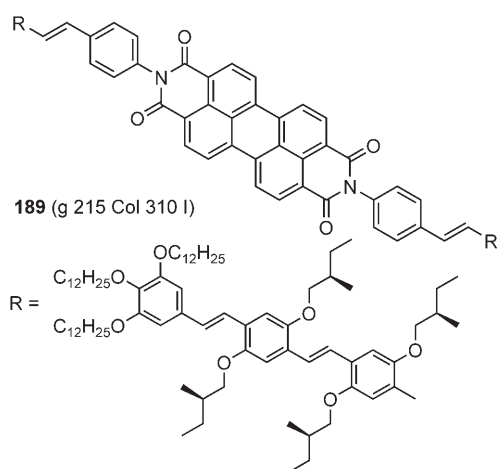
Scheme 81.

sub-picosecond electron-transfer reaction occurs in **189**. The lifetime of the charge-separated state in (ordered) thin films is markedly larger than in solution as a result of a decrease of geminate recombination by migration and spatial separation of charges in the film.

Unsymmetrical liquid-crystalline twin compounds that consist of rod-shaped and disk-shaped subunits have extensively been studied by the research groups of Mehl,[274] Luckhurst and Bruce.[275] While the building blocks **20g** and

190 displayed nematic and monotropic hexagonal columnar mesophases, respectively, a smectic A phase was observed for the twin **191** (Scheme 82).[275a]

20g (Cr 96 N 105 I)   **190** (Cr [23 Col$_h$ 51] I)

1) KOH, EtOH, THF, Δ   2) DCC, DMAP, TsOH

R =−(CH$_2$)$_{10}$O

191 (g 3 SmA 39 I)   R^1 = C$_6$H$_{13}$
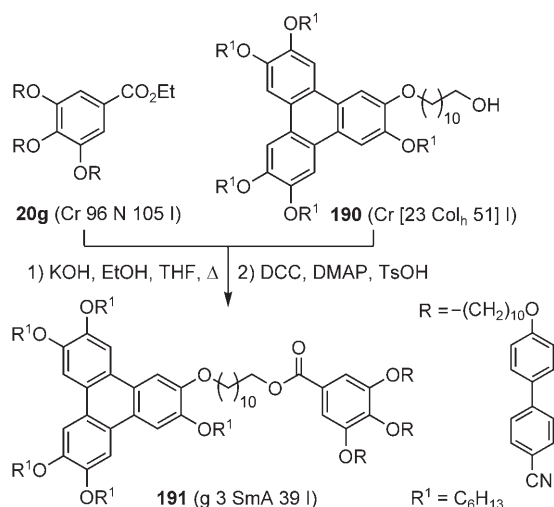
Scheme 82. Ts = *para*-toluenesulfonyl.

The possibility to grow highly ordered 2D and 3D structures of hybrid organic architectures has been demonstrated by Müllen and co-workers by using a soluble hexa-*peri*-hexabenzocoronene-pyrene hybrid **68d** (Scheme 83).[276]

68d R = 〜〜   (Cr 105 Col$_{ho}$ 136 I)
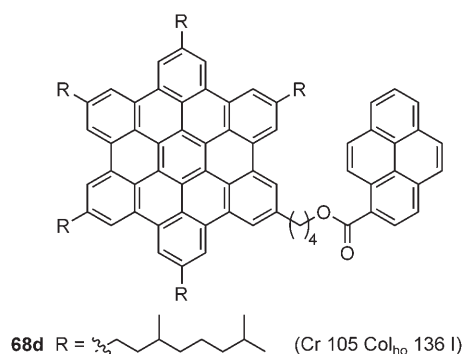
Scheme 83.

The novel dyad **68d** exhibits a more highly ordered columnar phase, but with a dramatically lowered isotropization temperature, which facilitates the homeotropic alignment in comparison with the symmetrical HBC derivative **63e** (Scheme 27).

These two features are important for processing such material into photovoltaic devices. STM studies allow a direct view on such highly ordered adsorbate of **68d** on HOPG with submolecular resolution (Figure 43).

4.15. Lyotropic systems

Lyotropic systems, based on rigid rodlike amphiphiles, have been extensively investigated by the research group of
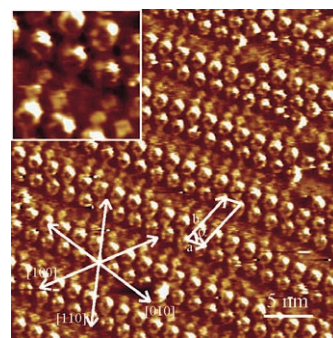
Figure 43. STM image of **68d** at the solid-liquid interface. Dimer row structures with smaller and darker bright spots between the dimer gaps. Figure taken from Ref. [276].

Tschierske,[277] and were discussed in a review by Kato.[247] Therefore, only 4-benzyloxy-4′-(2,3-dihydroxypropyloxy)biphenyl **192** will be presented (Scheme 84).[278] The neat

192 (Cr 128 Col$_{ob}$ 151 I)
saturated with glycerol **192** (Col 125 SmA 143 I)
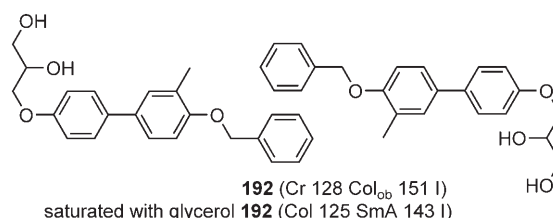
Scheme 84.

amphiphile **192** displays an oblique columnar mesophase. However, the mixture of **192**, which was saturated with glycerol, behaves differently. In the contact region between **192** and glycerol, the columnar mesophase is destabilized and the formation of a smectic A phase is observed.[277f]

Figure 44 presented the proposed arrangement of molecules of **192** in its mesophases. As the hydrophobic interactions between flexible alkyl chains in classical amphiphiles are replaced by interactions of rigid aromatic units in **192**, ribbon structures are formed.
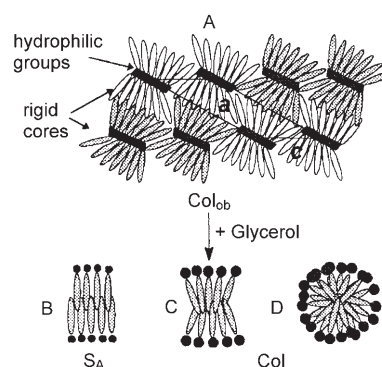
Figure 44. Proposed arrangement of **192** in its mesophases. Layer of a ribbon (C) and cylindrical aggregate (D). Reproduced from Ref. [277f].

4.16. Miscellaneous systems

Linear molecular structures are not excluded to generate columnar mesophases by themselves. Two typical examples **193** and **194** were reported by Nicoud, Donnio, and co-workers[279] and Ribeiro et al. (Scheme 85).[24]

193 R = $C_{12}H_{25}$ (Cr 64 M_{tet} 143 Col_h 156 I)

194 R = $C_{12}H_{25}$ (Cr 129 Col_r 149 Col_h 183 I)
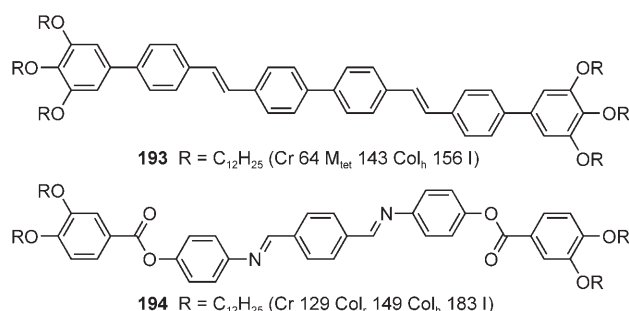
Scheme 85.

Columnar LCs based on bent-shaped mesogens with large lateral dipoles should be well-suited for optimal energy transport characteristics. To this goal, Swager and co-workers prepared 2,5-bis[4-(3,4,5-tridodecyloxyphenylcarbonyloxy)-phenylethynyl]-3,4-dicyanothiophene **195** (Scheme 86).[280]

195 R = $C_{12}H_{25}$ (Cr 43 Col_h 69 I)

antiparallel bent-rod structure
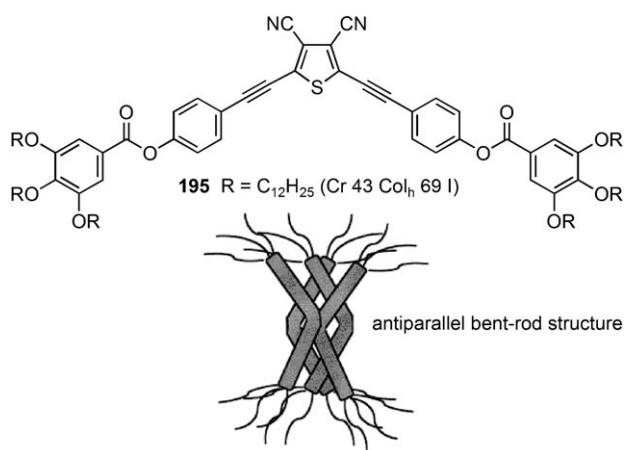
Scheme 86.

The emissive nature of the mesogen varies over the temperature range of the Col_h phase. The variation of the fluorescence emission band in this phase of **195** is due to varying degrees of rotational disorder between the mesogens. Furthermore, the bent-rod shape and highly dipolar nature of the mesogen promotes a high degree of antiparallel intermolecular correlations between the nearest neighbors.

The discovery of the so-called "banana phases" has caused much excitement because antiferroelectric switching is possible with these phases.[281] Tschierske and co-workers synthesized bent-core mesogens **196**, which form both an antiferroelectric switchable smectic and a rectangular columnar mesophase (Scheme 87).[282]

196 $R^1 = C_{10}H_{21}$
(Cr 89 $SmCP_A$ 107 Col_r 108 I)

197 $R^1 = C_{12}H_{25}$
(Cr_1 120 Cr_2 165 Col_r 203 I)

$R = $
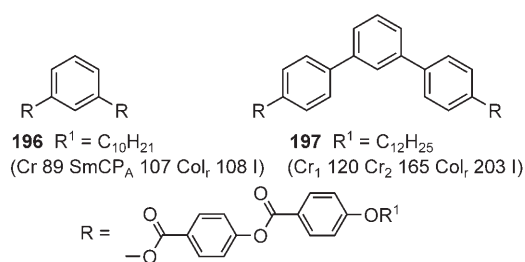
Scheme 87.

On extending the central *meta*-benzene core to a *meta*-terphenyl core, the stability of the columnar phase was improved at the expense of the $SmCP_A$ phase. A structural model for the Col_r phase is given in Figure 45.

$\alpha = 126°$
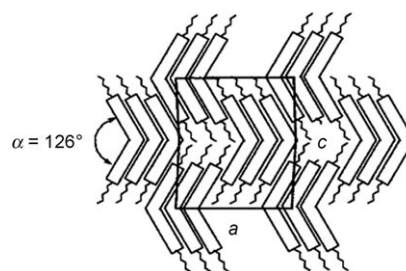
Figure 45. Structure model of a stable Col_r phase of molecules **196** and **197** with short chains or with large bent rigid cores. Reproduced from Ref. [282].

According to Kishikawa et al., even such structurally simple half-disk molecules such as 3,4,5-trialkoxybenzoic anhydrides **198** are able to form columnar mesophases through uneven-parallel association and one-directionally geared interdigitation (Scheme 88).[37] In the case of chiral

20d,h

AcOH
TsOH
toluene

198

198a R = $C_{10}H_{21}$ (Cr 15 Col 61 I)

198b R =

(Col 34 I)
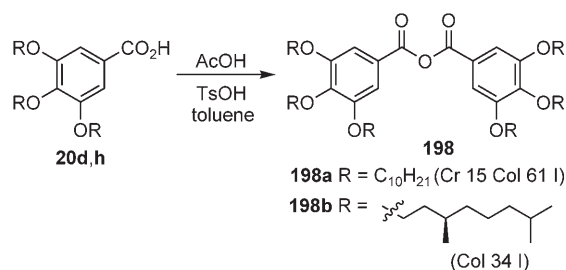
Scheme 88.

substituents, a chiral columnar structure (Figure 46) was found by CD spectroscopy. The mesogens **198b** with a central large dipole in a columnar phase are organized into a column, in which the molecules are piled up with an alternately antiparallel manner, and the columns interdigitate each other in one direction to give smaller intercolumnar distances than their columnar diameters.

The importance of microseggregation of incompatible molecular parts for mesophase formation was demonstrated
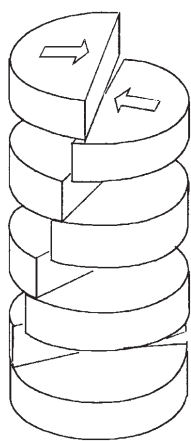
Figure 46. Model structure of a chiral columnar phase of compound **198 b**. Reproduced from Ref. [37].

independently by the research groups of Tschierske[283] and Laschat[89] for mesogens such as **199** and **200** to form tetrahedral columnar LCs (Scheme 89). Helical columnar LCs based on helicene systems **201** have been proposed by the research groups of Katz and Eichhorn (Scheme 90).[284]

Despite their propellerlike shape, tetraphenylethenes **203** are potential building blocks for liquid crystals. Tetraphenylethenes possess interesting photophysical properties and can easily undergo redox processes and photocyclizations (Scheme 91).[285] Compounds **203 c** were obtained by McMurry coupling of benzophenone **202** followed by demethylation and esterification with gallic acid (**20**).

On irradiation of tetraphenylethene **203 c** in the presence of iodine, the corresponding diphenylphenanthrene **204** was formed.[286] Although both compounds **203 c** and **204** displayed columnar mesophases, the mesophase range of **204** was shifted to higher temperatures probably as a result of the increased rigidity. Diphenylphenanthrene **204** differs by
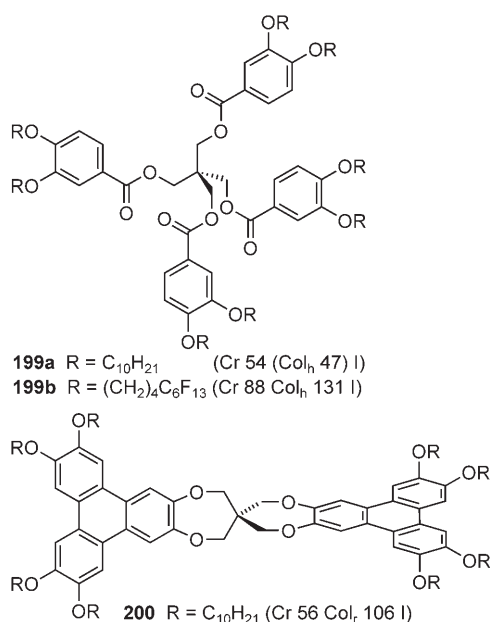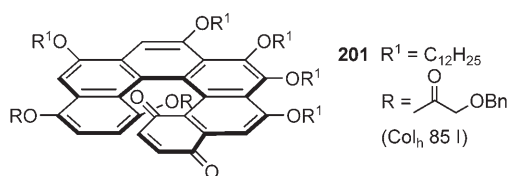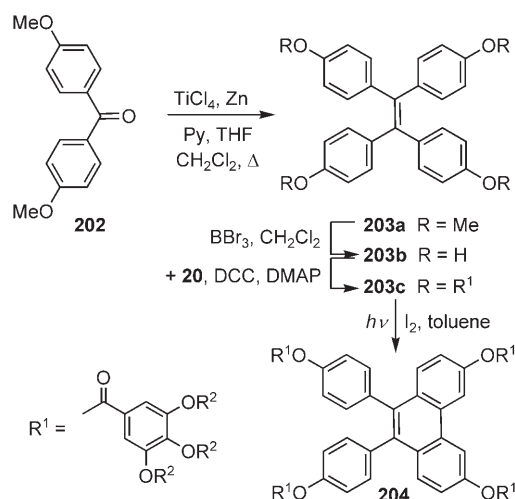
Scheme 91.

only one extra C–C bond from its precursor **203 c**, and the overall size of both molecules is identical. However, the lattice constant of phenanthrene **204** was much larger than the corresponding value for **203 c** (Figure 47). This result may be explained by a different packing behavior of the two mesogenic units.

199a R = C$_{10}$H$_{21}$ (Cr 54 (Col$_h$ 47) I)
199b R = (CH$_2$)$_4$C$_6$F$_{13}$ (Cr 88 Col$_h$ 131 I)

200 R = C$_{10}$H$_{21}$ (Cr 56 Col$_r$ 106 I)

Scheme 89.

201 R^1 = C$_{12}$H$_{25}$
R = $\overset{O}{\underset{\|}{C}}$–OBn
(Col$_h$ 85 I)
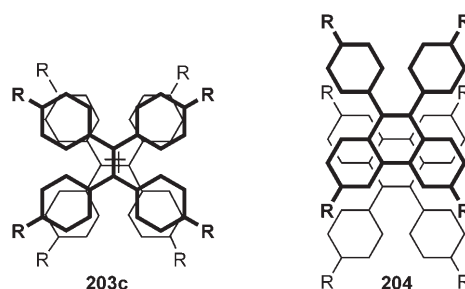
Scheme 90.

Figure 47. Possible arrangement of tetraphenylethenes and phenanthrenes in the Col$_h$ phase.[286]

A related example was reported by Toyne, Goodby, and co-workers (Scheme 92).[287,288] Only the octasubstituted board-like mesogen **206b** forms columnar mesophases, while the tetrasubstituted analogue **206a** displays a soft crystal phase (Scheme 92). A novel biaxial smectic liquid-crystalline phase formed by the rodlike 1,3-diazaazulene **207** was recently reported by Tschierske, Mori, and co-workers (Scheme 93).[289]

205a X = H (Cr 103 I)
205b X = OC$_8$H$_{17}$
(g −30 Col$_h$ 74 I)

R = C$_8$H$_{17}$
FeCl$_3$
CH$_2$Cl$_2$

206a X = H (CrysB 179 I)
206b X = OC$_8$H$_{17}$
(Cr 155 Col$_h$ 252 I)

Scheme 92.

207 (Cr₁ 110 Cr₂ 116 Col_L 121 SmC 127 I)
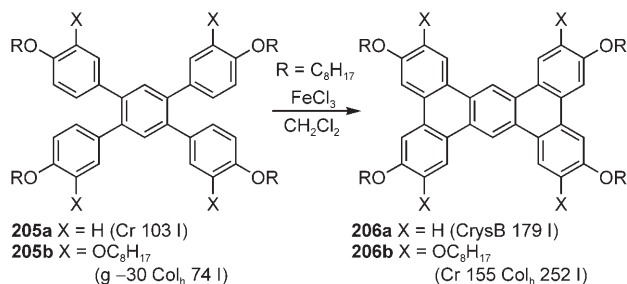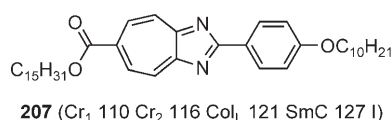
Scheme 93.

Tetrathiafulvalenes are very useful materials, in particular for organic conductors, and thus their chemistry has been extensively explored.[290] Nevertheless, it took until 1998 for the first columnar mesogen with a TTF core to be reported.[291] A TTF derivative **211b** with a rectangular columnar mesophase was prepared by the research group of Boden and Bushby by using the synthesis route outlined in Scheme 94.[292] It should be noted that its synthetic precursor, that is, the anhydride **211a**, displayed a smectic A mesophase. Compounds **211** behave as organic semiconductors.

210

R =

1) Ac₂O, DMAP
2) Hg(OAc)₂, HOAc
3) P(OMe)₃, Δ
4) RX, K₂CO₃, DMF
5) KOH, THF, MeOH, Δ
6) Δ

211a X = O (Cr 92 SmA 107 I)
211b X = NMe (Col_r 65 I)
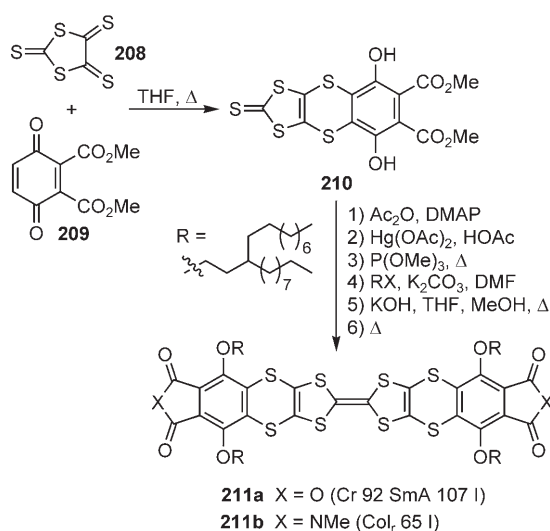
Scheme 94.

In 1998 the research group of Ros and Torroba made the surprising observation that even polarizable atoms such as sulfur or halogens, or polar groups such as cyano or carbonyl can act as the "soft regions" in the periphery of the discotic molecule.[293] Some typical examples are given in Scheme 95.

5. Applications

5.1. Phase-compensation filters in TN and STN liquid-crystal displays

In contrast to calamitic LCs, columnar LCs cannot be used as switching units in liquid crystal displays (LCDs).[294, 295] This is mainly due to the fact that these disk-shaped molecules do not have a central dipole moment, typically have a much higher viscosity than rod-shaped molecules of similar molecular weight, and are therefore difficult to orient by an electric field. Even if switching is possible, that is, reorientation of the bulk sample, switching times are too slow as compared to the

212 (Cr 205 Col_h 230 I)

214 (Cr 120 Col_h 144 I)

213a R=CN, R¹=R²=Cl   (Cr 184 Col_h 196 I)
213b R=R¹=Cl, R²=CN   (Cr 132 Col_h 152 I)
213c R=R²=Cl, R¹=CN   (Cr 97 M 160 Col_h 185 I)
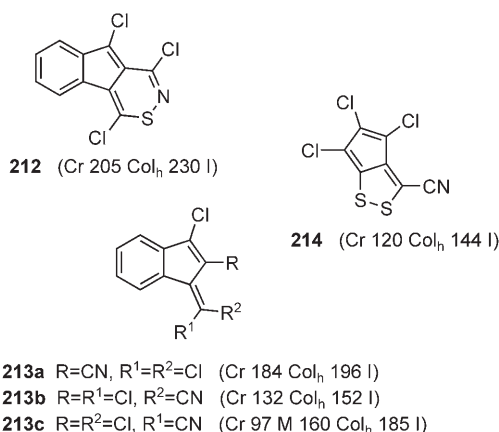
Scheme 95.

corresponding nematic or smectic compounds. However, this does not mean that columnar mesogens are completely useless for display applications. One serious limitation of current LCDs is the problem of the viewing angle: the brightness, contrast, and sharpness of focus are only optimal when the display is viewed at a certain angle. Furthermore an image inversion is observed because of the positive birefringence of the liquid-crystal layer. These effects can be suppressed by the use of compensation films, which should ideally have negative birefringence. The most promising materials for negative birefringence films are columnar LCs. Fuji has recently commercialized an optical phase compensation film using a triphenylene-based crosslinked polymer to overcome these problems.[296] These films are usually prepared by aligning the reactive monomer, a triphenylene benzoate ester, with up to six epoxide or acrylate groups homeotropically in the nematic discotic phase followed by photopolymerization. It should be noted that along with the optical-compensation films, the columnar LCs are not yet been ready for the market, but organic field-effect transistors (OFETs) and photovoltaic cells, particularly the OLEDs, seem likely to reach the market in the next couple of years.[297]

5.2. Xerographic processes

A commercially available photocopier or laser scanner consists of a rotating cylinder that is covered with a photoconducting surface, which moves over the original document with simultaneous irradiation.[134a] The light reflected by the document hits the photoconducting surface thereby leading to charge separation. An electrostatic image is generated on the cylinder surface. In the next step, the cylinder is covered with black toner particles (dry ink) that preferentially adsorb at the positive charges of the cylinder surface. On rotation of the cylinder over blank paper, the toner particles are transferred to the paper and the crude hardcopy is generated and submitted to thermal fixation.

There are several requirements for photoconducting materials for them to be useful for applications. To achieve a high contrast potential for image development, the photoreceptor must be an insulator or have low conductivity in the

dark and become conductive on exposure to light. A highly sensitive photoconductor not only requires less energy to generate the electrostatic image, but also increases the speed of the xerox process. Thus, photosensitivity and dark conductivity of a certain material must be assessed. In addition, the lifetime and processibility of the material must be considered. While copier applications require that the photoconductor is sensitive in the visible region (400–650 nm), the corresponding photoconducting materials of laser printers are sensitive in the IR region (750–850 nm).

A class of compounds which are particularly well suited for photoconducting devices that operate in the visible region are the perylene bisimides such as compound **57a** (Scheme 23).[136] The formation of 1D luminescent aggregates in solution and thin films from this compound was discussed in Section 4.3. In contrast, phthalocyanines have a strong absorption both in the visible and near infrared region. Eichhorn et al. discovered that mixtures, which contained amphitropic phthalocyanines such as **215** (Scheme 96) with a

215 (Cr –10 Col$_h$ 300 I)

M = Cu^{2+}, Zn^{2+}
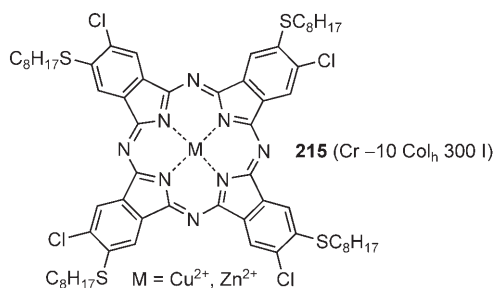
Scheme 96.

different substitution pattern, display much higher inter- and intracolumnar order than the single compounds.[200] In addition, macroscopic homeotropic alignment was simply achieved by mechanical shearing, thus providing an easy way to orient the material for laser printers.

5.3. Photovoltaic cells

The photovoltaic effect requires 1) the absorption of solar radiation and the photogeneration of electrons and holes, and 2) the charge separation, and the transport of electrons and holes for collection at the cathode and anode, respectively. For a typical photovoltaic blended device under short-circuit conditions, the energy-level diagram is in Figure 48.[298]

Both processes should be highly efficient and charge recombination should be kept to a minimum. Absorption is achieved by exciton formation. Charge separation is achieved by ionization of an exciton over a distributed interface between electron-donating and electron-accepting species. The separated carriers drift to external electrodes in the built-in field introduced by dissimilar electrodes. Müllen and coworkers have shown in a seminal contribution[12a] that thin films precipitated by self-organization of a mixture of columnar LCs and crystalline-conjugated materials directly from an xylene solution showed a photovoltaic response with
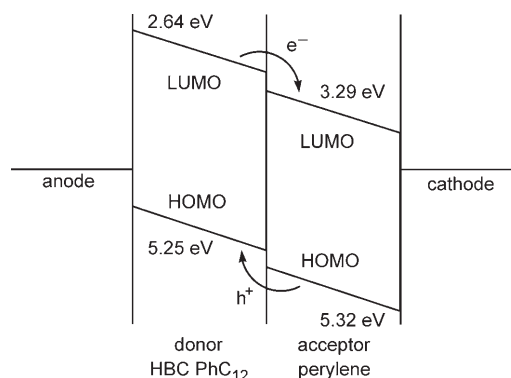
Figure 48. Energy-level diagram shows the charge separation and transport in a mixture that consists of an electron donor and acceptor placed between a dissimilar anode and cathode to provide a built-in field.[298]

external quantum efficiencies of greater than 34% at 490 nm and power efficiencies up to 2%. This material contains the vertically segregated nonmesomorphic electron-accepting perylene bisimide **58c** (Scheme 24) and the columnar-phase forming hole-accepting hexa-*peri*-hexabenzocoronene **63a** (Scheme 25) with a high interfacial surface as was shown by AFM, STM, and optical polarizing microscopy. The high efficiencies result from an efficient photoinduced charge transfer between **58c** and **63a** and an effective charge transport through the layered structure.

5.4. Organic light-emitting diodes

An OLED is a device, in which light is generated by electrical excitation. In a single-layer OLED, a thin film of an organic emitter is sandwiched between a transparent anode (for example, indium tin oxide (ITO)) and a metallic cathode.[298, 299] A multilayer device (Figure 49) consists of separate hole-transporting layer, emitter layer and electron-transporting layer. Electrons and holes, which are injected into the LUMO and HOMO, respectively, drift through the organic film under the influence of the applied electric field. The coulombic attraction between an electron and hole at the same chromophore site results in the formation of an exciton, a bound electron-hole pair, whose recombination produces
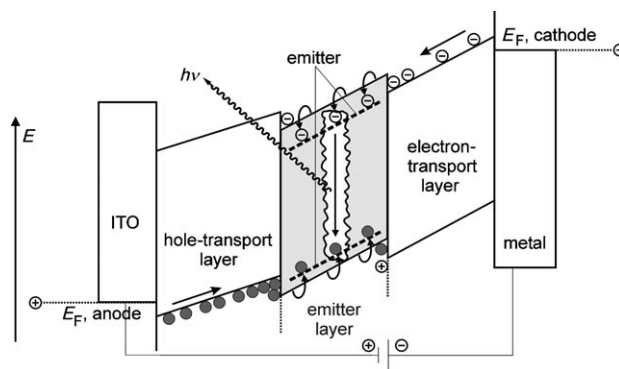
Figure 49. Energy diagram of a multilayer diode.[299]

luminescence. Efficient devices require the matching of energy levels to minimize the barriers for carrier injection and to trap both electron and holes exclusively in the emitter region. For OLED applications, columnar perylene derivatives have again been successfully used. For example, the research groups of Kitzerow and Bock[141, 142b, 300] described an all-columnar bilayer OLED that consisted of fluorescent columnar 3,4,9,10-tetra(alkoxycarbonyl)perylenes **59** (Scheme 24) as the luminescent electron-transport layer combined with columnar hexaalkoxytriphenylenes **35** (Scheme 12) as the hole-transport layer. A particular advantage of columnar LCs in such devices is their ability to expel defects in an annealing process which leads to increased lifetimes.

5.5. Organic field-effect transistors

The self-assembly properties of columnar LCs, in combination with their ability to provide anisotropic charge-carrier transport along the channel, makes them viable candidates for OFETs. A typical OFET device is shown in Figure 50.
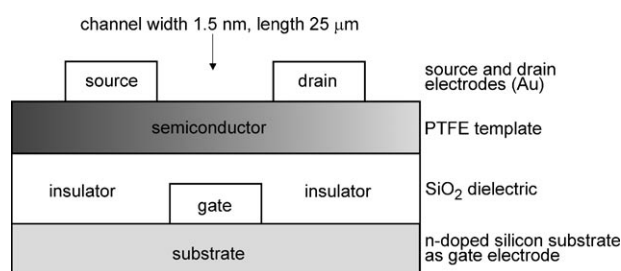
Figure 50. Schematic representation of an organic field-effect transistor.

For a p-type semiconductor, conduction of charge between the source and the drain electrodes is governed by the gate voltage. When the gate is positive with respect to the source, the semiconductor is depleted of carriers. When the gate is biased negatively, carriers accumulate in the channel between source and drain. The drain current is then proportional to the material mobility.[294] The extraordinary hole mobility for aligned hexa-*peri*-hexabenzocoronene **63 f** (HBC-C8,2; $\mu = 0.5-1.0 \times 10^{-3}$ cm^{2}V^{-1}s^{-1}) films on oriented PTFE has been used by the research group of Müllen.[166, 168] By meso-epitaxial solution-growths of the HBC semiconductor devices were built, which displayed on/off ratios of more than 10^4 and a turn-on voltage of -5 to -10 V. The solution processibility, uniaxial parallel orientation (by use of the PTFE alignment layer), and promising material and device stability under ambient conditions pave the way to the industrial production of these OFETs.

5.6. Holographic optical data storage

One of the common principles of reversible optical data storage relies on the *E/Z* isomerization of dyes such as azobenzenes and stilbenes. The imprinting with two linear-polarized laser-light beams induces a reorientation of the chromophores, which results in a change of the refractive index at the irradiated areas. The dye molecules are incorporated in a liquid-crystalline matrix, which strongly enhances the change in refractive index. The periodic modulation of the refractive index, induced by the writing laser beam, can be read out by a reading laser beam.

The columnar donor-acceptor triple compound **188** (Scheme 80) bears an azobenzene moiety as the chromophoric group.[272b, 301] The strong electron-acceptor TNF (Scheme 4) in combination with the electron donor pentakis-phenylalkynylbenzene resulted in the improved stability of the nematic columnar mesophase. As can be seen in Figure 51, at ambient temperature the refractive index of the photoinduced grating in this material differs by only 0.5%. On heating the sample to the nematic columnar mesophase, the diffraction efficiency increases to 4%.
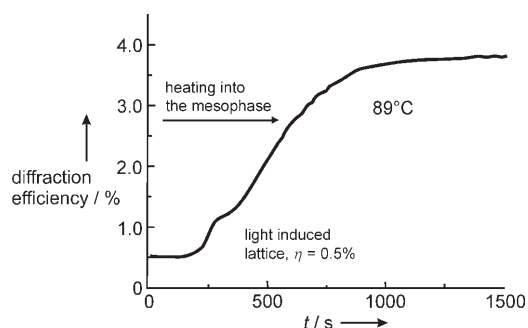
Figure 51. Thermal gain effect of the diffraction efficiency. Reproduced from Ref. [301].

Along these lines Wendorff, Janietz, and co-workers found that triazomelamine **216** (Scheme 97) is not only suitable for the light-induced isomerization of the azobenzene units to give rise to photo-reorientation, but also causes surface modulations.[302] Once more, a gain effect of these surface modulations was achieved by thermal treatment (Figure 52). It should be noted that triazomelamine **216** displays smectic and nematic mesophases despite its flat C_3-symmetrical structure.

216
(g 32 Sm 221 N 239 I)
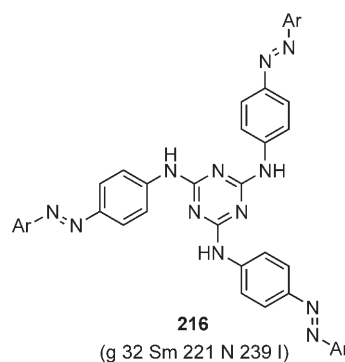
Scheme 97.
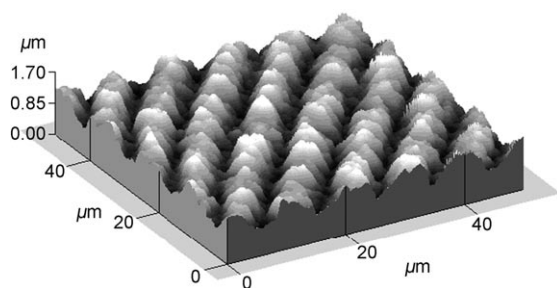
Figure 52. AFM image of an irradiated area after thermal treatment.[302]

molecules in disordered columns

sugar head groups   aliphatic chains

Figure 53. The disordered hexagonal columnar structure of derivatives **217** and **218**.[303]

5.7. Models for complex biological systems

Lyotropic columnar systems will not be discussed in this Review because of the recent discussion by Kato on this subject.[247] A single exception are the glycolipids such as **217** (Scheme 98), which were described by Plusquellec, Goodby

217 (g 65 Col$_{hd}$ 115 l)

218

Scheme 98.

and co-workers.[303] Compounds **217** and their derivatives serve as useful models for the self-organization of membrane lipids (for example, **218**) of archae bacteria. These extremophile microorganisms form a third class besides the classical procaryontic and eucaryontic cells. The most interesting feature of these membrane lipids is their bipolar structure and the presence of glucofuranose moieties, which are usually more easily hydrolyzed than the corresponding glucopyranoses.

Model lipids such as **217** form both thermotropic and lyotropic columnar mesophases. While a hexagonal columnar packing with polar head groups that point towards the center of the column (Figure 53) was assumed for the thermotropic mesophase, which is only partly miscible with water, the opposite orientation, and thus good miscibility with water,

was observed for the lyotropic mesophase, that is, the head groups that point to the outside of the columns. Furthermore, **217** forms tubes of about 10 μm long.

Induced fit is an important principle by which enzymes bind to substrates to convert them into certain products. Some binding proteins of nucleic acids also follow an induced-fit mechanism. These proteins are dimers and have the shape of a clip, as in the case of gene V protein encoded by bacteriophage M13, which binds to single-stranded DNA and changes the physical properties of the nucleic acid.[304] To mimic these biological recognition processes, Nolte and co-workers[305] developed a synthetic clip molecule **219** (Scheme 99), which can bind to a polymer chain by an induced-fit mechanism, thereby making it liquid crystalline. While the host–guest complex of **219** with methyl 3,5-dihydroxybenzoate (**220**) formed a nematic phase, a columnar phase was found for the corresponding host–guest complex of **219** with the copolymer **221**. Compound **219** exists as a mixture of three conformers. The guest changes the equilibrium of the conformers and thus the phase-transition temperature and aggregation behavior.

219 R = C$_{12}$H$_{25}$

220

219·220 (1:1) (Cr −4 N 110 l)
219·221 (1:1) (Cr 30 Col 141 l)

221
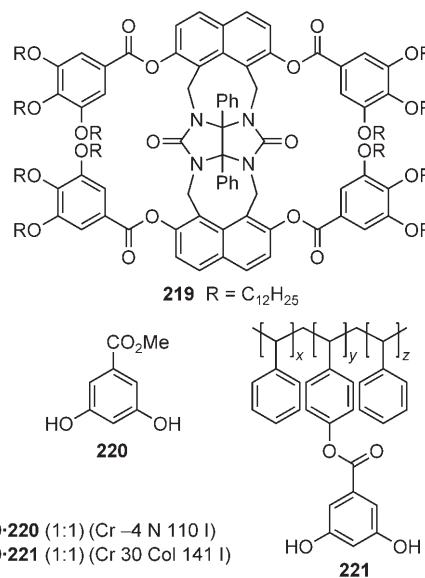
Scheme 99.
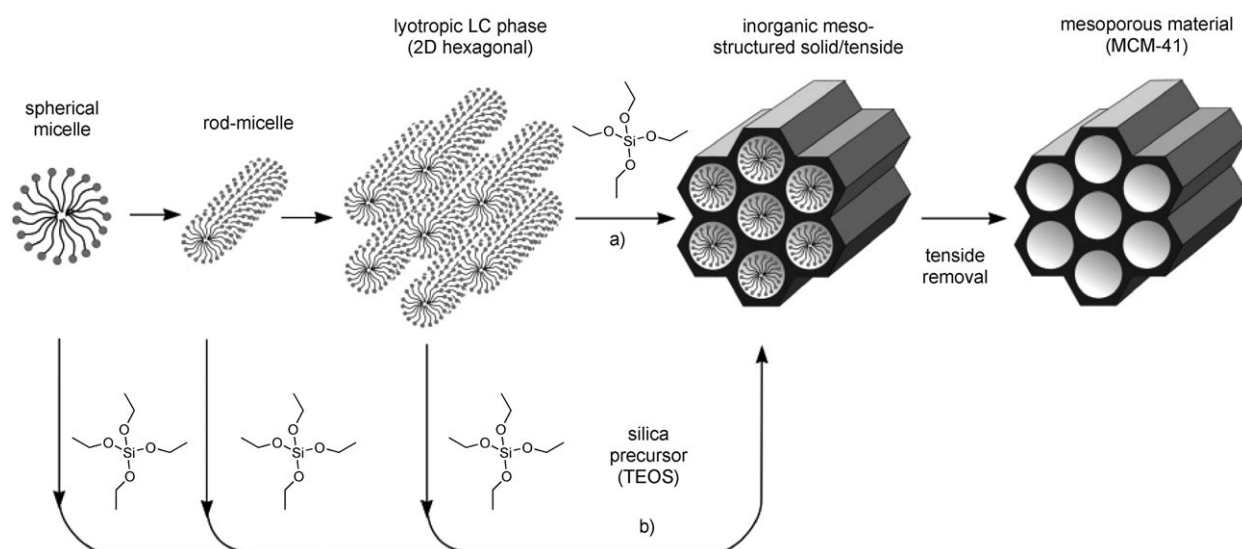
Figure 54. Formation of mesoporous materials by structure-directing agents: a) true and b) cooperative LC template mechanism. Reproduced from [306].

5.8. Mesoporous solids by template synthesis

Finally, one of the most important applications of columnar liquid crystals in general, and lyotropic liquid crystals in particular, is the template-assisted formation of mesoporous solids for heterogeneous catalysis. This issue has been discussed in detail in a recent review by Fröba and co-workers.[306] A ground-breaking discovery by the research group of Stucky[307] was that the self-assembly of amphiphiles such as hexadecyltrimethylammonium bromide into lyotropic hexagonal columnar rod-micelles could be used as a template for mesoporous solids. As shown in Figure 54, the initially formed composite of a mesostructured polysiloxane is converted into the mesoporous solid such as MCM-41 by removal of the tenside, and subsequent calcination. Such mesoporous materials have been found applications in adsorption and heterogeneous catalysis.[308]

6. Conclusions and Outlook

The tailormade synthesis of a wide variety of columnar mesogens is possible, thus giving access to novel materials that may be used as 1D molecular wires or have other applications in plastic electronics. Along with the optical compensatory films for LCDs based on thermotropic triphenylene derivatives and template-directed synthesis of zeolites based on lyotropic quaternary ammonium salts, the development of OLEDs based on perylenes, OFETs based on hexa-*peri*-hexabenzocoronenes and the LC-derived solar cells seem to be most advanced. However, applications of columnar liquid crystals are still in their infancy. For example, photovoltaic cells require both p-type and n-type materials. Whereas most columnar LCs are p-type materials, relatively few n-type materials are known. Thus, novel n-type liquid crystals with high electron mobilities are required.

Another problem is the stability of columnar liquid crystals over long periods that effect their application in optical and electronic devices. For example, blue-emitting OLEDs are severely hampered by the fact that the UV absorption and thus C−C bonds of the liquid-crystalline material are effected. Along with the development of possible applications in molecular electronics, further studies are needed to understand the correlation between molecular structure, that is, the type of core unit and side-chain lengths, and the physical properties such as mesophase type and phase transition temperatures. Currently we are a long way off predicting physical properties of a specific molecular structure. In addition, exciting results from the field of molecular biology should be expected. Although the columnar mesophases of DNA,[309] cellulose,[310] and other biomolecules have long been known, the mesophase behavior of biological systems needs to be intensively investigated to understand the influence of supramolecular assemblies and phase transitions on biological functions. Also, composite systems between columnar liquid crystals and polymers, inorganic solids, and biomolecules have only been rarely explored. It is our opinion that the field of liquid-crystal research and in particular the columnar systems will lead to exciting new discoveries.

[1] T. J. Sluckin, D. A. Dunmur, H. Stegemeyer, *Crystals that flow: Classic papers from the history of liquid crystals*, Taylor & Francis, London, **2004**.

[2] D. Vorländer, *Ber. Dtsch. Chem. Ges.* **1907**, *40*, 1970–1972.

[3] S. Chandrasekhar, B. K. Sadashiva, K. A. Suresh, *Pramana* **1977**, *9*, 471–480.

[4] A. Isihara, *J. Chem. Phys.* **1951**, *19*, 1142–1147.

[5] L. K. Runnels, C. Colvin in *Advances in Liquid Crystals, Vol. 3* (Eds.: G. H. Brown, M. M. Labes), Gordon und Breach, New York, **1972**.

[6] R. Alben, *Phys. Rev. Lett.* **1973**, *30*, 778–781.

[7] J. P. Straley, *Phys. Rev. A* **1974**, *10*, 1881–1887.

[8] J. D. Brooks, G. H. Taylor, *Carbon* **1965**, *3*, 185–186.

[9] J. Billard, J. C. Dubois, N. Huutinh, A. Zann, *Nouv. J. Chim.* **1978**, *2*, 535–540.

[10] A. M. Levelut, *J. Phys. Lett.* **1979**, *40*, L81–L84.

[11] S. Xiao, M. Myers, Q. Miao, S. Sanaur, K. Pang, M. L. Steigerwald, C. Nuckolls, *Angew. Chem.* **2005**, *117*, 7556–7560; *Angew. Chem. Int. Ed.* **2005**, *44*, 7390–7394.

[12] a) L. Schmidt-Mende, A. Fechtenkötter, K. Müllen, E. Moons, R. H. Friend, J. D. Mackenzie, *Science* **2001**, *293*, 1119–1122; b) J. Nelson, *Science* **2001**, *293*, 1059–1060.

[13] H. Kelker, B. Scheuerle, *Angew. Chem.* **1969**, *81*, 903–904; *Angew. Chem. Int. Ed. Engl.* **1969**, *8*, 884–885.

[14] B. Kohne, K. Praefcke, *Chimia* **1987**, *41*, 196–198.

[15] K. Praefcke, D. Singer, B. Kohne, M. Ebert, A. Liebmann, J. H. Wendorff, *Liq. Cryst.* **1991**, *10*, 147–159.

[16] a) The absence of perfect translational order in columns of disklike molecules is in perfect agreement with the so-called "Landau-Peierls instability"—a fundamental theorem in statistical physics that predicts the thermal instability of any infinitely extended 1D periodic structure; b) The absence of true 1D long-range translational order in smectics is again due to the Landau-Peiersl instability.

[17] P. Ekwall in *Advances in Liquid Crystals, Vol. 1* (Ed.: G. H. Brown), Academic Press, New York, **1975**.

[18] J. Malthete, A. M. Levelut, N. H. Tinh, *J. Phys. Lett.* **1985**, *46*, L875–L880.

[19] S. Chandrasekhar in *Handbook of Liquid Crystals, Vol. 2B* (Eds.: D. Demus, J. Goodby, G. W. Gray, H.-W. Spiess, V. Vill), Wiley-VCH, Weinheim, **1998**, p. 749.

[20] The abbreviations used herein conform with the recommendations of IUPAC: a) M. Barón, *Pure Appl. Chem.* **2001**, *73*, 845–895; b) C. Tschierske, G. Pelzl, S. Diele, M. Müller, *Angew. Chem.* **2004**, *116*, 6340–6368; reviews: c) S. Chandrasekhar, S. K. Prasad, D. S. S. Rao, V. S. K. Balagurusamy, *Proceedings of the Indian National Science Academy, Proc. Indian Acad. Sci. Sect. A* **2002**, *68*, 175–191; d) S. Krishna Prasad, D. S. S. Rao, S. Chandrasekhar, S. Kumar, *Mol. Cryst. Liq. Cryst.* **2003**, *396*, 121–139.

[21] E. Fontes, P. A. Heiney, M. Ohba, J. N. Haseltine, A. B. Smith III, *Phys. Rev. A* **1988**, *37*, 1329–1334.

[22] B. Donnio, B. Heinrich, H. Allouchi, J. Kain, S. Diele, D. Guillon, D. W. Bruce, *J. Am. Chem. Soc.* **2004**, *126*, 15258–15268.

[23] M. Lehmann, G. Kestemont, R. G. Aspe, C. Buess-Herman, M. H. J. Koch, M. G. Debije, J. Piris, M. P. de Haas, J. M. Warman, M. D. Watson, V. Lemaur, J. Cornil, Y. H. Geerts, R. Gearba, D. A. Ivanov, *Chem. Eur. J.* **2005**, *11*, 3349–3362.

[24] A. C. Ribeiro, B. Heinrich, C. Cruz, H. T. Nguyen, S. Diele, M. W. Schröder, D. Guillon, *Eur. Phys. J. E* **2003**, *10*, 143–151.

[25] A. Takada, T. Fukuda, T. Miyamoto, Y. Yakoh, J. Watanabe, *Liq. Cryst.* **1992**, *12*, 337–345.

[26] H. Zheng, C. K. Lai, T. M. Swager, *Chem. Mater.* **1995**, *7*, 2067–2077.

[27] C. Destrade, P. Foucher, H. Gesparoux, H. T. Nguyen, A. M. Levelut, J. Malthete, *Mol. Cryst. Liq. Cryst.* **1984**, *106*, 121–146.

[28] A. M. Levelut, *J. Chim. Phys.* **1983**, *80*, 149–161.

[29] F. C. Frank, S. Chandrasekhar, *J. Phys.* **1980**, *41*, 1285–1288.

[30] These three planar space groups refer to the tilted arrangement of the molecules over several columns, since the tilt direction of one column sets the tilt direction in the neighboring columns. In the case of columnar mesophases with nontilted arrangements of the molecules or columnar phases where no tilt direction can be defined (for example, for wedge-shaped molecules), 2D point groups should be used: $p2gg = P2_1/a$, $p2mg = P2/a$, $c2mm = C2/m$, and $p1 = P_1$; the last case applies for a columnar oblique mesophase.

[31] F. Morale, R. W. Date, D. Guillon, D. W. Bruce, R. L. Finn, C. Wilson, A. J. Blake, M. Schröder, B. Donnio, *Chem. Eur. J.* **2003**, *9*, 2484–2501.

[32] C. K. Lai, C.-H. Tsai, Y.-S. Pang, *J. Mater. Chem.* **1998**, *8*, 1355–1360.

[33] S. Chandrasekhar, *Adv. Liq. Cryst.* **1982**, *5*, 47–48.

[34] C. R. Safinya, K. S. Liang, W. A. Varady, N. A. Clark, G. Anderson, *Phys. Rev. Lett.* **1984**, *53*, 1172–1175.

[35] *International Tables for X-ray Crystallography, Vol. 1* (Eds.: N. F. M. Henry, K. Lonsdale), Kynoch Press, **1969**.

[36] J. Billard, J. C. Dubois, C. Vaucher, A. M. Levelut, *Mol. Cryst. Liq. Cryst.* **1981**, *66*, 115–122.

[37] K. Kishikawa, S. Furusawa, T. Yamaki, S. Kohmoto, M. Yamamoto, K. Yamaguchi, *J. Am. Chem. Soc.* **2002**, *124*, 1597–1605.

[38] H. T. Nguyen, C. Destrade, H. Gasparoux, *Phys. Lett. A* **1979**, *72*, 251–254.

[39] J. Malthete, C. Destrade, H. T. Nguyen, J. Jacques, *Mol. Cryst. Liq. Cryst. Lett. Sect.* **1981**, *64*, 233–238.

[40] C. Destrade, H. T. Nguyen, J. Malthete, J. Jacques, *Phys. Lett. A* **1980**, *79*, 189–192.

[41] K. Praefcke, D. Singer, L. Langner, B. Kohne, M. Ebert, A. Liebmann, J. H. Wendorff, *Mol. Cryst. Liq. Cryst.* **1992**, *215*, 121–126.

[42] H. Bengs, O. Karthaus, H. Ringsdorf, C. Baehr, M. Ebert, J. H. Wendorff, *Liq. Cryst.* **1991**, *10*, 161–168.

[43] Since the lamellar mesophase of discotic LCs has the same symmetry as the smectic phases of calamitics (for example, SmA or SmC), it can also be denoted as smectic.

[44] H. Sakashita, A. Nishitani, Y. Sumiya, H. Terauchi, K. Otha, I. Yamamoto, *Mol. Cryst. Liq. Cryst.* **1988**, *163*, 211–219.

[45] N. Steinke, W. Frey, A. Baro, S. Laschat, C. Drees, M. Nimtz, C. Hägele, F. Giesselmann, *Chem. Eur. J.* **2006**, *12*, 1026–1035.

[46] S. Méry, D. Haristoy, J.-F. Nicoud, D. Guillon, S. Diele, H. Monobe, Y. Shimizu, *J. Mater. Chem.* **2002**, *12*, 37–41.

[47] a) D. Markovitsi, *Mol. Cryst. Liq. Cryst.* **2003**, *397*, 389–398; b) K. Ohta, K. Hatsusaka, M. Sugibayashi, M. Ariyoshi, K. Ban, F. Maeda, R. Naito, K. Nishizawa, A. M. van de Craats, J. M. Warman, *Mol. Cryst. Liq. Cryst.* **2003**, *397*, 325–345; c) C. F. van Nostrum, *Adv. Mater.* **1996**, *8*, 1027–1030.

[48] R. J. Bushby, O. R. Lozman, *Curr. Opin. Solid State Mater. Sci.* **2002**, *6*, 569–578.

[49] G. B. M. Vaughan, P. A. Heiney, J. P. McCauley, Jr., A. B. Smith III, *Phys. Rev. B* **1992**, *46*, 2787.

[50] N. Boden, R. J. Bushby, J. Clements, M. V. Jesudason, P. F. Knowles, G. Williams, *Chem. Phys. Lett.* **1988**, *152*, 94.

[51] N. Boden, R. J. Bushby, J. Clements, *J. Mater. Sci. Mater. Electron.* **1994**, *5*, 83.

[52] I. Bleyl, C. Erdelen, H.-W. Schmidt, D. Haarer, *Philos. Mag. B* **1999**, *79*, 463.

[53] J. M. Warman, A. M. van De Craats, *Mol. Cryst. Liq. Cryst.* **2003**, *396*, 41.

[54] A. M. van de Craats, J. M. Warman, M. P. de Haas, D. Adam, J. Simmerer, D. Haarer, P. Schuhmacher, *Adv. Mater.* **1996**, *8*, 823.

[55] a) A. M. van de Craats, J. M. Warman, *Adv. Mater.* **2001**, *13*, 130; b) W. Pisula, M. Kastler, D. Wassefallen, M. Mondeshki, J. Piris, I. Schnell, K. Müllen, *Chem. Mater.* **2006**, *18*, 3634–3640.

[56] M. Kastler, W. Pisula, F. Laquai, A. Kumar, R. J. Davies, S. Baluschev, M.-C. Garcia-Gutierrez, D. Wasserfallen, H.-J. Butt, C. Riekel, G. Wegner, K. Müllen, *Adv. Mater.* **2006**, *18*, 2255–2259.

[57] V. Lemaur, D. A. da Silva Filho, V. Coropceanu, M. Lehmann, Y. Geerts, J. Piris, M. G. Debije, A. M. van de Craats, K. Senthilkumar, L. D. A. Siebbeles, J. M. Warman, J.-L. Bredas, J. Cornil, *J. Am. Chem. Soc.* **2004**, *126*, 3271.

[58] T. J. Philips, J.-C. Jones, *Liq. Cryst.* **1994**, *16*, 805–812.

[59] E. J. Foster, C. Lavigueur, Y.-C. Ke, V. E. Williams, *J. Mater. Chem.* **2005**, *15*, 4062–4068.

[60] a) S. Kumar, *Chem. Soc. Rev.* **2006**, *35*, 83–109; b) N. Boden, R. J. Bushby, O. R. Lozman, *Mol. Cryst. Liq. Cryst.* **2003**, *400*, 105–113; c) S. Kumar, *Pramana* **2003**, *61*, 199–203; d) K. Praefcke, A. Eckert, *Mol. Cryst. Liq. Cryst.* **2003**, *396*, 265–299; e) D. Guillon, B. Donnio, D. W. Bruce, F. D. Cukiernik, M. Rusjan, *Mol. Cryst. Liq. Cryst.* **2003**, *396*, 141–154; f) R. J. Bushby, O. R. Lozman, *Curr. Opin. Colloid Interface Sci.* **2002**, *7*, 343–354; g) D. Demus, *Mol. Cryst. Liq. Cryst.* **2001**, *364*, 25–91; h) C. Tschierske, *J. Mater. Chem.* **2001**, *11*, 2647–2671; i) C. Tschierske, *Annu. Rep. Prog. Chem. Sect. C* **2001**, *97*, 191–267; j) H. Bock in *Chirality in Liquid Crystals* (Eds.: H.-S. Kitzerow, C. Bahr), Springer, New York, **2001**, pp. 355–374; k) J. Kopitzke, J. H. Wendorff, *Chem. Unserer Zeit* **2000**, *34*, 4–16; l) S. Chandrasekhar, S. K. Prasad, *Contemp. Phys.* **1999**, *40*, 237–245; m) A. N. Cammidge, R. J. Bushby in *Handbook of Liquid Crystals*, *Vol. 2B* (Eds.: D. Demus, J. Goodby, G. W. Gray, H.-W. Spiess, V. Vill), Wiley-VCH, Weinheim, **1998**, pp. 693–798; n) S. Chandrasekhar, *Proceedings of the Indian National Science Academy*, *Proc. Indian Acad. Sci. Sect. A* **1993**, *59*, 1–15; o) S. Chandrasekhar, *Liq. Cryst.* **1993**, *14*, 3–14; p) J. W. Goodby, G. H. Mehl, I. M. Saez, R. P. Tuffin, G. Mackenzie, R. Auzély-Velty, T. Benvegnu, D. Plusquellec, *Chem. Commun.* **1998**, 2057–2070.

[61] S. Kumar, S. Kumar Varshney, *Angew. Chem.* **2000**, *112*, 3270–3272; *Angew. Chem. Int. Ed.* **2000**, *39*, 3140–3142.

[62] Review: S. Kumar, S. Kumar Varshney, D. Chauhan, *Mol. Cryst. Liq. Cryst.* **2003**, *396*, 241–250.

[63] a) P. H. J. Kouwer, W. F. Jager, W. J. Mijs, S. J. Picken, *J. Mater. Chem.* **2003**, *13*, 458–469; b) P. H. J. Kouwer, W. J. Mijs, W. F. Jager, S. J. Picken, *J. Am. Chem. Soc.* **2001**, *123*, 4645–4646.

[64] According to recent knowledge and IUPAC nomenclature, the columnar plastic phase is a hexagonal columnar phase frozen into the glassy state.

[65] S. Furumi, D. Janietz, M. Kidowaki, M. Nakagawa, S. Morino, J. Stumpe, K. Ichimura, *Chem. Mater.* **2001**, *13*, 1434–1437.

[66] A. Grafe, D. Janietz, T. Frese, J. H. Wendorff, *Chem. Mater.* **2005**, *17*, 4979–4984.

[67] a) H. Meier, *Angew. Chem.* **1992**, *104*, 1425–1446; *Angew. Chem. Int. Ed. Engl.* **1992**, *31*, 1399–1420; b) W. R. Salaneck, I. Lundström, B. Raanby, *Conjugated Polymers and Related Materials*, Oxford University Press, Oxford, **1993**; c) K. Müllen, G. Wegner, *Electronic Materials: The Oligomer Approach*, VCH, Weinheim, **1996**; d) H. Meier, U. Stalmach, M. Fetten, P. Seus, M. Lehmann, C. Schnorpfeil, *J. Inf. Rec.* **1998**, *24*, 47–60; e) R. E. Martin, F. Diederich, *Angew. Chem.* **1999**, *111*, 1440–1469; *Angew. Chem. Int. Ed.* **1999**, *38*, 1350–1377.

[68] a) H. Meier, M. Lehmann, *Angew. Chem.* **1998**, *110*, 666–669; *Angew. Chem. Int. Ed.* **1998**, *37*, 643–645; b) M. Lehmann, B. Schartel, M. Hennecke, H. Meier, *Tetrahedron* **1999**, *55*, 13377–13394; c) H. Meier, M. Lehmann, U. Kolb, *Chem. Eur. J.* **2000**, *6*, 2462–2469; d) M. Lehmann, I. Fischbach, H. W. Spiess, H. Meier, *J. Am. Chem. Soc.* **2004**, *126*, 772–784; e) M. Lehmann, C. Köhn, H. Meier, S. Renker, A. Oehlhof, *J. Mater. Chem.* **2006**, *16*, 441–451.

[69] J. Y. Chang, J. R. Yeon, Y. S. Shin, M. J. Han, S.-K. Hong, *Chem. Mater.* **2000**, *12*, 1076–1082.

[70] M. Lehmann, R. I. Gearba, M. H. J. Koch, D. A. Ivanov, *Chem. Mater.* **2004**, *16*, 374–376.

[71] R. I. Gearba, A. Bondar, M. Lehmann, B. Goderis, W. Bras, M. H. J. Koch, D. A. Ivanov, *Adv. Mater.* **2005**, *17*, 671–676.

[72] A. R. A. Palmans, J. A. J. M. Vekemans, R. A. Hikmet, H. Fischer, E. W. Meijer, *Adv. Mater.* **1998**, *10*, 873–876.

[73] A. R. A. Palmans, J. A. J. M. Vekemans, H. Fischer, R. A. Hikmet, E. W. Meijer, *Chem. Eur. J.* **1997**, *3*, 300–307.

[74] J. van Gestel, A. R. A. Palmans, B. Titulaer, J. A. J. M. Vekemans, E. W. Meijer, *J. Am. Chem. Soc.* **2005**, *127*, 5490–5494.

[75] A. Omenat, J. Barberá, J. L. Serrano, S. Houbrechts, A. Persoons, *Adv. Mater.* **1999**, *11*, 1292–1295.

[76] a) S. Ito, H. Inabe, N. Morita, H. Ohta, T. Kitamura, K. Imafuku, *J. Am. Chem. Soc.* **2003**, *125*, 1669–1680; b) S. Ito, M. Ando, A. Nomura, N. Morita, C. Kabuto, H. Mukai, K. Ohta, J. Kawakami, A. Yoshizawa, A. Tajiri, *J. Org. Chem.* **2005**, *70*, 3939–3949.

[77] D. Demus, J. Goodby, G. W. Gray, H.-W. Spiess, V. Vill, *Handbook of Liquid Crystals*, *Vol. 2A*, Wiley-VCH, Weinheim, **1998**, pp. 3–21.

[78] L. Eshdat, R. E. Hoffman, A. Fechtenkötter, K. Müllen, M. Rabinovitz, *Chem. Eur. J.* **2003**, *9*, 1844–1851.

[79] S. Kumar, *Liq. Cryst.* **2004**, *31*, 1037–1059.

[80] S. Kumar, *Liq. Cryst.* **2005**, *32*, 1089–1113.

[81] G. Cooke, V. Sage, T. Richomme, *Synth. Commun.* **1999**, *29*, 1767–1771.

[82] N. Boden, R. C. Borner, R. J. Bushby, A. N. Cammidge, M. V. Jesudason, *Liq. Cryst.* **1993**, *15*, 851–858.

[83] S. Kumar, M. Manickam, *Chem. Commun.* **1997**, 1615–1616.

[84] H. Naarmann, M. Hanack, R. Mattmer, *Synthesis* **1994**, 477–478.

[85] S. Kumar, S. K. Varshney, *Synthesis* **2001**, 305–311.

[86] S. Kumar, B. Lakshmi, *Tetrahedron Lett.* **2005**, *46*, 2603–2605.

[87] N. Boden, R. J. Bushby, Z. Lu, G. Headdock, *Tetrahedron Lett.* **2000**, *41*, 10117–10120.

[88] J. L. Schulte, S. Laschat, *Synthesis* **1999**, 475–478.

[89] J. L. Schulte, S. Laschat, V. Vill, E. Nishikawa, H. Finkelmann, M. Nimtz, *Eur. J. Org. Chem.* **1998**, 2499–2506.

[90] F. C. Krebs, N. C. Schiødt, W. Batsberg, K. Bechgaard, *Synthesis* **1997**, 1285–1290.

[91] a) F. Closs, L. Häußling, P. Henderson, H. Ringsdorf, P. Schuhmacher, *J. Chem. Soc. Perkin Trans. 1* **1995**, 829–837; b) G. Cooke, F. Hell, S. Violini, *Synth. Commun.* **1997**, *27*, 3745–3748.

[92] P. T. Wright, I. Gillies, J. D. Kilburn, *Synthesis* **1997**, 1007–1009.

[93] S. Kumar, M. Manickam, *Synthesis* **1998**, 1119–1122.

[94] R. J. Bushby, Z. Lu, *Synthesis* **2001**, 763–767.

[95] For other recent syntheses of triphenylenes, see: a) E. Brenna, C. Fuganti, S. Serra, *J. Chem. Soc. Perkin Trans. 1* **1998**, 901–904; b) H. Krempl, R. Mattmer, M. Hanack, *Synthesis* **2000**, 1705–1708; c) D. Peña, S. Escudero, D. Pérez, E. Guitián, L. Castedo, *Angew. Chem.* **1998**, *110*, 2804–2806; *Angew. Chem. Int. Ed.* **1998**, *37*, 2659–2661.

[96] a) R. Breslow, B. Jaun, R. Q. Kluttz, C.-Z. Xia, *Tetrahedron* **1982**, *38*, 863–867; b) E. Fontes, P. A. Heiney, W. H. de Jeu, *Phys. Rev. Lett.* **1988**, *61*, 1202–1205; c) C. Mertesdorf, H. Ringsdorf, J. Stumpe, *Liq. Cryst.* **1991**, *9*, 337–357.

[97] S. J. Cross, J. W. Goodby, A. W. Hall, M. Hird, S. M. Kelly, K. J. Toyne, C. Wu, *Liq. Cryst.* **1998**, *25*, 1–11.

[98] I. Paraschiv, P. Delforterie, M. Giesbers, M. A. Posthumus, A. T. M. Marcelis, H. Zuilhof, E. J. R. Sudhölter, *Liq. Cryst.* **2005**, *32*, 977–983.

[99] H. Bock, W. Helfrich, *Liq. Cryst.* **1992**, *12*, 697–703.

[100] G. Heppke, D. Krüerke, M. Müller, H. Bock, *Ferroelectrics* **1996**, *179*, 203–209.

[101] C. V. Yelamaggad, V. Prasad, M. Manickam, S. Kumar, *Mol. Cryst. Liq. Cryst.* **1998**, *325*, 33–41.

[102] M. Weck, A. R. Dunn, K. Matsumoto, G. W. Coates, E. B. Lobkovsky, R. H. Grubbs, *Angew. Chem.* **1999**, *111*, 2909–2912; *Angew. Chem. Int. Ed.* **1999**, *38*, 2741–2745.

[103] A. Schultz, S. Laschat, M. Morr, S. Diele, M. Dreyer, G. Bringmann, *Helv. Chim. Acta* **2002**, *85*, 3909–3918.

[104] a) D. Adam, F. Closs, T. Frey, D. Funhoff, D. Haarer, H. Ringsdorf, P. Schuhmacher, K. Siemensmeyer, *Phys. Rev. Lett.* **1993**, *70*, 457–460; b) H. Bengs, F. Closs, T. Frey, D. Funhoff, H. Ringsdorf, K. Siemensmeyer, *Liq. Cryst.* **1993**, *15*, 565–574; c) D. Haarer, D. Adam, J. Simmerer, F. Closs, D. Funhoff, L. Häussling, K. Siemensmeyer, H. Ringsdorf, P. Schumacher, *Mol. Cryst. Liq. Cryst.* **1994**, *252*, 155–164.

[105] D. Adam, P. Schuhmacher, J. Simmerer, L. Häussling, K. Siemensmeyer, K. H. Etzbach, H. Ringsdorf, D. Haarer, *Nature* **1994**, *371*, 141.

[106] N. Mizoshita, H. Monobe, M. Inoue, M. Ukon, T. Watanabe, Y. Shimizu, K. Hanabusa, T. Kato, *Chem. Commun.* **2002**, 428–429.

[107] For other photoconductivity studies of triphenylenes, see: a) B. Rose, H. Meier, *Z. Naturforsch. B* **1998**, *53*, 1031–1034; b) I. Bleyl, C. Erdelen, K.-H. Etzbach, W. Paulus, H.-W. Schmidt, K. Siemensmeyer, D. Haarer, *Mol. Cryst. Liq. Cryst.* **1997**, *299*, 149–155.

[108] K. Scott, K. J. Donovan, T. Kreouzis, J. C. Bunning, R. J. Bushby, N. Boden, O. R. Lozman, *Mol. Cryst. Liq. Cryst.* **2003**, *397*, 253.

[109] D. Hirst, S. Diele, S. Laschat, M. Nimtz, *Helv. Chim. Acta* **2001**, *84*, 1190–1196.

[110] N. Boden, R. J. Bushby, A. N. Cammidge, S. Duckworth, G. Headdock, *J. Mater. Chem.* **1997**, *7*, 601–605.

[111] K. Praefcke, A. Eckert, D. Blunk, *Liq. Cryst.* **1997**, *22*, 113–119.

[112] S. Kumar, M. Manickam, *Chem. Commun.* **1998**, 1427–1428.

[113] A. Kettner, J. H. Wendorff, *Liq. Cryst.* **1999**, *26*, 483–487.

[114] B. Glüsen, A. Kettner, J. H. Wendorff, *Mol. Cryst. Liq. Cryst.* **1997**, *303*, 115–120.

[115] B. Brandl, J. H. Wendorff, *Liq. Cryst.* **2005**, *32*, 425–430.

[116] a) J. A. Rego, S. Kumar, H. Ringsdorf, *Chem. Mater.* **1996**, *8*, 1402–1409; b) S. Kumar, P. Schuhmacher, P. Henderson, J. Rego, H. Ringsdorf, *Mol. Cryst. Liq. Cryst.* **1996**, *288*, 211–222.

[117] S. Kumar, M. Manickam, *Mol. Cryst. Liq. Cryst.* **1998**, *309*, 291–295.

[118] N. Boden, R. J. Bushby, Z. B. Lu, A. N. Cammidge, *Liq. Cryst.* **1999**, *26*, 495–499.

[119] M. Ikeda, M. Takeuchi, S. Shinkai, *Chem. Commun.* **2003**, 1354–1355.

[120] H. Ringsdorf, R. Wüstefeld, E. Zerta, M. Ebert, J. H. Wendorff, *Angew. Chem.* **1989**, *101*, 934–938; *Angew. Chem. Int. Ed. Engl.* **1989**, *28*, 914–918.

[121] N. Boden, R. J. Bushby, J. F. Hubbard, *Mol. Cryst. Liq. Cryst.* **1997**, *304*, 195–200.

[122] L. Calucci, H. Zimmermann, E. J. Wachtel, R. Poupko, Z. Luz, *Liq. Cryst.* **1997**, *22*, 621–630.

[123] B. Brandl, J. H. Wendorff, *Liq. Cryst.* **2005**, *32*, 553–563.

[124] H. Allinson, N. Boden, R. J. Bushby, S. D. Evans, P. S. Martin, *Mol. Cryst. Liq. Cryst.* **1997**, *303*, 273–278.

[125] G. Li, J. Luo, T. Wang, E. Zhou, J. Huang, H. Bengs, H. Ringsdorf, *Mol. Cryst. Liq. Cryst.* **1998**, *309*, 73–91.

[126] P. Wu, Q. Zeng, S. Xu, C. Wang, S. Yin, C.-L. Bai, *ChemPhysChem* **2001**, *2*, 750–754.

[127] a) H. Monobe, K. Awazu, Y. Shimizu, *Adv. Mater.* **2006**, *18*, 607–610; b) J. K. Vij, A. Kocot, T. S. Perova, *Mol. Cryst. Liq. Cryst.* **2003**, *397*, 531–544; c) S. H. Eichhorn, A. Adavelli, H. S. Li, N. Fox, *Mol. Cryst. Liq. Cryst.* **2003**, *397*, 347–358; d) V. G. Chigrinov, V. M. Kozenkov, H. S. Kwok in *Optical Applications of Liquid Crystals* (Ed.: L. Vicari), Institute of Physics Publishing, Bristol, **2003**, pp. 201–244; e) T. S. Perova, J. K. Vij, A. Kocot, *Adv. Chem. Phys.* **2000**, *113*, 341–486.

[128] B. Kevenhörster, J. Kopitzke, A. M. Seifert, V. Tsukruk, J. H. Wendorff, *Adv. Mater.* **1999**, *11*, 246–250.

[129] K. Ichimura, S. Furumi, S. Morino, M. Kidowaki, M. Nakagawa, M. Ogawa, Y. Nishiura, *Adv. Mater.* **2000**, *12*, 950–953.

[130] H. Monobe, K. Awazu, Y. Shimizu, *Adv. Mater.* **2000**, *12*, 1495–1499.

[131] N. Terasawa, H. Monobe, K. Kiyohara, Y. Shimizu, *Chem. Commun.* **2003**, 1678–1679.

[132] W. Kranig, C. Boeffel, H. W. Spiess, O. Karthaus, H. Ringsdorf, R. Wüstefeld, *Liq. Cryst.* **1990**, *8*, 375–388.

[133] H. Zollinger, *Color: A Multidisciplinary Approach*, Wiley-VCH, Weinheim, **1999**, p. 228.

[134] a) K.-Y. Law, *Chem. Rev.* **1993**, *93*, 449–486; b) H. Langhals, *Heterocycles* **1995**, *40*, 477–500; c) F. Würthner, *Chem. Commun.* **2004**, 1564–1579.

[135] a) U. Anton, C. Göltner, K. Müllen, *Chem. Ber.* **1992**, *125*, 2325–2330; b) C. Göltner, D. Pressner, K. Müllen, H. W. Spieß, *Angew. Chem.* **1993**, *105*, 1722–1724; *Angew. Chem. Int. Ed. Engl.* **1993**, *32*, 1660–1662.

[136] F. Würthner, C. Thalacker, S. Diele, C. Tschierske, *Chem. Eur. J.* **2001**, *7*, 2245–2253.

[137] F. Würthner, Z. Chen, V. Dehm, V. Stepanenko, *Chem. Commun.* **2006**, 1188–1190.

[138] C. W. Struijk, A. B. Sieval, J. E. J. Dakhorst, M. van Dijk, P. Kimkes, R. B. M. Koehorst, H. Donker, T. J. Schaafsma, S. J. Picken, A. M. van de Craats, J. M. Warman, H. Zuilhof, E. J. R. Sudhölter, *J. Am. Chem. Soc.* **2000**, *122*, 11057–11066.

[139] G. Zucchi, B. Donnio, Y. H. Geerts, *Chem. Mater.* **2005**, *17*, 4273–4277.

[140] S. Méry, D. Haristoy, J.-F. Nicoud, D. Guillon, H. Monobe, Y. Shimizu, *J. Mater. Chem.* **2003**, *13*, 1622–1630.

[141] S. Benning, H.-S. Kitzerow, H. Bock, M.-F. Achard, *Liq. Cryst.* **2000**, *27*, 901–906.

[142] a) I. Seguy, P. Jolinat, P. Destruel, R. Mamy, H. Allouchi, C. Courseille, M. Cotrait, H. Bock, *ChemPhysChem* **2001**, *2*, 448–452; b) T. Hassheider, S. A. Benning, H.-S. Kitzerow, M.-F. Achard, H. Bock, *Angew. Chem.* **2001**, *113*, 2119–2122; *Angew. Chem. Int. Ed.* **2001**, *40*, 2060–2063.

[143] For a review on polyaromatic hydrocarbons, see: a) R. G. Harvey, *Polycyclic Aromatic Hydrocarbons*, Wiley, New York, **1997**; b) V. Enkelmann, *Synth. Met.* **1991**, *42*, 2547–2552; c) K. Yoshizawa, A. Chano, A. Ito, K. Tanaka, T. Yamabe, H. Fujita, J. Yamauchi, M. Shiro, *J. Am. Chem. Soc.* **1992**, *114*, 5994–5998; d) M. Baumgarten, K. Müllen, *Top. Curr. Chem.* **1994**, *169*, 1–103.

[144] P. Herwig, C. W. Kayser, K. Müllen, H. W. Spiess, *Adv. Mater.* **1996**, *8*, 510–513.

[145] For reviews on hexa-*peri*-hexabenzocoronenes, see: a) A. J. Berresheim, M. Müller, K. Müllen, *Chem. Rev.* **1999**, *99*, 1747–1785; b) M. D. Watson, A. Fechtenkötter, K. Müllen, *Chem. Rev.* **2001**, *101*, 1267–1300; c) A. C. Grimsdale, J. Wu, K. Müllen, *Chem. Commun.* **2005**, 2197–2204.

[146] R. Goddard, M. W. Haenel, W. C. Herndon, C. Krüger, M. Zander, *J. Am. Chem. Soc.* **1995**, *117*, 30–41.

[147] S. P. Brown, I. Schnell, J. D. Brand, K. Müllen, H. W. Spiess, *J. Am. Chem. Soc.* **1999**, *121*, 6712–6718.

[148] A. Fechtenkötter, K. Saalwächter, M. A. Harbison, K. Müllen, H. W. Spiess, *Angew. Chem.* **1999**, *111*, 3224–3228; *Angew. Chem. Int. Ed.* **1999**, *38*, 3039–3042.

[149] S. Ito, M. Wehmeier, J. D. Brand, C. Kübel, R. Epsch, J. R. Rabe, K. Müllen, *Chem. Eur. J.* **2000**, *6*, 4327–4342.

[150] J. D. Brand, C. Kübel, S. Ito, K. Müllen, *Chem. Mater.* **2000**, *12*, 1638–1647.

[151] J. Wu, M. D. Watson, L. Zhang, Z. Wang, K. Müllen, *J. Am. Chem. Soc.* **2004**, *126*, 177–186.

[152] A. Fechtenkötter, N. Tchebotareva, M. Watson, K. Müllen, *Tetrahedron* **2001**, *57*, 3769–3783.

[153] Z. Tomovic, M. D. Watson, K. Müllen, *Angew. Chem.* **2004**, *116*, 773–777; *Angew. Chem. Int. Ed.* **2004**, *43*, 755–758.

[154] W. Pisula, Z. Tomovic, C. Simpson, M. Kastler, T. Pakula, K. Müllen, *Chem. Mater.* **2005**, *17*, 4296–4303.

[155] a) J. Wu, A. Fechtenkötter, J. Gauss, M. D. Watson, M. Kastler, C. Fechtenkötter, M. Wagner, K. Müllen, *J. Am. Chem. Soc.* **2004**, *126*, 11311–11321; b) J. Wu, J. Li, U. Kolb, K. Müllen, *Chem. Commun.* **2006**, 48–50.

[156] W. Pisula, M. Kastler, D. Wasserfallen, T. Pakula, K. Müllen, *J. Am. Chem. Soc.* **2004**, *126*, 8074–8075.

[157] B. Alameddine, O. F. Aebischer, W. Amrein, B. Donnio, R. Deschenaux, D. Guillon, C. Savary, D. Scanu, O. Scheidegger, T. A. Jenny, *Chem. Mater.* **2005**, *17*, 4798–4807.

[158] A. M. van de Craats, J. M. Warman, K. Müllen, Y. Geerts, J. D. Brand, *Adv. Mater.* **1998**, *10*, 36–38.

[159] A. M. van de Craats, J. M. Warman, A. Fechtenkötter, J. D. Brand, M. A. Harbison, K. Müllen, *Adv. Mater.* **1999**, *11*, 1469–1472.

[160] C.-Y. Liu, A. Fechtenkötter, M. D. Watson, K. Müllen, A. J. Bard, *Chem. Mater.* **2003**, *15*, 124–130.

[161] M. G. Debije, J. Piris, M. P. de Haas, J. M. Warman, Z. Tomovic, C. D. Simpson, M. D. Watson, K. Müllen, *J. Am. Chem. Soc.* **2004**, *126*, 4641–4645.

[162] a) J. M. Warman, J. Piris, W. Pisula, M. Kastler, D. Wasserfallen, K. Müllen, *J. Am. Chem. Soc.* **2005**, *127*, 14257–14262; b) M. Kastler, J. Schmidt, W. Pisula, D. Sebastiani, K. Müllen, *J. Am. Chem. Soc.* **2006**, *128*, 9526–9534.

[163] N. Reitzel, T. Hassenkam, K. Balashev, T. R. Jensen, P. B. Howes, K. Kjaer, A. Fechtenkötter, N. Tchebotareva, S. Ito, K. Müllen, T. Bjørnholm, *Chem. Eur. J.* **2001**, *7*, 4894–4901.

[164] M. Lee, J.-W. Kim, S. Peleshanko, K. Larson, Y.-S. Yoo, D. Vaknin, S. Markutsya, V. V. Tsukruk, *J. Am. Chem. Soc.* **2002**, *124*, 9121–9128.

[165] O. Bunk, M. M. Nielsen, T. I. Sølling, A. M. van de Craats, N. Stutzmann, *J. Am. Chem. Soc.* **2003**, *125*, 2252–2258.

[166] A. M. van de Craats, N. Stutzmann, O. Bunk, M. M. Nielsen, M. Watson, K. Müllen, H. D. Chanzy, H. Sirringhaus, R. H. Friend, *Adv. Mater.* **2003**, *15*, 495–499.

[167] A. Tracz, J. K. Jeszka, M. D. Watson, W. Pisula, K. Müllen, T. Pakula, *J. Am. Chem. Soc.* **2003**, *125*, 1682–1683.

[168] W. Pisula, A. Menon, M. Stepputat, I. Lieberwirth, U. Kolb, A. Tracz, H. Sirringhaus, T. Pakula, K. Müllen, *Adv. Mater.* **2005**, *17*, 684–689.

[169] J. Piris, W. Pisula, A. Tracz, T. Pakula, K. Müllen, J. M. Warman, *Liq. Cryst.* **2004**, *31*, 993–996.

[170] For reviews on switchable columnar phases, see: H. Takezoe, K. Kishikawa, E. Gorecka, *J. Mater. Chem.* **2006**, *16*, 2412–2416.

[171] J. W. Goodby in *Handbook of Liquid Crystals, Vol. 1* (Eds.: D. Demus, J. Goodby, G. W. Gray, H.-W. Spiess, V. Vill), Wiley-VCH, Weinheim, **1998**, pp. 115–132.

[172] a) H. Zimmermann, R. Poupko, Z. Luz, J. Billard, *Z. Naturforsch. A* **1985**, *40*, 149–160; b) N. Spielberg, M. Sarkar, Z. Luz, R. Poupko, J. Billard, H. Zimmermann, *Liq. Cryst.* **1993**, *15*, 311–330.

[173] C. Garcia, J. Malthête, A. Collet, *Bull. Soc. Chim. Fr.* **1993**, *130*, 93–95.

[174] a) V. Percec, C. G. Cho, C. Pugh, *J. Mater. Chem.* **1991**, *1*, 217–222; b) V. Percec, C. G. Cho, C. Pugh, *Macromolecules* **1991**, *24*, 3227–3234; c) V. Percec, C. G. Cho, C. Pugh, D. Tomazos, *Macromolecules* **1992**, *25*, 1164–1176.

[175] a) H. Budig, S. Diele, P. Göring, R. Paschke, C. Sauer, C. Tschierske, *J. Chem. Soc. Chem. Commun.* **1994**, 2359–2360; b) H. Budig, R. Lunkwitz, R. Paschke, C. Tschierske, U. Nütz, S. Diele, G. Pelzl, *J. Mater. Chem.* **1996**, *6*, 1283–1289; c) R. Lunkwitz, C. Tschierske, S. Diele, *J. Mater. Chem.* **1997**, *7*, 2001–2011.

[176] For optical resolution of monosubstituted tribenzocyclononatrienes see: C. Schmuck, W. Wienand, *Synthesis* **2002**, 655–663.

[177] O. B. Akopova, A. A. Bronnikova, *J. Struct. Chem.* **1998**, *39*, 384–387.

[178] E. Wuckert, M. Dix, S. Laschat, A. Baro, J. L. Schulte, C. Hägele, F. Giesselmann, *Liq. Cryst.* **2004**, *31*, 1305–1309.

[179] E. Wuckert, S. Laschat, A. Baro, C. Hägele, F. Giesselmann, H. Luftmann, *Liq. Cryst.* **2006**, *33*, 103–107.

[180] H. Zimmermann, V. Bader, R. Poupko, E. J. Wachtel, Z. Luz, *J. Am. Chem. Soc.* **2002**, *124*, 15286–15301.

[181] D. Felder, B. Heinrich, D. Guillon, J.-F. Nicoud, J.-F. Nierengarten, *Chem. Eur. J.* **2000**, *6*, 3501–3507.

[182] K. Pieterse, A. Lauritsen, A. P. H. J. Schenning, J. A. J. M. Vekemans, E. W. Meijer, *Chem. Eur. J.* **2003**, *9*, 5597–5604.

[183] G. Lattermann, H. Höcker, *Mol. Cryst. Liq. Cryst.* **1986**, *133*, 245–257.

[184] W. Mormann, C. Irle, J. Zimmermann, *Polym. Prepr. Am. Chem. Soc. Div. Polym. Chem.* **1993**, *34*, 704–705.

[185] S. Mahlstedt, M. Bauer, *Polym. Mater. Sci. Eng.* **1994**, *71*, 801–802.

[186] W.-J. Lo, Y.-L. Hong, R.-H. Lin, J.-L. Hong, *Mol. Cryst. Liq. Cryst.* **1997**, *308*, 133–146.

[187] C. J. Lee, S. J. Lee, J. Y. Chang, *Tetrahedron Lett.* **2002**, *43*, 3863–3866.

[188] H. Lee, D. Kim, H.-K. Lee, W. Qiu, N.-K. Oh, W.-C. Zin, K. Kim, *Tetrahedron Lett.* **2004**, *45*, 1019–1022.

[189] C.-W. Chien, K.-T. Liu, C. K. Lai, *Liq. Cryst.* **2004**, *31*, 1007–1017.

[190] a) J. Barberá, M. Bardaji, J. Jiménez, A. Laguna, M. P. Martínez, L. Oriol, J. L. Serrano, I. Zaragozano, *J. Am. Chem. Soc.* **2005**, *127*, 8994–9002; b) J. Barberá, J. Jiménez, A. Laguna, L. Oriol, S. Perez, J. L. Serrano, *Chem. Mater.* **2006**, *18*, 5437–5445.

[191] B. Mohr, G. Wegner, K. Ohta, *J. Chem. Soc. Chem. Commun.* **1995**, 995–996.

[192] S. Kumar, E. J. Wachtel, E. Keinan, *J. Org. Chem.* **1993**, *58*, 3821–3827.

[193] a) E. J. Foster, J. Babuin, N. Nguyen, V. E. Williams, *Chem. Commun.* **2004**, 2052–2053; b) E. J. Foster, R. B. Jones, C. Lavigueur, V. E. Williams, *J. Am. Chem. Soc.* **2006**, *128*, 8569–8574.

[194] J. Babuin, J. Foster, V. E. Williams, *Tetrahedron Lett.* **2003**, *44*, 7003–7005.

[195] E. J. Foster, C. Lavigueur, Y.-C. Ke, V. E. Williams, *J. Mater. Chem.* **2005**, *15*, 4062–4068.

[196] N. Saettel, N. Katsonis, A. Marchenko, M.-P. Teulade-Fichou, D. Fichou, *J. Mater. Chem.* **2005**, *15*, 3175–3180.

[197] a) M. Lehmann, G. Kestemont, R. G. Aspe, C. Buess-Herman, M. H. J. Koch, M. G. Debije, J. Piris, M. P. de Haas, J. M. Warman, M. D. Watson, V. Lemaur, J. Cornil, Y. H. Geerts, R. Gearba, D. A. Ivanov, *Chem. Eur. J.* **2005**, *11*, 3349–3362; b) G. Kestemont, V. de Halleux, M. Lehmann, D. A. Ivanov, M. Watson, Y. H. Geerts, *Chem. Commun.* **2001**, 2074–2075.

[198] N. Boden, R. J. Bushby, K. Donovan, Q. Liu, Z. Lu, T. Kreouzis, A. Wood, *Liq. Cryst.* **2001**, *28*, 1739–1748.

[199] a) M. K. Engel, P. Bassoul, L. Bosio, H. Lehmann, M. Hanack, J. Simon, *Liq. Cryst.* **1993**, *15*, 709–722; b) J. Simon, C. Sirlin, *Pure Appl. Chem.* **1989**, *61*, 1625–1629; c) M. J. Cook, *Chem. Rec.* **2002**, *2*, 225–236.

[200] H. Eichhorn, D. W. Bruce, D. Wöhrle, *Adv. Mater.* **1998**, *10*, 419–422.

[201] a) P. G. Schouten, J. F. van der Pol, J. W. Zwikker, W. Drenth, S. J. Picken, *Mol. Cryst. Liq. Cryst.* **1991**, *195*, 291–305; b) C. F. van Nostrum, A. W. Bosman, G. H. Gelinck, P. G. Schouten,

J. M. Warman, A. P. M. Kentgens, M. A. C. Devillers, A. Meijerink, S. J. Picken, U. Sohling, A.-J. Schouten, R. J. M. Nolte, *Chem. Eur. J.* **1995**, *1*, 171–182; c) H. Engelkamp, C. F. van Nostrum, S. J. Picken, R. J. M. Nolte, *Chem. Commun.* **1998**, 979–980.

[202] H. Iino, J. Hanna, R. Bushby, B. Movaghar, B. J. Whitaker, M. J. Cook, *Appl. Phys. Lett.* **2005**, *87*, 132102.

[203] P. Samorí, H. Engelkamp, P. de Witte, A. E. Rowan, R. J. M. Nolte, J. P. Rabe, *Angew. Chem.* **2001**, *113*, 2410–2412; *Angew. Chem. Int. Ed.* **2001**, *40*, 2348–2350.

[204] a) B. R. Patel, K. S. Suslick, *J. Am. Chem. Soc.* **1998**, *120*, 11802–11803; further porphyrin-based LCs: b) A. Segade, M. Castella, F. Lopez-Calaborra, D. Velasco, *Chem. Mater.* **2005**, *17*, 5366–5374.

[205] a) B. Donnio, D. Guillon, R. Deschenaux, D. W. Bruce in *Comprehensive Coordination Chemistry II*, *Vol. 7* (Eds.: J. A. McCleverty, T. J. Meyer), Elsevier, Oxford, **2004**, pp. 357–627; b) J. L. Serrano, T. Sierra, *Coord. Chem. Rev.* **2003**, *242*, 73–85; c) K. Binnemans, C. Görller-Walrand, *Chem. Rev.* **2002**, *102*, 2303–2345; d) S. R. Collinson, F. Martin, K. Binnemans, R. Van Deun, D. W. Bruce, *Mol. Cryst. Liq. Cryst.* **2001**, *364*, 745–752; e) N. Hoshino, *Coord. Chem. Rev.* **1998**, *174*, 77–108; f) J. Barberá in *Metallomesogens* (Hrsg.: J. L. Serrano), VCH, Weinheim, **1996**, pp. 131–192; g) A. M. Giroud-Godquin in *Handbook of Liquid Crystals*, *Vol. 2B* (Eds.: D. Demus, J. Goodby, G. W. Gray, H.-W. Spiess, V. Vill), Wiley-VCH, Weinheim, **1998**, pp. 901–932; h) P. Espinet, M. A. Esteruelas, L. A. Oro, J. L. Serrano, E. Sola, *Coord. Chem. Rev.* **1992**, *117*, 215–274; i) S. A. Hudson, P. M. Maitlis, *Chem. Rev.* **1993**, *93*, 861–885; j) C. Piguet, J.-C. G. Bünzli, B. Donnio, D. Guillon, *Chem. Commun.* **2006**, 3755–3768; k) A.-M. Giroud-Godquin, P. M. Maitlis, *Angew. Chem.* **1991**, *103*, 370–398; *Angew. Chem. Int. Ed. Engl.* **1991**, *30*, 375–402.

[206] H. Zheng, B. Xu, T. M. Swager, *Chem. Mater.* **1996**, *8*, 907–911.

[207] C.-W. Chien, K.-T. Liu, C. K. Lai, *J. Mater. Chem.* **2003**, *13*, 1588–1595.

[208] J. Barberá, R. Iglesias, J. L. Serrano, T. Sierra, M. R. de la Fuente, B. Palacios, M. A. Pérez-Jubindo, J. T. Vázquez, *J. Am. Chem. Soc.* **1998**, *120*, 2908–2918.

[209] J.-Q. Jiang, Z.-R. Shen, J. Lu, P.-F. Fu, Y. Lin, H.-D. Tang, H.-W. Gu, J. Sun, P. Xie, R.-B. Zhang, *Adv. Mater.* **2004**, *16*, 1534–1539.

[210] J. Szydlowska, A. Krówczynski, U. Pietrasik, A. Rogowska, *Liq. Cryst.* **2005**, *32*, 651–658.

[211] a) U. Pietrasik, J. Szydlowska, A. Krówczynski, *Chem. Mater.* **2004**, *16*, 1485–1492; b) U. Pietrasik, J. Szydlowska, A. Krówczynski, D. Pociecha, E. Górecka, D. Guillon, *J. Am. Chem. Soc.* **2002**, *124*, 8884–8890.

[212] a) J. Barberá, R. Giménez, N. Gimeno, M. Marcos, M. D. C. Pina, J. L. Serrano, *Liq. Cryst.* **2003**, *30*, 651–661; b) M. Marcos, A. Omenat, J. Barberá, F. Durán, J. L. Serrano, *J. Mater. Chem.* **2004**, *14*, 3321–3327.

[213] R. W. Date, D. W. Bruce, *Liq. Cryst.* **2004**, *31*, 1435–1444.

[214] a) K. Binnemans, K. Lodewyckx, B. Donnio, D. Guillon, *Chem. Eur. J.* **2002**, *8*, 1101–1105; b) K. Binnemans, K. Lodewyckx, B. Donnio, D. Guillon, *Eur. J. Inorg. Chem.* **1998**, 1506–1513.

[215] K. Ohta, R. Higashi, M. Ikejima, I. Yamamoto, N. Kobayashi, *J. Mater. Chem.* **1998**, *8*, 1979–1991.

[216] a) T. Hegmann, J. Kain, S. Diele, B. Schubert, H. Bögel, C. Tschierske, *J. Mater. Chem.* **2003**, *13*, 991–1003; b) C. Damm, G. Israel, T. Hegmann, C. Tschierske, *J. Mater. Chem.* **2006**, *16*, 1808–1816; c) B. Bilgin-Eran, C. Tschierske, S. Diele, U. Baumeister, *J. Mater. Chem.* **2006**, *16*, 1136–1144; d) B. Bilgin-Eran, C. Tschierske, S. Diele, U. Baumeister, *J. Mater. Chem.* **2006**, *16*, 1145–1153.

[217] a) D. M. Huck, H. L. Nguyen, B. Donnio, D. W. Bruce, *Liq. Cryst.* **2004**, *31*, 503–507; b) M. C. Torralba, D. M. Huck, H. L.

[218] A. El-ghayoury, L. Douce, A. Skoulios, R. Ziessel, *Angew. Chem.* **1998**, *110*, 2327–2331; *Angew. Chem. Int. Ed.* **1998**, *37*, 2205–2208.

[219] L. Douce, T. H. Diep, R. Ziessel, A. Skoulios, M. Césario, *J. Mater. Chem.* **2003**, *13*, 1533–1539.

[220] E. Terazzi, S. Torelli, G. Bernardinelli, J.-P. Rivera, J.-M. Bénech, C. Bourgogne, B. Donnio, D. Guillon, D. Imbert, J.-C. G. Bünzli, A. Pinto, D. Jeannerat, C. Piguet, *J. Am. Chem. Soc.* **2005**, *127*, 888–903.

[221] J. Barberá, A. Elduque, R. Giménez, L. A. Oro, J. L. Serrano, *Angew. Chem.* **1996**, *108*, 3048–3051; *Angew. Chem. Int. Ed. Engl.* **1996**, *35*, 2832–2835.

[222] M. Enomoto, A. Kishimura, T. Aida, *J. Am. Chem. Soc.* **2001**, *123*, 5608–5609.

[223] C.-R. Wen, Y.-J. Wang, H.-C. Wang, H.-S. Sheu, G.-H. Lee, C. K. Lai, *Chem. Mater.* **2005**, *17*, 1646–1654.

[224] B. A. Minch, W. Xia, C. L. Donley, R. M. Hernandez, C. Carter, M. D. Carducci, A. Dawson, D. F. O'Brien, N. R. Armstrong, *Chem. Mater.* **2005**, *17*, 1618–1627.

[225] a) G. W. Kabalka, S. K. Guchhait, A. Naravane, *Tetrahedron Lett.* **2004**, *45*, 4685–4687; b) A. N. Cammidge, H. Gopee, *Chem. Commun.* **2002**, 966–967.

[226] J.-H. Lee, S.-M. Choi, B. D. Pate, M. H. Chisholm, Y.-S. Han, *J. Mater. Chem.* **2006**, *16*, 2785–2791.

[227] M. Yu, G. Liu, Y. Cheng, W. Xu, *Liq. Cryst.* **2005**, *32*, 771–780.

[228] Z. Belarbi, C. Sirlin, J. Simon, J.-J. Andre, *J. Phys. Chem.* **1989**, *93*, 8105–8110.

[229] a) A. A. Dembek, R. R. Burch, A. E. Feiring, *J. Am. Chem. Soc.* **1993**, *115*, 2087–2089; b) A. A. Dembek, R. R. Burch, A. E. Feiring, *Polym. Prepr. Am. Chem. Soc. Div. Polym. Chem.* **1993**, *34*, 172–173; c) A. A. Dembek, P. J. Fagan, M. Marsi, *Macromolecules* **1993**, *26*, 2992–2994; d) A. A. Dembek, R. R. Burch, A. E. Feiring, *Macromol. Symp.* **1994**, *77*, 303–313.

[230] E. Campillos, R. Deschenaux, A.-M. Levelut, R. Ziessel, *J. Chem. Soc. Dalton Trans.* **1996**, 2533–2536.

[231] a) C. Destrade, H. T. Nguyen, A. Roubineau, A.-M. Levelut, *Mol. Cryst. Liq. Cryst.* **1988**, *159*, 163–171; b) A.-M. Levelut, Y. Fang, C. Destrade, *Liq. Cryst.* **1989**, *4*, 441–448.

[232] J. L. Schulte, S. Laschat, R. Schulte-Ladbeck, V. von Arnim, A. Schneider, H. Finkelmann, *J. Organomet. Chem.* **1998**, *552*, 171–176.

[233] Review: C. F. van Nostrum, *Adv. Mater.* **1996**, *8*, 1027–1030.

[234] For reviews on nonconventional LCs, see: a) C. Tschierske, *Annu. Rep. Prog. Chem. Sect. C* **2001**, *97*, 191–267; b) C. Tschierske, *J. Mater. Chem.* **1998**, *8*, 1485–1508.

[235] a) G.-X. He, F. Wada, K. Kikukawa, S. Shinkai, T. Matsuda, *J. Org. Chem.* **1990**, *55*, 541–548; b) V. Percec, G. Johansson, *J. Mater. Chem.* **1993**, *3*, 83–96; c) J. A. Schröter, C. Tschierske, M. Wittenberg, J. H. Wendorff, *Angew. Chem.* **1997**, *109*, 1160–1163; *Angew. Chem. Int. Ed. Engl.* **1997**, *36*, 1119–1121.

[236] A. J. Blake, D. W. Bruce, J. P. Danks, I. A. Fallis, D. Guillon, S. A. Ross, H. Richtzenhain, M. Schröder, *J. Mater. Chem.* **2001**, *11*, 1011–1018.

[237] For other azamacrocycles see: a) R. P. Tuffin, K. J. Toyne, J. W. Goodby, *J. Mater. Chem.* **1996**, *6*, 1271–1282; b) A. Liebmann, C. Mertesdorf, T. Plesnivy, H. Ringsdorf, J. H. Wendorff, *Angew. Chem.* **1991**, *103*, 1358–1361; *Angew. Chem. Int. Ed. Engl.* **1991**, *30*, 1359–1361; c) H. Richtzenhain, A. J. Blake, D. W. Bruce, I. A. Fallis, W.-S. Li, M. Schröder, *Chem. Commun.* **2001**, 2580–2581.

[238] A. Schultz, S. Laschat, A. Saipa, F. Gießelmann, M. Nimtz, J. L. Schulte, A. Baro, B. Miehlich, *Adv. Funct. Mater.* **2004**, *14*, 163–168.

[239] a) V. Percec, G. Johansson, J. Heck, G. Ungar, S. V. Batty, *J. Chem. Soc. Perkin Trans. 1* **1993**, 1411–1420; b) V. Percec, W.-

D. Cho, G. Ungar, D. J. P. Yeardley, *Chem. Eur. J.* **2002**, *8*, 2011 – 2025.

[240] a) U. Beginn, G. Zipp, M. Möller, *Chem. Eur. J.* **2000**, *6*, 2016 – 2023; b) U. Beginn, G. Zipp, M. Möller, *Adv. Mater.* **2000**, *12*, 510 – 513; c) U. Beginn, G. Zipp, A. Mourran, P. Walther, M. Möller, *Adv. Mater.* **2000**, *12*, 513 – 516.

[241] H.-T. Jung, S. O. Kim, S. D. Hudson, V. Percec, *Appl. Phys. Lett.* **2002**, *80*, 395 – 397.

[242] a) C. Schnorpfeil, M. Fetten, H. Meier, *J. Prakt. Chem.* **2000**, *342*, 785 – 790; b) R. Yu, A. Yakimansky, I. G. Voigt-Martin, M. Fetten, C. Schnorpfeil, D. Schollmeyer, H. Meier, *J. Chem. Soc. Perkin Trans. 2* **1999**, 1881 – 1890; c) K. Müller, H. Meier, H. Bouas-Laurent, J. P. Desvergne, *J. Org. Chem.* **1996**, *61*, 5474 – 5480; d) H. Meier, K. Müller, *Angew. Chem.* **1995**, *107*, 1598 – 1600; *Angew. Chem. Int. Ed. Engl.* **1995**, *34*, 1437 – 1439; e) H. Kretzschmann, K. Müller, H. Kolshorn, D. Schollmeyer, H. Meier, *Chem. Ber.* **1994**, *127*, 1735 – 1745; f) H. Meier, H. Kretzschmann, M. Lang, *J. Photochem. Photobiol. A* **1994**, *80*, 393 – 398; g) H. Meier, H. Kretzschmann, H. Kolshorn, *J. Org. Chem.* **1992**, *57*, 6847 – 6852.

[243] H. Meier, M. Fetten, *Tetrahedron Lett.* **2000**, *41*, 1535 – 1538.

[244] C. Schnorpfeil, H. Meier, M. Irie, *Helv. Chim. Acta* **2001**, *84*, 2467 – 2475.

[245] a) M. Fischer, G. Lieser, A. Rapp, I. Schnell, W. Mamdouh, S. De Feyter, F. C. De Schryver, S. Höger, *J. Am. Chem. Soc.* **2004**, *126*, 214 – 222; b) S. Höger, *Angew. Chem.* **2005**, *117*, 3872 – 3875; *Angew. Chem. Int. Ed.* **2005**, *44*, 3806 – 3808; c) S. Höger, X. H. Cheng, A.-D. Ramminger, V. Enkelmann, A. Rapp, M. Mondeshki, I. Schnell, *Angew. Chem.* **2005**, *117*, 2862 – 2866; *Angew. Chem. Int. Ed.* **2005**, *44*, 2801 – 2805.

[246] J. Zhang, J. S. Moore, *J. Am. Chem. Soc.* **1994**, *116*, 2655 – 2656.

[247] T. Kato, N. Mizoshita, K. Kishimoto, *Angew. Chem.* **2006**, *118*, 44 – 74; *Angew. Chem. Int. Ed.* **2006**, *45*, 38 – 68.

[248] a) C. M. Paleos, D. Tsiourvas, *Angew. Chem.* **1995**, *107*, 1839 – 1855; *Angew. Chem. Int. Ed. Engl.* **1995**, *34*, 1696 – 1711; b) U. Beginn, *Prog. Polym. Sci.* **2003**, *28*, 1049 – 1105.

[249] R. I. Gearba, M. Lehmann, J. Levin, D. A. Ivanov, M. H. J. Koch, J. Barberá, M. G. Debije, J. Piris, Y. H. Geerts, *Adv. Mater.* **2003**, *15*, 1614 – 1618.

[250] K. Kishikawa, S. Nakahara, Y. Nishikawa, S. Kohmoto, M. Yamamoto, *J. Am. Chem. Soc.* **2005**, *127*, 2565 – 2571.

[251] F. Artzner, M. Veber, M. Clerc, A.-M. Levelut, *Liq. Cryst.* **1997**, *23*, 27 – 33.

[252] M. Yoshio, T. Mukai, H. Ohno, T. Kato, *J. Am. Chem. Soc.* **2004**, *126*, 994 – 995.

[253] D. Kim, S. Jon, H.-K. Lee, K. Baek, N.-K. Oh, W.-C. Zin, K. Kim, *Chem. Commun.* **2005**, 5509 – 5511.

[254] S. Kumar, S. Kumar Pal, *Tetrahedron Lett.* **2005**, *46*, 4127 – 4130.

[255] S. Kumar, S. Kumar Pal, *Tetrahedron Lett.* **2005**, *46*, 2607 – 2610.

[256] J. Motoyanagi, T. Fukushima, T. Aida, *Chem. Commun.* **2005**, 101 – 103.

[257] a) C. F. J. Faul, *Mol. Cryst. Liq. Cryst.* **2006**, *450*, 55 – 65; b) D. Franke, M. Vos, M. Antonietti, N. A. J. M. Sommerdijk, C. F. J. Faul, *Chem. Mater.* **2006**, *18*, 1839 – 1847; c) J. Kadam, C. F. J. Faul, U. Scherf, *Chem. Mater.* **2004**, *16*, 3867 – 3871; d) F. Camerel, P. Strauch, M. Antonietti, C. F. J. Faul, *Chem. Eur. J.* **2003**, *9*, 3764 – 3771.

[258] a) M. M. Green, H. Ringsdorf, J. Wagner, R. Wüstefeld, *Angew. Chem.* **1990**, *102*, 1525 – 1528; *Angew. Chem. Int. Ed. Engl.* **1990**, *29*, 1478 – 1481; b) H. Ringsdorf, H. Bengs, O. Karthaus, R. Wüstefeld, M. Ebert, J. H. Wendorff, B. Kohne, K. Praefcke, *Adv. Mater.* **1990**, *2*, 141 – 144.

[259] K. Praefcke, J. D. Holbrey, *J. Inclusion Phenom. Mol. Recognit. Chem.* **1996**, *24*, 19 – 41.

[260] D. Markovitsi, H. Bengs, H. Ringsdorf, *J. Chem. Soc. Faraday Trans.* **1992**, *88*, 1275 – 1279.

[261] V. V. Tsukruk, J. H. Wendorff, O. Karthaus, H. Ringsdorf, *Langmuir* **1993**, *9*, 614 – 618.

[262] S. J. Lee, J. Y. Chang, *Tetrahedron Lett.* **2003**, *44*, 7493 – 7497.

[263] L. Y. Park, D. G. Hamilton, E. A. McGehee, K. A. McMenimen, *J. Am. Chem. Soc.* **2003**, *125*, 10586 – 10590.

[264] a) N. Boden, R. J. Bushby, G. Cooke, O. R. Lozman, Z. Lu, *J. Am. Chem. Soc.* **2001**, *123*, 7915 – 7916; b) E. O. Arikainen, N. Boden, R. J. Bushby, O. R. Lozman, J. G. Vinter, A. Wood, *Angew. Chem.* **2000**, *112*, 2423 – 2426; *Angew. Chem. Int. Ed.* **2000**, *39*, 2333 – 2336; c) R. J. Bushby, I. W. Hamley, Q. Liu, O. R. Lozman, J. E. Lydon, *J. Mater. Chem.* **2005**, *15*, 4429 – 4434; d) R. J. Bushby, J. Fisher, O. R. Lozman, S. Lange, J. E. Lydon, S. R. McLaren, *Liq. Cryst.* **2006**, *33*, 653 – 664.

[265] D. Guillon, R. Deschenaux, *Curr. Opin. Solid State Mater. Sci.* **2002**, *6*, 515 – 525.

[266] a) A. Ciferri, *Liq. Cryst.* **2004**, *31*, 1487 – 1493; b) G. Ungar, *Mol. Cryst. Liq. Cryst.* **2003**, *396*, 155 – 168; c) P. Xie, R. Zhang in *Thermotropic Liquid Crystal Polymers* (Ed.: T.-S. Chung), CRC, Lanchaster, **2001**, pp. 257 – 279; d) G. Ungar, *Prog. Colloid Polym. Sci.* **1992**, *87*, 53 – 56; e) H. Ringsdorf, R. Wüstefeld, *Proc. R. Soc. London Ser. A* **1990**, *430*, 95 – 108; f) V. Abetz, *Adv. Polym. Sci. 190* (*Block Copolymers II*), Springer, Berlin, **2005**; g) V. Abetz, *Adv. Polym. Sci. 189 (Block Copolymers I)*, Springer, Berlin, **2005**; h) I. W. Hamley, *Development in Block Copolymer Science and Technology*, Wiley, Chichester, **2004**.

[267] S. Zamir, E. J. Wachtel, H. Zimmermann, S. Dai, N. Spielberg, R. Poupko, Z. Luz, *Liq. Cryst.* **1997**, *23*, 689 – 698.

[268] S. Kumar, S. K. Varshney, *Org. Lett.* **2002**, *4*, 157 – 159.

[269] M. Möller, V. V. Tsukruk, J. H. Wendorff, H. Bengs, H. Ringsdorf, *Liq. Cryst.* **1992**, *12*, 17 – 36.

[270] A. Schultz, S. Laschat, A. P. Abbott, M. Langner, T. B. Reeve, *J. Chem. Soc. Perkin Trans. 1* **2000**, 3356 – 3361.

[271] G. Cooke, N. Kaushal, N. Boden, R. J. Bushby, Z. Lu, O. Lozman, *Tetrahedron Lett.* **2000**, *41*, 7955 – 7959.

[272] a) S. Mahlstedt, D. Janietz, A. Stracke, J. H. Wendorff, *Chem. Commun.* **2000**, 15 – 16; b) A. Stracke, J. H. Wendorff, D. Janietz, S. Mahlstedt, *Adv. Mater.* **1999**, *11*, 667 – 670.

[273] E. Peeters, P. A. van Hal, S. C. J. Meskers, R. A. J. Janssen, E. W. Meijer, *Chem. Eur. J.* **2002**, *8*, 4470 – 4474.

[274] a) P. H. J. Kouwer, J. Pourzand, G. H. Mehl, *Chem. Commun.* **2004**, 66 – 67; b) P. H. J. Kouwer, C. J. Welch, G. McRobbie, B. J. Dodds, L. Priest, G. H. Mehl, *J. Mater. Chem.* **2004**, *14*, 1798 – 1803; c) P. H. J. Kouwer, G. H. Mehl, *J. Am. Chem. Soc.* **2003**, *125*, 11172 – 11173; d) P. H. J. Kouwer, G. H. Mehl, *Angew. Chem.* **2003**, *115*, 6197 – 6200; *Angew. Chem. Int. Ed.* **2003**, *42*, 6015 – 6018.

[275] a) J. J. Hunt, R. W. Date, B. A. Timimi, G. R. Luckhurst, D. W. Bruce, *J. Am. Chem. Soc.* **2001**, *123*, 10115 – 10116; b) R. W. Date, D. W. Bruce, *J. Am. Chem. Soc.* **2003**, *125*, 9012 – 9013.

[276] N. Tchebotareva, X. Yin, M. D. Watson, P. Samorì, J. P. Rabe, K. Müllen, *J. Am. Chem. Soc.* **2003**, *125*, 9734 – 9739.

[277] a) M. Prehm, S. Diele, M. K. Das, C. Tschierske, *J. Am. Chem. Soc.* **2003**, *125*, 614 – 615; b) M. Kölbel, T. Beyersdorff, C. Tschierske, S. Diele, J. Kain, *Chem. Eur. J.* **2000**, *6*, 3821 – 3837; c) M. Kölbel, T. Beyersdorff, I. Sletvold, C. Tschierske, J. Kain, S. Diele, *Angew. Chem.* **1999**, *111*, 1146 – 1149; *Angew. Chem. Int. Ed.* **1999**, *38*, 1077 – 1080; d) K. Borisch, C. Tschierske, P. Göring, S. Diele, *Chem. Commun.* **1998**, 2711 – 2712; e) J. A. Schröter, C. Tschierske, M. Wittenberg, J. H. Wendorff, *J. Am. Chem. Soc.* **1998**, *120*, 10669 – 10675; f) M. Kölbel, C. Tschierske, S. Diele, *Chem. Commun.* **1998**, 1511 – 1512; g) C. Tschierske, F. Hildebrandt, J. A. Schröter, J. H. Wendorff, R. Festag, M. Wittenberg, *Adv. Mater.* **1997**, *9*, 564 – 567.

[278] a) M. Lee, B.-K. Cho, K. J. Ihn, W.-K. Lee, N.-K. Oh, W.-C. Zin, *J. Am. Chem. Soc.* **2001**, *123*, 4647 – 4648; b) M. Lee, D.-W. Jang, Y.-S. Kang, W.-C. Zin, *Adv. Mater.* **1999**, *11*, 1018 – 1021;

c) M. Lee, D.-W. Lee, B.-K. Cho, J.-Y. Yoon, W.-C. Zin, *J. Am. Chem. Soc.* **1998**, *120*, 13258–13259; d) M. Lee, B.-K. Cho, H. Kim, W.-C. Zin, *Angew. Chem.* **1998**, *110*, 661–663; *Angew. Chem. Int. Ed.* **1998**, *37*, 638–640.

[279] F. Lincker, P. Bourgun, P. Masson, P. Didier, L. Guidoni, J.-Y. Bigot, J.-F. Nicoud, B. Donnio, D. Guillon, *Org. Lett.* **2005**, *7*, 1505–1508.

[280] I. A. Levitsky, K. Kishikawa, S. H. Eichhorn, T. M. Swager, *J. Am. Chem. Soc.* **2000**, *122*, 2474–2479.

[281] Review: G. Pelzl, S. Diele, W. Weissflog, *Adv. Mater.* **1999**, *11*, 707–724.

[282] D. Shen, A. Pegenau, S. Diele, I. Wirth, C. Tschierske, *J. Am. Chem. Soc.* **2000**, *122*, 1593–1601.

[283] a) X. H. Cheng, S. Diele, C. Tschierske, *Angew. Chem.* **2000**, *112*, 605–608; *Angew. Chem. Int. Ed.* **2000**, *39*, 592–595; b) A. Pegenau, T. Hegmann, C. Tschierske, S. Diele, *Chem. Eur. J.* **1999**, *5*, 1643–1660.

[284] a) C. Nuckolls, T. J. Katz, *J. Am. Chem. Soc.* **1998**, *120*, 9541–9544; b) L. Vyklicky, S. H. Eichhorn, T. J. Katz, *Chem. Mater.* **2003**, *15*, 3594–3601.

[285] A. Schultz, S. Diele, S. Laschat, M. Nimtz, *Adv. Funct. Mater.* **2001**, *11*, 441–446, and references therein.

[286] A. Schultz, S. Laschat, S. Diele, M. Nimtz, *Eur. J. Org. Chem.* **2003**, 2829–2839.

[287] M. C. Artal, K. J. Toyne, J. W. Goodby, J. Barberá, D. J. Photinos, *J. Mater. Chem.* **2001**, *11*, 2801–2807.

[288] K. Lau, J. Foster, V. Williams, *Chem. Commun.* **2003**, 2172–2173.

[289] A. Mori, M. Yokoo, M. Hashimoto, S. Ujiie, S. Diele, U. Baumeister, C. Tschierske, *J. Am. Chem. Soc.* **2003**, *125*, 6620–6621.

[290] Reviews: a) M. R. Bryce, *J. Mater. Chem.* **1995**, *5*, 1481–1496; b) J. Garin, *Adv. Heterocycl. Chem.* **1995**, *62*, 249–304; c) G. Schukat, E. Fanghänel, *Sulfur Rep.* **1996**, *18*, 1–294.

[291] R. Andreu, J. Garín, J. Orduna, J. Barberá, J. L. Serrano, T. Sierra, M. Sallé, A. Gorgues, *Tetrahedron* **1998**, *54*, 3895–3912.

[292] a) R. A. Bissell, N. Boden, R. J. Bushby, C. W. G. Fishwick, E. Holland, B. Movaghar, G. Ungar, *Chem. Commun.* **1998**, 113–114; b) R. A. Bissell, N. Boden, S. J. Brown, R. J. Bushby, *Mol. Cryst. Liq. Cryst.* **1999**, *332*, 149–154.

[293] a) J. Barberá, O. A. Rakitin, M. B. Ros, T. Torroba, *Angew. Chem.* **1998**, *110*, 308–312; *Angew. Chem. Int. Ed.* **1998**, *37*, 296–299; b) S. Basurto, S. García, A. G. Neo, T. Torroba, C. F. Marcos, D. Miguel, J. Barberá, M. B. Ros, M. R. de la Fuente, *Chem. Eur. J.* **2005**, *11*, 5362–5376.

[294] a) N. Boden, B. Movaghar in *Handbook of Liquid Crystals*, *Vol. 2B* (Eds.: D. Demus, J. Goodby, G. W. Gray, H.-W. Spiess, V. Vill), Wiley-VCH, Weinheim, **1998**, pp. 781–798; b) N. Boden, R. J. Bushby, J. Clements, B. Movaghar, *J. Mater. Chem.* **1999**, *9*, 2081–2086.

[295] Reviews: a) C. Borchard-Tuch, *Chem. Unserer Zeit* **2004**, *38*, 58–59; b) K. Blankenbach, *Phys. Bl.* **1999**, *55*, 33–38; c) I. C.

Sage in *Handbook of Liquid Crystals*, *Vol. 1* (Eds.: D. Demus, J. Goodby, G. W. Gray, H.-W. Spiess, V. Vill), Wiley-VCH, Weinheim, **1998**, pp. 731–762; d) T. Sergan, J. Kelly, O. Yaroshchuk, L.-C. Chien, *Mol. Cryst. Liq. Cryst.* **2004**, *409*, 153–162.

[296] a) K. Kawata, *Chem. Rec.* **2002**, *2*, 59–80; b) H. Mori, Y. Itoh, Y. Nishiura, T. Nakamura, Y. Shinagawa, *Jpn. J. Appl. Phys.* **1997**, *36*, 143–147; c) F. Leenhouts, *Jpn. J. Appl. Phys.* **2000**, *39*, L741–L743.

[297] G. P. Crawford, R. H. Hurt, *Encycl. Nanosci. Nanotechnol.* **2004**, *6*, 879–905.

[298] Review: a) M. O'Neill, S. M. Kelly, *Adv. Mater.* **2003**, *15*, 1135–1146; b) N. R. Armstrong, B. Kippelen, D. F. O'Brien, S. M. Marder, J.-L. Bredas, *Proceedings—NCPV Program Review Meeting, Lakewood* **2001**, 328–329; c) S. Kumar, *Curr. Sci.* **2002**, *82*, 256–257.

[299] Review: D. Hertel, C. D. Müller, K. Meerholz, *Chem. Unserer Zeit* **2005**, *39*, 336–347.

[300] I. Seguy, P. Destruel, H. Bock, *Synth. Met.* **2000**, *111*, 15–18.

[301] Review: J. Kopitzke, J. H. Wendorff, *Chem. Unserer Zeit* **2000**, *34*, 4–16.

[302] A. Stracke, J. H. Wendorff, D. Goldmann, D. Janietz, B. Stiller, *Adv. Mater.* **2000**, *12*, 282–285.

[303] R. Auzély-Velty, T. Benvegnu, D. Plusquellec, G. Mackenzie, J. A. Haley, J. W. Goodby, *Angew. Chem.* **1998**, *110*, 2665–2668; *Angew. Chem. Int. Ed.* **1998**, *37*, 2511–2515.

[304] R. H. A. Folmer, M. Nilges, P. J. M. Folkers, R. N. H. Konings, C. W. Hilbers, *J. Mol. Biol.* **1994**, *240*, 341–357.

[305] J. L. M. van Nunen, B. F. B. Folmer, R. J. M. Nolte, *J. Am. Chem. Soc.* **1997**, *119*, 283–291.

[306] Review: F. Hoffmann, M. Cornelius, J. Morell, M. Fröba, *Angew. Chem.* **2006**, *118*, 3290–3328; *Angew. Chem. Int. Ed.* **2006**, *45*, 3216–3251.

[307] a) A. Monnier, F. Schüth, Q. Huo, D. Kumar, D. Margolese, R. S. Maxwell, G. D. Stucky, M. Krishnamurty, P. Petroff, A. Firouzi, M. Janicke, B. Chmelka, *Science* **1993**, *261*, 1299–1303; b) Q. Huo, D. I. Margolese, U. Ciesla, P. Feng, T. E. Gier, P. Sieger, R. Leon, P. M. Petroff, F. Schüth, G. D. Stucky, *Nature* **1994**, *368*, 317–321; c) Q. Huo, D. I. Margolese, U. Ciesla, D. G. Demuth, P. Feng, T. E. Gier, P. Sieger, A. Firouzi, B. F. Chmelka, F. Schüth, G. D. Stucky, *Chem. Mater.* **1994**, *6*, 1176–1191.

[308] F. Di Renzo, A. Galarneau, P. Trens, F. Fajulas in *Handbook of Porous Solids*, *Vol. 3* (Eds.: F. Schüth, K. S. W. Sing, J. Weitkamp), Wiley-VCH, Weinheim, **2002**, pp. 1311–1395.

[309] Review: S. Hoffmann in *Handbook of Liquid Crystals*, *Vol. 3* (Eds.: D. Demus, J. Goodby, G. W. Gray, H.-W. Spiess, V. Vill), Wiley-VCH, Weinheim, **1998**, pp. 393–452.

[310] Review: P. Zugenmaier in *Handbook of Liquid Crystals*, *Vol. 3* (Eds.: D. Demus, J. Goodby, G. W. Gray, H.-W. Spiess, V. Vill), Wiley-VCH, Weinheim, **1998**, pp. 453–482.